Role of zinc containing compounds in nitrile rubber based micro- and nanocomposites

Von der Fakultät Maschinenwesen

der

Technische Universität Dresden

Zur

Erlangung des akademischen Grades

Doktoringenieur (Dr.-Ing.)

angenommene Dissertation

M.Sc. Debdipta Basu

Geb. am 16.01.1985 in Hooghly, Indien

Tag der Einreichung: 18.06.2015

Gutachter: Prof. Dr. rer. nat. habil. Gert Heinrich

Prof. Dr. rer. nat. Ulrich Giese

*I dedicate this thesis to my **Baba** and **Ma** who are the best support systems to me*

Acknowledgement

I would like to express my sincerest and heartfelt gratitude to Prof. Gert Heinrich for providing me with the opportunity to work on my Ph.D thesis at Leibniz-Institut für Polymerforschung (IPF) Dresden e.V., Germany. His strong faith in me to carry out the task for the doctoral thesis has been an immense source of motivation. I am thankful for the valuable discussions and comments he made towards my topics. It is indeed a privilege to work with such a humble and wonderful human being like him.

I am extremely indebted to Dr. Amit Das for his guidance and encouragement. He has been a constant source of inspiration to me. I have never hesitated to rush to him to share both of my success and failure. His affection and love did not ever let me feel away from home. During my stay here, I have been enriched to a great extent by the scientific discussions and technical suggestions I had with him. His simplicity in every approach of life has taught me a great lesson. I hope to maintain this relationship with him and his family for the rest of my life. I am equally grateful to Dr. Klaus Werner Stöckelhuber for helping me with valuable technical advices for numerous times to execute the scientific works successfully. I am deeply touched by his humble and kind nature. I express my deep gratitude to Dr. De-Yi Wang for his support and encouragement. I am thankful to Dr. Sven Wießner and Dr. Andreas Leuteritz for their scientific inputs.

I thankfully acknowledge the support of Mr. Réne Jurk for demonstrating me all the necessary instruments in the elastomer laboratory. I would like to thank Dr. Petr Formanek for spending some fruitful time in discussions and carrying out the TEM analysis. I am extremely thankful to Mrs. Uta Reuter for TEM characterization, Mrs. Sabina Krause for thermal analysis, Dr. Mikhail Malanin for FTIR characterization and Mr. Holger Scheibner for stress-strain analysis. I am grateful to Mrs. Gudrun Schwarz and Mrs. Anne Hofmann for their assistance whenever needed. It is my great pleasure to mention the names of couple of my friends, Mr. Jianhong Chen and Mr. Nguyen Hoai An Tran and Mr. Dan Xiao who made my stay in Dresden memorable. I will definitely cherish the moments I spent travelling to various places as well as doing other extra-curricular activities together. I enjoyed my life here in Dresden with friends and colleagues like Chayan da, Subhas da, Jatin da, Babu anna, Tahir, Kalaivani, Gaurav bhaiya, Sourav, Hirak, Sujit, Krishanu, Sthitadhi.

Finally, I want to give the utmost credit to my family to stand as the strongest support system for me. My Baba and Ma are the most important persons in my life. I have perpetual love and respect for them. It is their bliss and affection which have empowered me to come abroad and pursue my dream. I personally owe a lot to Debi kaku for his inspiration and support. I am extremely thankful to other family members and well-wishers, Thakuma, Didi, Mama, Munai, Chhodda, Niladri da, Uttam, Bate, Arpana and so many. Last but not the least, I offer my sincerest respect to the revered Thakur, Ma and Swamiji for blessing me throughout the journey.

Eidesstattliche Erklärung

Hiermit versichere ich, dass ich die vorliegende Arbeit ohne unzulässige Hilfe Dritter und ohne Benutzung anderer als der angegebenen Hilfsmittel angefertigt habe; die aus fremden Quellen direkt oder indirekt übernommenen Gedanken sind als solche kenntlich gemacht. Die Arbeit wurde bisher weder im Inland noch im Ausland in gleicher oder ähnlicher Form einer anderen Prüfungsbehörde vorgelegt.

Die Promotionsordnung wird anerkannt.

Dresden, den 18.06.2014

Abstract

A detailed understanding of the mechanisms of rubber vulcanization of di-ene rubbers remains one of the most challenging issues in rubber chemistry and technology. The sulfur vulcanization of rubber is a traditional but very sophisticated process by which modern tyres are produced. In this chemical process zinc oxide plays a crucial role along with other sulfur vulcanization ingredients. To improve the performance of a sulfur vulcanized rubber product the mechanistic pathways of the chemical crosslinking and the role of zinc containing compounds in the vulcanization process should be well understood. For example, the performance of tyres could be optimized by establishing proper sulfur/or other type of network structures. Nitrile rubbers, the most non-tyre rubber used in the world and of course being categorized as specialty elastomers draw significant interest for research to understand the unique chemistry of crosslinking while cured with zinc compounds and the associated properties of composites prepared with such system.

In this work effort has been paid to understand the role of different types of zinc compounds in the sulfur vulcanization of carboxylated nitrile rubbers. In this extensive and in depth study the formation of a new type of polymer phase inside the rubber has been firmly established. By this finding the dynamic mechanical behavior of such polymers can be well understood.

Certain part of this work deals with the exploration of the role of zinc chloride in nitrile rubbers. It was found that the zinc chloride has a profound effect on the chemical crosslinking of NBR where other rubber additive/curing agent was totally absent. The rubber thus cured was found to be very hydrophilic as contrary to general behavior of the rubber compounds. A detail analysis based on the novel crosslinking network structure established by co-ordination linkage between zinc atom of zinc chloride and nitrile rubber is carried out. The carboxylated nitrile rubber was explored to develop some functional rubber compounds with the development of very interesting flame retardant properties. In this topic, zinc containing layered double hydroxide (LDH) was used as multifunctional fillers in XNBR rubbers. Apart from the flame retardancy behavior, LDH shows its unique features as reinforcing filler and its sulfur vulcanizing activation effects simultaneously.

Finally, another zinc containing compound e.g., zinc stearate has been used to develop thermo- responsive or mechano- adaptive elastomeric materials by adjusting the crystalline/amorphous character of this compound. This type of work can pave the ways to understand and develop the concept of adaptive tyres in future.

Kurzzusammenfassung

Ein fundiertes Verständnis der Mechanismen der Gummi-Vulkanisation von Dien-Kautschuken ist noch immer eine der größten Herausforderungen in der Chemie und Technologie der Elastomere. Die Schwefelvulkanisation von Elastomerwerkstoffen ist ein seit langem verwendeter, aber dennoch sehr anspruchsvoller Prozess, mit dessen Hilfe moderne Reifen hergestellt werden. Bei dieser chemischen Reaktion spielt Zinkoxid, zusammen mit den anderen Hilfsstoffen der Schwefelvulkanisation eine entscheidende Rolle. Um die Produkteigenschaften von mit Schwefel vulkanisierten Elastomermaterialien zu verbessern, sollten die Mechanismen der chemischen Vernetzung - und insbesondere auch die Rolle von Zink enthaltenden Verbindungen bei der Vulkanisationsreaktion besser verstanden werden. Zum Beispiel könnte das Eigenschaftsprofil von Reifen durch die Ausbildung von geeigneten Netzwerken aus Schwefel oder anderen Netzknoten optimiert werden. Nitrilkautschke aus der Klasse der Spezialelastomere und die meisten nicht-Tire- Kautschuk in der ganzen Welt eingesetzt, wecken ein großes Interesse der Forschung wegen ihrer einzigartigen Vulkanisationschemie bei der Vernetzung mittels Zinkverbindungen und wegen der besonderen Eigenschaften der dadurch erzeugten Elastomerwerkstoffe.

In dieser Arbeit wurde besonderes Augenmerk darauf gelegt, die Rolle von verschiedenen Zinkverbindungen in der Schwefelvulkanisation von carboxylierten Nitrilkautschuken zu verstehen. In der vorliegenden umfangreichen und eingehenden Untersuchung konnte die Ausbildung einer weiteren Polymerphase im Elastomer nachgewiesen werden. Durch dieses Ergebnis kann nun das dynamische mechanische Verhalten von solchen Polymerwerkstoffen besser verstanden werden.

Teile dieser Arbeit beschäftigen sich mit der Erforschung der Rolle von Zinkchlorid bei der Vernetzung von Nitrilkautschuken. Hierzu wurde festgestellt, dass Zinkchlorid einen besonderen Einfluss auf die chemische Vernetzung des NBR aufweist, auch in Abwesenheit anderer Vernetzungs- oder Vulkanisationsadditive. Die so vernetzten Elastomere weisen ein stark hydrophiles Verhalten auf, im Gegensatz zu den allgemeinen Eigenschaften solcher Elastomerwerkstoffe. Eine detaillierte Analyse dieser neuartigen Netzwerkstruktur, gebildet durch eine Koordinationsbindung zwischen dem Zinkatom des Zinkchlorids und dem Nitrilkautschuk, wurde durchgeführt. Carboxylierter Nitrilkautschuk (XNBR) wurde ebenfalls eingesetzt, um funktionale Kautschukmischungen mit neuartigen flammhemmenden Eigenschaften zu entwickeln. Zu dieser Thematik wurden Zink enthaltende Doppelhydroxide (Layered Doube Hydroxides, LDH) als multifunktionale Füllstoffe in XNBR-Kautschuk eingesetzt. Neben dem Flammschutzverhalten zeigt LDH einzigartige Eigenschaften als verstärkenden Füllstoff und gleichzeitig als aktivierendes Additiv für die Schwefel-vulkanisation.

Eine weitere Zink enthaltenden Verbindung, Zinkstearat, wurde eingesetzt um mechano-adaptive elastomere Materialien durch gezieltes Einstellen des kristallinen bzw. amorphen Charakters dieser Verbindung zu entwickeln. Dies könnte einen wichtigen Beitrag zur Entwicklung zukünftiger Reifenmaterialien mit intrinsisch adaptiven Eigenschaften liefern.

Contents

Chapter 1

Introduction

1.1 Aim and approach of this work

Over the long decades since the vulcanization of rubber is discovered, the trends in use of additives have been pretty similar. The rubber compounds we see in our day to day lives, spanning from tire to a shoe sole or pencil eraser are a mixture of a number of various ingredients. The gum (unvulcanized raw rubber) is elastic in nature and hence mechanically weak and subject to swelling by different solvents. In order to improve these properties to a significant extent, they need to be compounded with different additives [1]. The raw rubber is usually vulcanized with the aids of different chemical substances. Apart from the essential crosslinking agent e.g., sulfur, peroxides or electron induced radiation [2-6], some other curing additives are also practically used in the process. The final properties and the performance of a rubber item largely depend on the network structure of the polymers. A fine tuning of the network structure can offer immense opportunities to develop high performance elastomeric materials. For example, a fuel efficient tyre could be developed if the sulfur network structure is tailored according to the desirable way. For this purpose the role of each sulfur vulcanization chemicals should be well explored [7,8]. Particularly, in sulfur vulcanization, the role of zinc oxide still remains unclear to the rubber chemists. For this process zinc oxide and stearic acid have been two indispensable chemical aids in rubber compounding. It is reported that zinc oxide is generally used at the level of 2-3% by weight of zinc (4-5 phr ZnO) in the whole rubber compound [9]. The rubber industries in the European Union (EU) consume approximately 10^5 tons of zinc oxide per year. This figure of consumption of zinc oxide and other forms of zinc compounds in rubber industries is approximately 40% of the total usage of zinc oxide in the world [7, 9]. It has been noticed that mostly their use has been practiced in case of sulfur crosslinking process. Zinc oxide reacts with stearic acid and forms zinc stearate which accelerates the rate of the sulfur vulcanization process by releasing soluble zinc ions that activate the crosslinking reactions. Some amount of zinc sulfide is also believed to take part in the crosslinking process [7]. With sulfur only in the curing recipe, the whole process of vulcanization takes longer time which is a very key issue

to handle in both industrial and academic fields. Thus, both these chemical substances are established as crucial components for basic rubber compounding. Till date the exact role of zinc oxide in sulfur vulcanization process is not explored properly.

Over the years, zinc oxide has been considered to be relatively non-toxic compound [8]. Recent issues, however, compelled to restrict the use of this material to limited levels [7-9]. It is reported that zinc oxide is generally used at the level of 2-3% by weight of zinc (4-5 phr ZnO) in the whole rubber compound [9]. The rubber industries in the European Union (EU) consume approximately 10^5 tons of zinc oxide per year. This figure of consumption of zinc oxide and other forms of zinc compounds in rubber industries is approximately 40% of the total usage of zinc oxide in the world [7, 9]. The aquatic flora and fauna are observed to be greatly affected by the intake of zinc oxides to a significant extent. These organisms, reckoned to be sensitive to a very low levels of zinc need to be saved. To take care of this sensitive issue remedies are being found and discussed in details within the scope of this study.

In search to find a suitable replacement material of zinc oxide in the conventional rubber compounding process, layered double hydroxides (LDH) evolved as a potential material [10-12]. Especially, Zn-Al LDH contains the zinc ions which aid the vulcanization process. If modified with some stearate salts, use of stearic acid can also be avoided in the curing ingredients [10-13]. LDH being a relatively new material to rubbers is not explored a lot [11]. There is immense scope to exploit the versatility of this inorganic clay in rubbers because it provides a wide range of properties due to its unique structure. The potential of this inorganic material as mechanical reinforcing, flame retardant, aging resistant material have been explored in nitrile rubber within the scope of this work. Detailed studies are carried out to understand the fundamental mechanisms involved with LDH in nitrile rubber compared to other zinc salts used in the curing process. This study is also focused with a goal to introduce and establish layered double hydroxides as potential multi-functional filler in rubber technology.

Nitrile rubber, especially NBR and its modified form named as XNBR find applications in sealings, automotives, laboratory gloves, bowling pin setters, hoses, O-rings, gaskets, oil and gas pipes, high abrasion resistance shoes, printing rolls, rice dehusking roles. This work is motivated to develop rubber components made of zinc compounds based nitrile rubber composites which find new fields of potential applications in flame retardant wires and

cables, active dampers for racing cars, water seals for tanks and washing machines, wiper blades for cars, thermotropic shades for solar panels, low heat build-up rubber rolls, floor and roofing materials etc. as shown in Fig. 1.1.

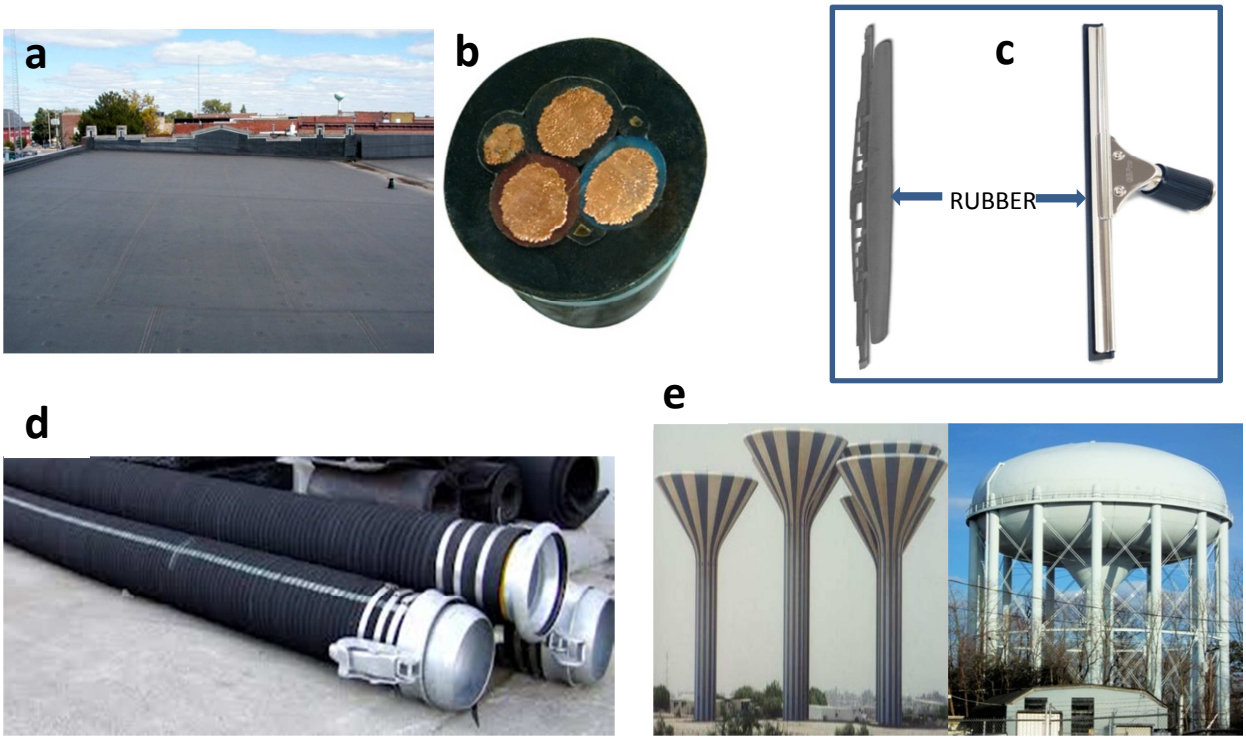

Fig. 1.1 Potential fields of application of zinc based nitrile rubber composites: a) flame retardant roof mat, b) flame retardant electrical cables, c) wiper blades for cars, d) water hoses and e) water seals for tanks

The main aim and objectives of this work is therefore to investigate the role of different zinc compounds viz. zinc oxide (ZnO), Zn-Al Layered Double Hydroxides (LDH), zinc chloride ($ZnCl_2$) , zinc stearate ($C_{36}H_{70}O_4Zn$) etc. in nitrile rubber in different aspects.

1.2 Role of zinc in curing of nitrile rubbers

Introduction of zinc ion as an activator in curing of rubbers has been realized by the following two ways:

i) Zinc ions have been potentially delivered using the most common source material, like zinc oxide for conventional sulfur curing of rubber compounds. Stearic acid has been an indispensable aid in this curing recipe to promote the crosslinking process further.

ii) In the curing process where sulfur is not used, zinc ions form some coordination complexes with the host rubber (mostly polar rubber). Thus, the ionic association between the polar (mostly acidic) part of the rubber and metal cation help crosslink the rubber. These types of rubber compounds are termed as ionic elastomers [14-17].

1.2.1 Zinc oxide in sulfur vulcanization of rubber

Invented by Charles Goodyear, chemical cross-linking of rubbers by sulfur vulcanization is the only method by which modern automobile tyres are manufactured [18]. The cured product does not flow under deformation like the uncured raw mass, does not get stiff at cold condition or neither it does soften at elevated temperatures. Rather, it is more elastic in nature and gets back to its original shape after unloading the stress and shows higher abrasion resistance too. Nevertheless, vulcanization process without any accelerator in the recipe used to take 6 hours at 142°C. Addition of a certain amount of organic accelerator, the vulcanization time was reduced dramatically [19, 20]. In this process, zinc oxide (ZnO) acts an activator, increasing the efficiency of the organic accelerators. In spite of the fact that sulfur vulcanization is employed for almost 200 years, till now, the exact mechanistic pathways of such crosslinking process is not completely understood and remains subject of study [21-25]. A number of mechanisms have been evolved, but due to the complexity of the systems involved with multi-components in the cured mass, elucidations of those mechanisms becomes difficult. As a result, convergence of so many theories of sulfur vulcanizations in presence of zinc oxide into uniform acceptance is still not possible amongst the rubber technologists. Significant statements from the two renowned rubber scientists in this century prove the scenario. As per Scheele [26], *"Perhaps nowhere in chemistry is there encountered a field which even in its literature alone shows so many uncertainties and (possibly only apparent) contradictions as that of the vulcanization of rubber."* Bateman *et al* [27] further added to the previous statement, *"Whilst it has long been appreciated, albeit intuitively, that sulfur vulcanization is a very complex chemical process, the actual complexity… is probably far in excess of what has ever been envisaged."*

1.2.2 Zinc ions as activator in classical sulfur curing process

Over a long decade now, it is quite widely accepted that zinc ions play the role of the potential activator in sulfur curing process of rubbers. The schematic displayed in Fig. 1.2 explains the

overall mechanism of zinc activation in sulfur curing process. Several mechanisms have evolved over the years to interpret the probable mechanism involved in formation of vulcanizates through sulphurating complexes. In one hand, some authors have advocated that the active sulphurating complex is indeed the accelerator polysulphide, Ac – S_x – Ac instead

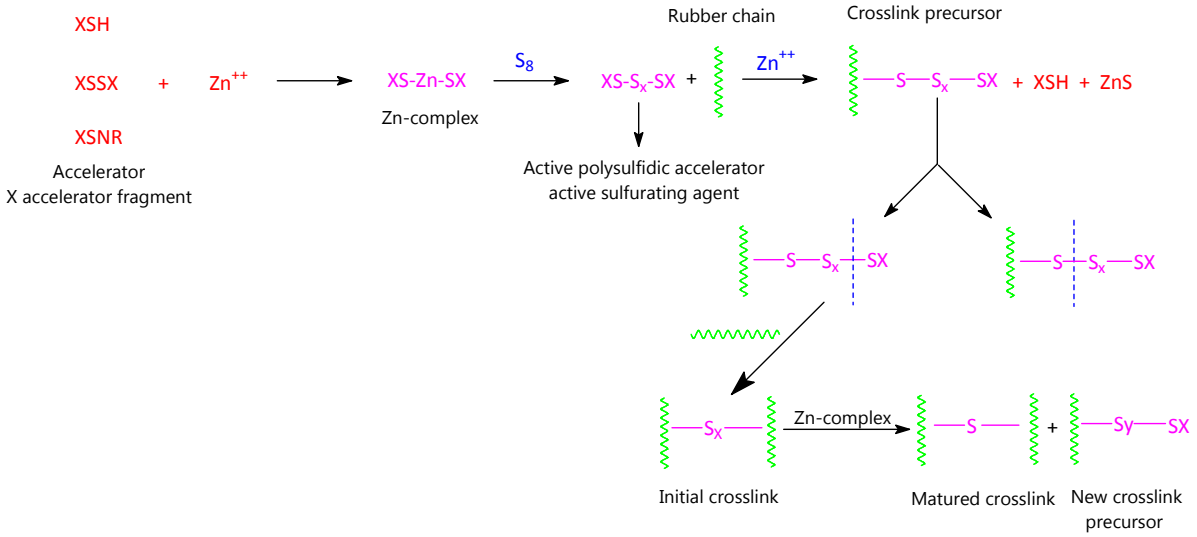

Fig. 1.2 Schematic representation of accelerated sulfur vulcanization in the presence of zinc ions (Zinc cations are produced by the reaction of zinc oxide and stearic acid or zinc stearate or other zinc containing compounds)

of the zinc complex, on the other hand others came up with the conclusions that both the zinc complex and polysulphide act as the sulphurating agent [9]. Role of zinc oxide is also vital to stabilize and further strengthen the precursor S – S bond in the crosslinking process. Zinc oxide, by the virtue of releasing Zn^{2+} ions during the vulcanization process forms a chelating compound which stabilizes other sulfur bonds and prevents the breaking of S – S bond [28]. Amongst different metal oxides exploited with rubber to act as vulcanization activators, zinc has been reckoned as one of the most easily available and less expensive source to form the required coordination bond with the rubber chains [29]. The following order of stability confirms the above statement:

$$Cu^{2+}, Hg^{2+} > Ni^{2+}, Zn^{2+}, Cd^{2+}, In^{2+} > Mg^{2+}, Ca^{2+}$$

1.2.3 Zinc ions as self crosslinker – Ionic elastomer

Ionomers are categorized as a special class of polymer where incorporation of relatively small amount of ionic groups (10 mol %) in the form of inorganic salts into hydrocarbon chains generates unique physical properties of the whole material. Ionic elastomers are fabricated when these ionomer units are effectively cross-linked through the ionic association and in

some cases form ionic multiplets and clusters as exhibited in Fig. 1.3. At the outset, the ion pairs are formed followed by the formation of multiplets. Multiplets are basically termed as aggregates consisting of several ion pairs (approximately 6 to 8) [30]. They act primarily as

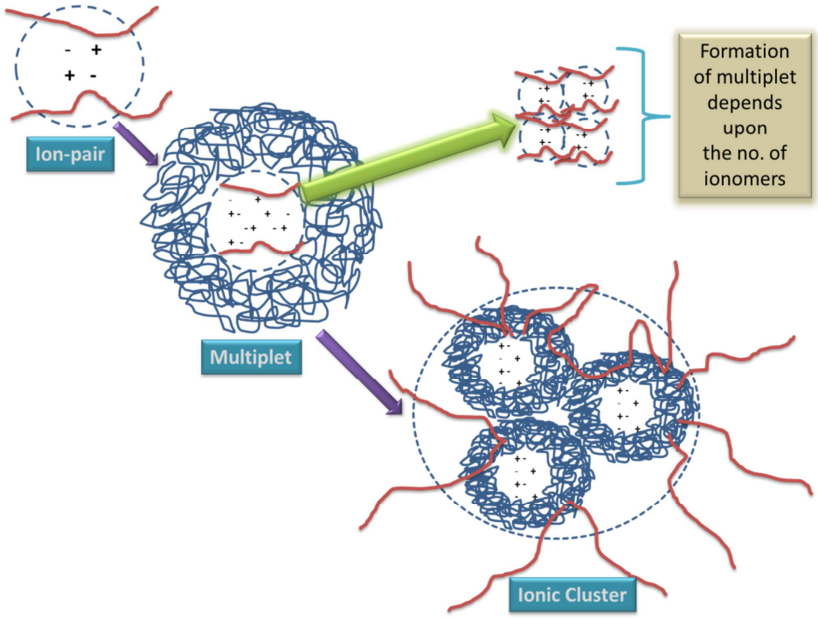

Fig. 1.3 Schematic of hierarchical structure of ionomer formation

physical crosslinks. Several factors are believed to be controlling the number of ion pairs in a multiplet e.g., the size of the ion content, ion pair, and steric effects of the polymer chain segments adjoined to the ion pairs [31]. These multiplets exist in the form of quadrapoles, hexapoles, or octapoles. It is noteworthy to mention that low dielectric constant and low glass transition temperature (T_g) of the host polymer favour ionic aggregation, while high dielectric constant and/or high T_g inhibit multiplet formation. Specific interactions between plasticizer, if present in the system and backbone of the ionic groups also influence the ionic crosslinking process. These multiplets are believed [31] to be dispersed in the hydrocarbon matrix and hence do not form any separate phase.The average gap between the multiplets decreases as the ion contents gradually increase. Thus, ion clusters are formed. These ionic clusters typically exhibit the characteristics of phase-separated regions having their own T_g. The Strong intermolecular ionic interactions between the moieties and the ultimate physical properties of the rubber compound depend strongly on the type of host polymer, ionic content, nature of the ionic moiety (carboxylate, sulfonate , phosphonate) degree of neutralization and obviously the types of cations and anions [14,32]. The clusters contain a large amount of ion pairs and considerable amount of non-ionic hydrocarbon as well. They typically demonstrate some of the properties of a separate phase, including some type of relaxation behavior at

elevated temperature, and subsequently behave like reinforcing fillers in addition to their function as physical crosslinks [33]. The ratio of ionic groups available in these two forms in any particular ionomer is determined by the nature of the hydrocarbon backbone, the concentration of salt groups and their chemical nature [34].

Though, a significantly wide range of ionic elastomers are of both academic and commercial interests, we would mostly highlight the carboxylated elastomers here within the scope of the present study. Typically 6-7 % carboxylic groups are incorporated in the acrylonitrile-butadiene rubber (NBR) in order to enhance various elastomeric properties. Thus, carboxylated acrylonitrile-butadiene rubber (XNBR) is produced. The structural modification is displayed in chapter 2 (Fig. 3.2). The worldwide production of carboxylated based ionic elastomers are reported to be approximately 0.5 million tons per year [35]. Basically, carboxylated ionic elastomers are categorized into following two classes [32]:

i) **Conventional carboxylated ionic elastomer** – These classes of ionic elastomers are produced in bulk.

ii) **Telechelic carboxylated ionic elastomer** – Low molecular weight difunctional carboxyl terminated buta di-ene based elastomers fall in the category of telechelic ionomers.

Incorporation of optimum level of acidic groups in the hydrocarbon chains of di-ene rubbers improves many properties. These specially modified elastomers while neutralized with suitable metal oxides, very significant property changes are observed. For instance, XNBR when vulcanized (or, neutralized) with zinc oxide, stable and neutral salt in the form of COO – Zn – COO is eventually obtained. As a result, increase in the glass transition temperature and enhancement of rubbery modulus at high temperature is observed as well in these rubber products.

These types of ionic elastomers are commercially used in adhesives, impact modifiers, shoe soles, garden hose, rubber roll, floor materials etc.

1.2.4 Zinc in nitrile rubbers

The use of zinc in the form of various zinc compounds as the preliminary sources has been pretty inevitable in nitrile rubber compounds. The fundamental reasons supporting this statement has been described briefly in the previous sections. Although over the years, zinc oxide and zinc peroxide have been the most common sources used in nitrile rubbers, current

research trends introduce some relatively uncommon sources of zinc e.g., zinc chloride [36], zinc aluminium layered double hydroxides, zinc di-methacrylate [37,38], zinc disorbate [39] etc. in nitrile rubber compounds. The end results attained from these rubber composites have diversified to a wide extent because of their multi-functional aspects as curing ingredients or filler materials. Zinc based nitrile rubber compounds not only are limited in research purpose in the academic fields, but also gained a significant interest amongst the industries because of the smart properties obtained from these elastomeric products. Thermotropicity, flame retardancy, stimuli-responsive properties etc. are some of the unique properties exhibited by these compounds. The ability to form ionic or co-ordination compounds with the polar nitrile rubbers (NBR or XNBR) eases the dispersion of various zinc compounds. Therefore, the mechanical properties along with thermal, optical properties are improved as well.

1.3 Synopsis of the thesis

The current study highlights both very fundamental role of zinc in nitrile rubbers in various aspects and the commercial aspects of the elastomeric products prepared as well. Intensive literatures survey was carried out to gain an updated and comprehensive knowledge on this field.

Chapter 2 presents a comprehensive overview about the state of the art of the relevant body of work. Over a decade, various zinc compounds e.g., zinc oxide, zinc peroxide etc. have been extensively used with di-ene rubber as curing recipe. Mostly their roles have been exploited as curing activator. A couple of relatively rare zinc sources, zinc chloride and zinc based layered double hydroxides have also been explored particularly in nitrile rubber in a limited number of literatures. Synthesis, structural features, properties and applications of these zinc sources have been discussed. XNBR based rubber compounds in the presence of zinc sources form ionomers which find considerable academic and commercial interests. Self-healing polymers based on XNBR and zinc systems are also reviewed and critically discussed.

Chapter 3 is mainly comprised of the experimental parts carried out for this thesis work. Materials used, experimental techniques followed to prepare rubber compounds and characterization tools used to analyze and interpret the data obtained are discussed in this chapter in detail.

Chapter 4 illustrates the results and discussions related to this work. This chapter is mainly divided into 4 subchapters. The first subchapter deals with the fundamental understanding of

the ionomeric characteristics associated with carboxylated nitrile rubber and different zinc sources. In-depth studies in the lights of FT-IR, HRTEM, DMA, WAXS techniques are carried out to extract the underlying mechanism involved with the phase behavior of XNBR while cured with zinc compounds. Second subchapter basically is devoted to explore the role of a zinc based clay material namely Zn-Al LDH as a multifunctional filler for XNBR. Despite integrating any functional groups into the interlayers, LDH proved to be acting as a remarkable filler material with XNBR. Curing characteristics, mechanical, dynamic mechanical and thermal properties were substantially improved by introducing LDH with the XNBR. Moreover, flame retardancy of the rubber composites enhanced to a considerable extent after incorporating higher amount of LDH clay. The third subchapter describes how the addition of nano-crystalline zinc stearate into the ionomeric mixture of XNBR and ZnO could lead to thermos-responsive or mechano-adaptive elastomer. The dynamic behavior of the corresponding compounds filled with zinc stearate could be tuned accordingly with temperature due to the melting nature of zinc stearate at high temperature. Combined presence of 'micro-islands' comprised of nano particles of zinc stearate and the phase separated lamellar structures formed by the association of XNBR and ZnO increased the mechanical properties of the final products. Detailed chemical interaction between the functional groups in the ionic elastomers is presented in the lights of FT-IR study. Finally, subchapter 4 reports the fabrication of rubber compounds obtained by novel crosslinking method. Nitrile rubber when cured with $ZnCl_2$ forms a co-ordination network established by the reaction of Zn^{2+} atom and the –CN group attributed to the host polymer. Detailed reaction mechanism was studied and demonstrated in this subchapter. The reaction schemes proposed are well supported by the FT-IR study. For the very first time, the DMA spectra of the nitrile rubber exhibited an extra transition at lower temperature apart from the usual transition at T_g. The transition at lower temperature is attributed to the β-relaxation whereas the transition involved with T_g is termed as α-relaxation. The rubber compound obtained by the co-ordination crosslinking showed substantial swelling behavior. A new zinc based co-ordination compound formed after hydrolysis was the primary reason attributing to this permanent swelling nature.

Eventually, **chapter 5** summarizes the whole work with some final remarks. A brief outlook illustration the future scope of work is also presented in this chapter.

Chapter 2

Literature review

(Some results of this chapter are published in Prog. in Polym. Sci. 39, 594-626, 2014)

2.1 Various zinc compounds used in nitrile rubbers

As discussed in section 1.2.3, various zinc compounds have been used with nitrile rubbers to obtain a wide range of properties, we would discuss in the following sections about the most commonly used zinc compounds in nitrile rubbers.

2.1.1 Zn-Al Layered Double Hydroxides (LDH)

Layered double hydroxides (LDH) belong to a typical class of layered minerals that are quite often termed *anionic clay* minerals. These clay materials are a broad class of inorganic layered compounds with basic character and a high capacity for anion intercalation. LDH is available in nature as well as can be synthesized or modified in the laboratories. Amongst the commercially available LDH clays, Mg-Al LDH and Zn-Al LDH are the most common ones.

2.1.1.1 Structural features of LDH

The chemical formula for LDH is $[M_{1-x}^{II}M^{III}(OH)_2]^{x+}(A^{n-})_{x/n}\cdot yH_2O$, where M^{II} represents a divalent cation, e.g., Mg^{2+}, Ca^{2+}, Zn^{2+}, etc.; M^{III} represents a trivalent cation, e.g., Al^{3+},Cr^{3+}, Fe^{3+},Co^{3+}, etc.; and A^{n-} represents an anion, e.g., Cl^-, CO_3^{2-}, NO_3^-, etc. A^{n-} basically maintain the electro-neutrality of the inorganic sheets. Both the anions and the water molecules are hosted in the interlayer region [11]. A broad range of x values are reported to exist for synthesizing a LDH structure; however, the pure LDH phase contains a narrow range of x values: $0.2 \leq x \leq 0.33$ giving rise to a large class of isostructural materials [40]. As stated earlier, hydrotalcite with the chemical formula $Mg_6Al_2(OH)_{16}CO_3{\cdot}4H_2O$ is the most naturally occurring LDH because of its lowest Gibbs free energy of formation. Back in 1842, Hochstetter [41] first found natural hydrotalcite which was later synthesized by Feitknecht [42] 100 years later. The hydrotalcite structure resulting from the stacking of brucite like layers $[Mg(OH)_2]$contains a positive residual charge arising from the partial isomorphous

substitution of Mg^{2+}cations by Al^{3+}cations (in Mg-Al LDH). Different other types of LDH are also available where, the bivalent cations, such as Zn^{2+}, Ni^{2+}, Co^{2+}, etc., are replaced by

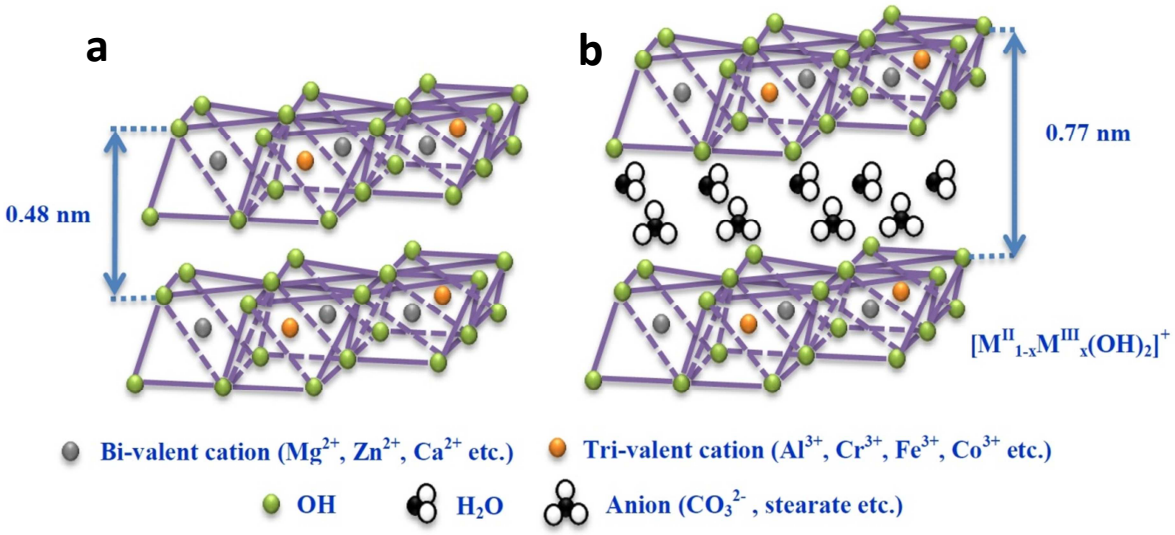

Fig. 2.1 Chemical structures of (a) brucite [$Mg(OH)_2$] and (b) modified form of layered double hydroxides (LDH)

trivalent cations, such as Cr^{3+}, Fe^{3+}, etc. This excess positive charge produced from this kind of substitution is counterbalanced by the carbonate anions, which occupy the interlamellar spaces [11]. LDH and brucite both have similar chemical structures. Hence, a comparative analogy would be useful in this context. Fig. 2.1 exhibits a schematic illustration comparing the structures of brucite and LDH. Brucite consists of a hexagonal close packing of hydroxyl ions with alternate octahedral sites occupied by Mg^{2+} ions. It is quite obvious that the metal hydroxide sheets in the brucite crystal structure have neither a positive nor a negative charge, and they are connected with each other via weak Van der Waals forces, producing a basal spacing of approximately 0.48 nm. In contrast, in the LDH structure, some of the divalent cations of the brucite-like sheets as shown in Fig. 2.1a are isomorphously replaced by a trivalent cation. As a consequence, the mixed metal hydroxide layer, i.e.,$[M_{1-x}{}^{II}M_x{}^{III}(OH)_2]^{x+}$, that is formed attains a net positive charge. Eventually, this excess positive charge on the metal hydroxide layers is neutralized by the anions present in the interlayer region. Some water molecules, which are sometimes required for stabilizing the crystal structure, also exist in the interlayer region of LDHs. The combined presence of anions and water molecules ultimately causes an increase of the basal spacing from 0.48 nm in brucite to approximately 0.77 nm in the modified form of LDH (Fig. 2.1). This type of modification is possible with any types of metal atoms of choice. Mg-Al LDH has been a very preferred choice with

various thermoplastics due to its ease of availability, modification and compatibility, whereas, use of Zn-Al LDH in the polymers has not been explored to a much extent. Intensive studies are being conducted to elucidate various properties of Zn-Al LDH on nitrile rubber in this thesis within the scope of the work.

2.1.1.2 Synthesis and modification of LDH

The ease to synthesize as well as modify layered double hydroxides in the laboratory made this inorganic filler as a very preferable candidate to be used with polymers. The chemical modification is necessary to make this inorganic filler compatible with polymer matrix and to provide sufficient space for the intercalation of polymer chains in between two crystalline layers. Apart from being synthesized in laboratory scale, a few commercial grades of LDH materials are also available in the market. One of the main advantageous features of layered double hydroxide is the employment of similar technique to both synthesize and modify its structure. A flow chart displaying the route to modify LDH from unmodified material is provided in Fig. 2.2. Ability to tune the structure by incorporating the metal atoms of one's own choice as per requirement makes this inorganic clay materials a very preferable filler to explore. Among the various methods to synthesize and modify LDH materials, the most common are co-precipitation, homogeneous precipitation, structure reconstruction, sol–gel, hydrothermal and the anion exchange method. Vaccari presented in his review [43] that the co-precipitation method is the most common and useful method for synthesizing large amounts of LDH. Modifications of unmodified LDH materials have been carried out as per the requirement.

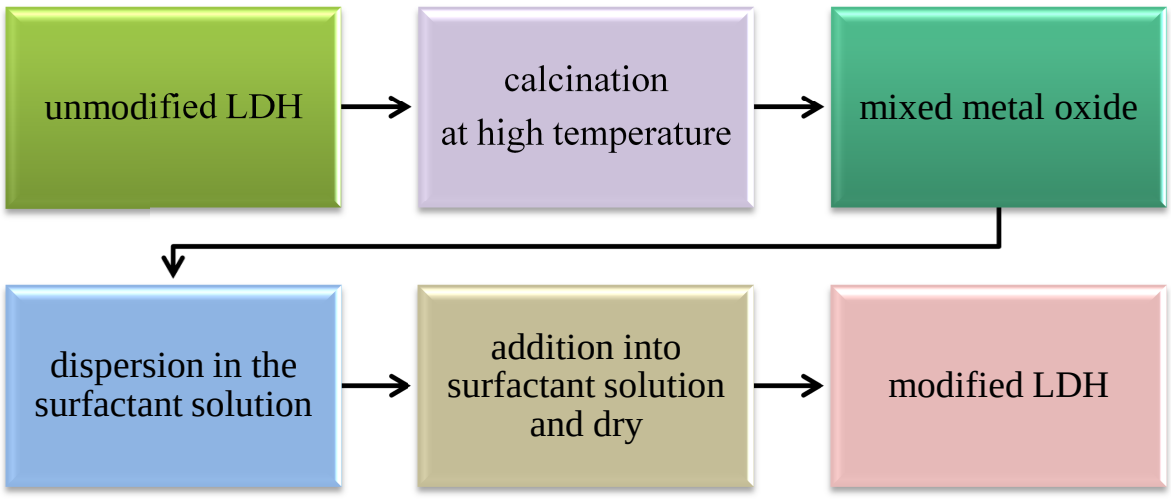

Fig. 2.2 Flowchart of the process to modify LDH

As discussed in the above paragraph, modification of the LDH is necessary in order to get more intercalated and sometimes exfoliated morphology of the layered crystalline particles. By proper modification a large LDH particle can be dissociated into several thousand single layers resulting into a good degree of rubber-filler interactions. Thus, the rubber matrix is reinforced and it can offer enhanced mechanical properties. For these reasons some organic anionic compounds are incorporated into the interlayers in between the layered double hydroxides sheets to increase the gallery gap. This enhancement of the gallery width facilitates the intercalation of the rubber chains. Mostly, till date, either Zn-Al LDH [10-12] or Mg-Al LDH [11, 44-47] has been modified by the incorporation of carbonate (CO_3^{2-}), sulfonate (dodecyl benzene sulfonate), sulfate (dodecyl sulfate) or stearate atoms etc. to be used with various elastomers like carboxylated nitrile buta di-ene rubber (XNBR), ethylene propylene di-ene monomer rubber (EPDM), chloroprene rubber, solution styrene buta di-ene rubber (SSBR), nitrile rubber (NBR), silicone rubber etc.

2.1.1.3 Applications of LDH

Layered double hydroxides (LDH) being a multi-functional filler has various applications in rubber composites. The complete range of the fields of application of LDH is exhibited in Fig. 2.3. Some of the key areas of the applications are as follows:

i. Reinforcing agent

The reinforcing nature of layered double hydroxides has been explored to a great extent with different polar and non-polar rubbers [44, 47]. High aspect ratio and the anisotropic nature of this inorganic layered material make it a suitable candidate to be considered as reinforcing filler for elastomers.

ii. Zinc activator for sulfur vulcanization

The role of layered double hydroxide as the essential curing additives in rubber compounding is extensively studied. Due to some issues by European Union, the use of zinc oxide in the rubber compounding is restricted. Zinc oxide, being a very important additive in sulfur vulcanization of rubbers needs to be substituted by a chemical which will not compromise with the mechanical properties of the composite. LDH, especially Zn-Al LDH showed an enormous potential as a suitable replacement in this regard [10-11]. This LDH material not only cures the rubbers to a great extent but also imparts reasonably higher mechanical properties to the rubbers.

iii. Transparent elastomers (including thermotropic character)

Transparent elastomeric composite based on LDH and solution styrene butadiene rubber (SSBR) was successfully prepared for optical applications [48]. Reversible thermotropic nature of LDH in the rubber is also studied. Fabrication of smart materials like temperature sensors for automobile tyres or flexible organic light-emitting diode (OLED) is possible with such a novel thermoreversible transparent rubber composite

iv. Flame retardant rubber composites

Higher loading of layered double hydroxides into rubbers leads to flame retardant rubber composites [49]. The virtue of being flame retardant in nature makes LDH a very promising candidate for industries. The conventional flame retardants available in the market are either very toxic for environments or expensive. LDH takes care of both these issues. LDH based rubber compounds find applications in various electrical fields like conduits, cables etc.

Fig. 2.3 LDH as multi-functional filler for rubbers

2.1.1.4 Commercial manufacturers of LDH

Versatility in functionalities and chemical structures makes LDH robust materials to gain considerable interests for the industries. A few companies produce layered double hydroxides

all over the world under different trade names. These commercial products have a wide range of applications. A short list is provided in Table 2.1.

Table 2.1 Manufacturers, types and applications of commercial grades of LDHs

Manufacturers	Type of LDH	Trade name	Typical applications
Akzonobel, The Netherlands	Mg-Al LDH	PERKALITE	Flame retardant
Süd-Chemie AG, Germany	Mg-Al LDH	SORBACID, HYCITE	Eco-friendly stabilizer
Sasol Germany GmbH	Mg-Al LDH	PURAL, CATAPAL, DISPERAL, DISPAL	Food packaging, polymer additives
Kisuma Chemicals BV, The Netherlands	Mg-Al LDH Zn-Al LDH	Alcamizer, DHT-4A	Heat stabilizer, Acid scavenger

It is worthy to mention that both the existing and new chemical industries are approaching towards manufacturing LDH filled polymers recently because of the unique features of the compounds in various applications.

2.1.2 Zinc oxide and zinc peroxide

Zinc oxide is an amphoteric oxide. Zincite mineral is the source of naturally occurring zinc oxide. A couple of metallurgical processes based on roasting of zincite ore, direct (American) process and indirect (French) process are widely used over the years. Zinc oxide is termed type A obtained by the former process and type B obtained by the later process [50]. In the direct process, the zincite ore is reduced by heating at elevated temperature with the help of anthracite coal followed by the oxidation of zinc vapor in the same reactor, in a single production cycle. The resulting zinc oxide obtained by this process often contains impurities consisting of other metal compounds. On the other hand, in the indirect process, metallic zinc is treated at very higher temperature of 900°C. Therefore, it is melted and subsequently vaporized. The vapor of metallic zinc reacts with oxygen in the air to produce zinc oxide. Then the particles are cooled down and collected in bag filters. Zinc oxide particles obtained by indirect process has superior purity than the particles obtained by direct process. Laboratory synthesis of zinc oxide is scaled up by mechano-chemical process to obtain both

micro and nanoparticles [50]. Relatively low cost of production, narrow distribution of particle size and high degree of homogeneity and crystallinity are the prime advantages of this process. The precursor materials utilized in this process are anhydrous $ZnCl_2$ and Na_2CO_3. Reaction of these two anhydrous chemicals yields NaCl (reaction 1). NaCl primarily serves as a reaction medium and separates the nanoparticles as well. $ZnCO_3$ formed from the reaction is milled in a ball mill and then calcined at a temperature of 400–800 °C in a furnace (reaction 2). Nano (20-40 nm) zinc oxide particles of white colour are produced by this process.

$$ZnCl_2 + Na_2CO_3 \longrightarrow ZnCO_3 + 2\,NaCl \quad (1)$$

$$ZnCO_3 \xrightarrow{400\text{-}800°C} ZnO + CO_2 \quad (2)$$

Various others chemical synthesis techniques e.g., controlled precipitation route ($ZnSO_4$ precursor), sol-gel route (zinc-2-ethylhexanoate or zinc acetate dehydrate as precursors), solvo-thermal and hydrothermal route ($ZnCl_2$ or $Zn(OH)_2$ precursors) etc. are also employed commercially to produce micro or nano zinc oxide. Owing to possess unique physical and chemical features, zinc oxide is widely consumed globally in diversified areas. Even though, mostly consumed in rubber industries as an additive, zinc oxide finds applications in other fields as well like components of cosmetics in pharmaceutical and cosmetic industries, absorber of UV radiation in textile industries, semiconductors and photo-electronic goods in solar and electronic industries etc. [50, 51].

Zinc peroxide (ZnO_2) has been a preferred accelerator over the years in the vulcanization of polysulphide rubber especially for nitrile rubber compounds in order to produce oil and aging resistant rubber products like sealants, tubes, rollings, etc. Zinc peroxide compounds are utilized as curing agents in XNBR by forming metal carboxylate bonds. Zinc peroxide cured nitrile rubber compounds are observed to have improved scorch resistance and storage stability. Zinc peroxide also seems to function as an oxidant and oxygen donor in compositions or mixtures containing explosive materials. This inorganic powder is yellow in appearance and normally chemically synthesized by the reaction of zinc chloride and hydrogen peroxide. Zinc peroxide finds applications in medical use as a special drug for curing of swollen prepuce. It is also used in the blowing composition in manufacturing a foamed object of high-melting resin e.g., polyesters, polycarbonates, polyamides etc.

2.1.3 Zinc chloride

Zinc chloride is a white powder known to be extremely hygroscopic and deliquescent in nature. This crystalline inorganic salt is extracted from the naturally occurring mineral simonkolleite ($Zn_5(OH)_8Cl_2.H_2O$). The synthesis route of zinc chloride in the laboratory is revealed with the help of reaction 3 as follows:

$$Zn + 2\,HCl \longrightarrow ZnCl_2 + H_2 \uparrow \qquad (3)$$

At first scrap zinc or roasted zinc or raw zinc oxide is heated in hydrochloric acid. Hydrogen gas is removed by this reaction. The zinc chloride solution obtained this way is usually purified by the means of several ways, depending on the percentage of impurities in the starting material. Iron (Fe) and manganese (Mn) can be precipitated as oxides by the addition of zinc oxide or sodium hypochlorite. Heavy metals are normally removed with the help of zinc powder. The solution is then concentrated by boiling and hydrochloric acid is added to prevent the formation of basic chlorides. Zinc chloride finds applications in dental fillings and mouthwash liquid due to its potential as a metallurgical flux. Zinc chloride is also a very common source of Lewis acid catalyst for many organic syntheses like Fischer indole synthesis and Friedel-Crafts acylation reaction. Others applications of this inorganic compound have been observed in textile processing, antiseptic products, deodorants, disinfecting fluid materials, smoke grenades etc. Zinc chloride is a relatively less explored curing agent for nitrile rubber compared to other zinc salts. Crosslinking process induced by the coordination bonding between zinc and polar groups of nitrile rubber made this inorganic compound a very interesting candidate to be considered in rubber processing [36].

2.2 Overview of XNBR – zinc based LDH composites

Carboxylated acrylonitrile buta di-ene rubber or carboxylated nitrile rubber (XNBR) is a special type of modified form of nitrile buta di-ene rubber. These types of rubbers generally contain one or more acrylic type of acid as a terpolymer. So basically the resultant chain is almost identical to nitrile rubber except with the existence of carboxyl functionalities occurring about every 100 to 200 carbon atoms. This modification improves several properties like enhanced abrasion resistance, higher tensile and tear strength, improved hardness, improved low temperature brittleness and better retention of the physical properties

after hot-oil and air ageing when compared to pristine nitrile rubber. Despite being a very promising polar synthetic rubber based on the impressive properties listed above, there has been very limited number of studies on XNBR and LDH. LDH being multi-functional filler can potentially be a very interesting candidate to be explored with XNBR.

2.2.1 Curing properties

The curing characteristic of both Mg-Al LDH [44, 46, 49] and Zn-Al LDH [10, 12, 52-53] have been investigated. Laskowska *et al* [39] reported that hydrotalcites (Mg-Al LDH) can cure the XNBR efficiently without the presence of conventional curing additives in the compounds. Curing curves displays gradual increase in the torque values with the addition of hydrotalcite (2.5, 5, 10, 20, 30 phr) in XNBR. The increase in the crosslink density primarily enhances the torque values of the composites.

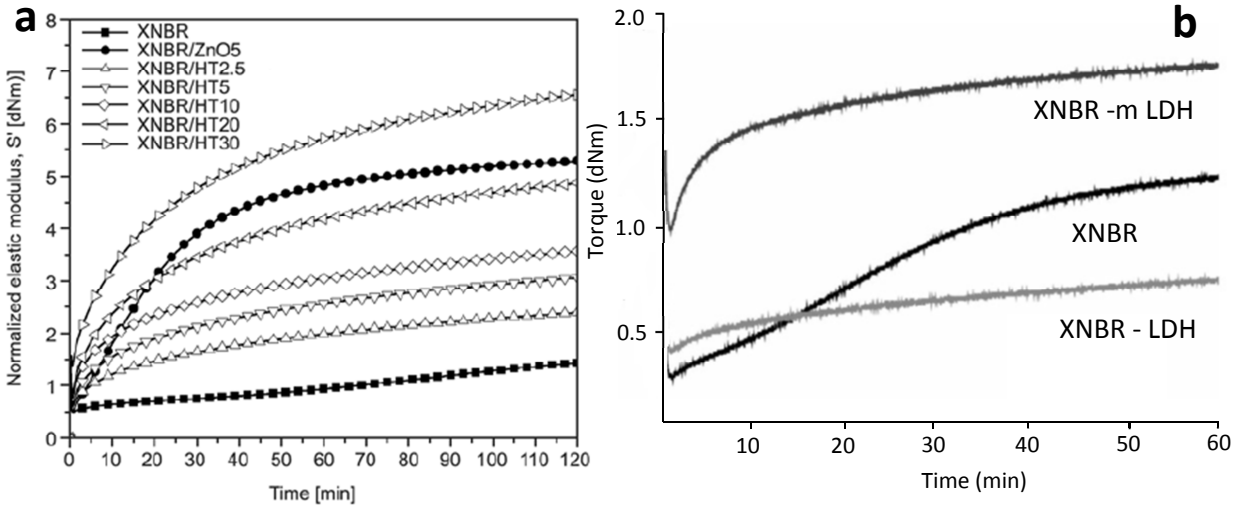

Fig. 2.4 Rheometric torque-time plots of (a) XNBR – Mg-Al LDH composites [49], (b) XNBR – Zn-Al LDH composites [53]

The scorch time was also claimed to be shorter for the hydrotalcite cured rubber compounds than the ZnO cured compounds (XNBR/ZnO 5). However a steady plateau for the hydrotalcite (HT) cured XNBR samples was reached slower than the samples cured with ZnO (Fig. 2.4a).

Fig. 2.4b exhibits the torque-time plot of XNBR cured with unmodified LDH and modified LDH (modified with surfactant SDBS). The abrupt increase in the torque value of pristine XNBR after certain time (~ 10 min) is attributed to the self-healing phenomenon of XNBR due to the formation of anhydride linkage at 160°C [54-55]. LDH, as obvious from Fig. 2.4b, suppresses the formation of such anhydride bonds and consequently, the torque value drops

down. After suitable modification, due to the increase in the gallery gap of the LDH molecule, intercalation of XNBR chains take place and eventually the torque value increases to a great extent.

2.2.2 Mechanical properties

Fig. 2.5 depicts the mechanical properties of XNBR compounds cured with two different types of LDH materials, Mg-Al LDH and Zn-Al LDH. It is quite clear from Fig. 2.5a that the addition of Mg-Al LDH modified with surfactant sodium-1-decanesulfonate has a strong impact on the mechanical properties of the corresponding rubber composites. As the amount of modified LDH increases, the stress-strain values increase as well. The successful intercalation of the XNBR chains into the interlayer galleries of the surfactant modified LDH

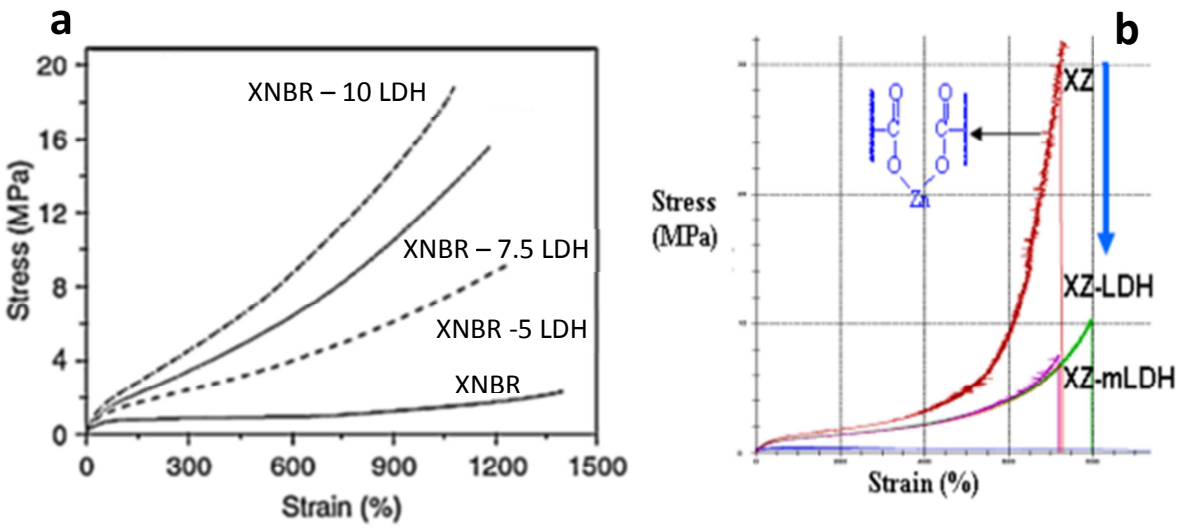

Fig. 2.5 Stress-strain plots (a) XNBR – Mg-Al LDH composites [46], (b) XNBR – Zn-Al LDH composites [53]

molecule reinforces the rubber matrix [36]. The polar-ionic interaction between XNBR and the modified LDH is also attributed to the enhancement of the mechanical properties of the composites.

Thakur *et al* [53] investigated the role of Zn-Al LDH in the ionic crosslinking nature of XNBR molecules which is very common with zinc oxide. As Fig. 2.5b suggests, Zn-Al LDH was reported to decrease the tensile properties of the composites by the virtue of inhibiting the formation of ionic cluster between the carboxylic group of XNBR and zinc ion from LDH molecule.

The phenomena of strain-induced crystallization and limited chain extensibility were explored intensively by Costa *et al* for the XNBR – LDH composites [44, 46]. Presence of LDH nanoparticles along with relatively larger amount of anionic surfactant molecules at the rubber – filler interface favors orientation of rubber chains during elongation. However, according to this work, this effect is only clearly visible in the case of LDH modified with sodium-1-decanesulfonate, whereas modification of XNBR with 1-hexadecanesulfonate, which has 16 carbon atoms, does not yield any strain-induced crystallization.

2.2.3 Flame retardancy

Layered Double Hydroxides (LDH) due to its unique chemical structure, showed a lot of promise as a halogen free flame retardant material. The presence of water molecules in the interlayer galleries of LDHs facilitates fire retardancy. Although the detailed flame retardant mechanism of LDH is not being known till date, speculations are being made that the condensed phase of flame retardant LDH material would form reinforced char layers during combustion, leading to the low volatiles produced. On the other side, another flame retardant mechanism was proposed based on the cooling and dilution effect from the released water during crosslinking reaction and the produced inflammable gas during the carbonaceous procedures, respectively.

As of now, very few numbers of literatures [52, 56] are available on rubber – LDH composites exploring the flame retardancy aspect. Certain part of this thesis is devoted to investigate the role of LDH (Zn-Al LDH) as potential flame retardant filler for XNBR.

2.3 XNBR and zinc based ionic elastomers

Typically, carboxyl-based ionic elastomers are obtained by direct copolymerization of relatively small amount of acrylic or methacrylic acid with ethylene or styrene by free radical copolymerization. For instance, XNBR molecules contain acrylonitrile buta di-ene random copolymer with usually 7-8 % carboxylic functionalities incorporated to the hydrocarbon chains. The carboxylic acid groups of XNBR are neutralized during vulcanization to the desired extent with different types of metal oxides [14, 16, 57-60], metal peroxides [59, 61-62] and similar kind of salts. The pristine XNBR rubber after vulcanized with divalent metal oxide like zinc oxide yields very high green strength as compared to sulfur-vulcanized buta di-ene elastomers. It is evident now courtesy to a good volume of research works that the final

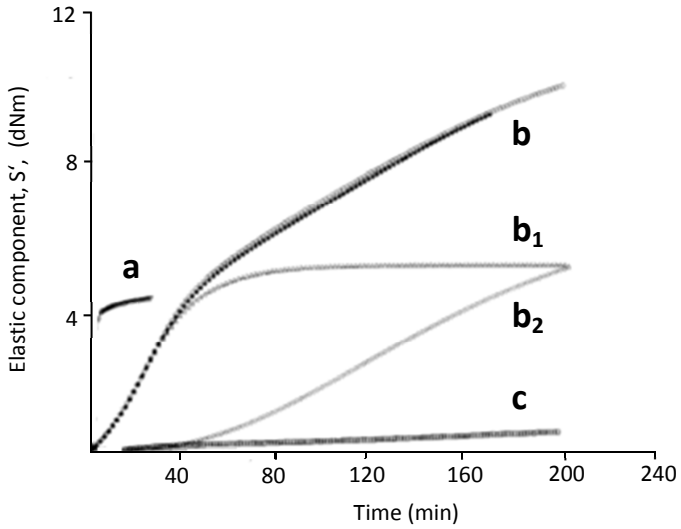

Fig. 2.6 Torque-time plots of (a) XNBR – ZnO system, (b) XNBR – ZnO – Zinc peroxide system ($b=b_1+b_2$) and (c) NBR – ZnO – Zinc peroxide system [59]

product after neutralization is a mixture of some free acid and mixed salts. As a consequence, the final product displays fluidity at higher temperature, extra dynamic relaxation at elevated temperature, high stress relaxation and poor compression set. These properties are quite consistent with the chemically combined crosslinks along with secondary bonding due to the obvious ionic association.

Different mechanistic pathways have been explored by Ibarra *et al* [59] in case of curing XNBR with the combined presence of zinc oxide and zinc peroxide. XNBR when cured with only zinc oxide, a single maximum (Fig. 2.6a) was found attributing to the improvement on the ordering on the ionic groups associated with carboxylic functionalities of XNBR and zinc atom from zinc oxide. On the other hand, XNBR when cured with the combined presence of zinc oxide and zinc peroxide, some covalent crosslinking has also been achieved along with the ionic association. Henceforth, the rheometric curve was observed to be splitting into two contributions (Fig. $2.6b_1$ and $2.6b_2$). In case of NBR, the catalytic activity supposedly available from the carboxylic acid group of XNBR is absent. As a result, no ionic crosslinking would take place. Therefore, the curing behavior of NBR – ZnO – zinc peroxide is quite different from the curing behavior of XNBR – ZnO – zinc peroxide (Fig. 2.6c). NBR in this case is reported to be only cured by zinc peroxide forming covalent crosslinking points [59].

Ionic elastomers formed by XNBR and zinc oxide are known to show unique dynamic behavior. An extra high temperature transition peak is usually observed in dynamic mechanical analysis for such kinds of ionomers. Zinc carboxylate which is formed as an ionic

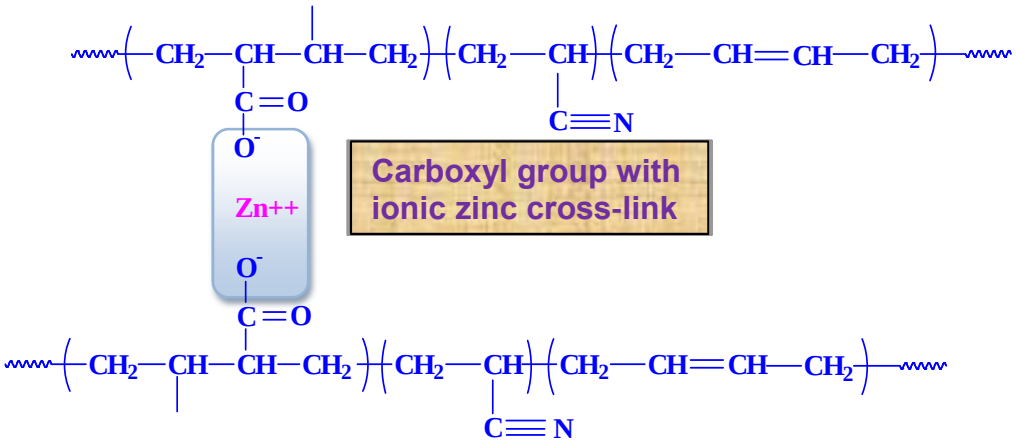

Fig. 2.7 Chemical structure of ionic zinc carboxylate by the reaction of zinc and carboxylic group

aggregate due to the association of zinc and carboxylic group (Fig. 2.7) is believed to be primarily responsible to form a phase separated region in the matrix [14, 16]. Therefore, an additional glass transition like behavior at elevated temperature is obtained for such compounds [14]. Ammonia is believed to act as a plasticizer which can chemically dissolve and break the ionic association and thus resulting in the disappearance of the high temperature transition peak in the dynamic mechanical spectra.

Results based on mechanical stress-strain are in excellent conformity with those of dynamic mechanical analysis. It is noticed that the ionic elastomers based on XNBR and zinc oxide usually show enhanced tensile strength, stress at 100% and 200% strains, tear strength, hardness, abrasion resistance compared to the green rubber.

Thermo-shrinkable nature of XNBR with zinc oxide is also explored [63]. Ionic crosslinking points generated during the curing process of XNBR with nano-sized zinc oxide particles served as memory points and increases the heat shrinkability. The XNBR vulcanizates revealed thermo-shrinkability to almost 50% and the percentage of shape recovery was reported to be in the range of 90-100%. The thermo-shrinkability value and shape recovery ratio had a very obvious correlation with the percentage ionic crosslink of the elastomer network. The ionic crosslinks density was reduced by heating the samples above their ionic transition temperature. Higher ionic crosslink density and their more significant decomposition corresponded to vulcanizates with greater thermo-shrinkability.

The influence of particle size of zinc oxide while mixed with XNBR on the crosslinking process was also explored by Przybyszewska *et al* [64]. In their study, it is claimed that the

morphological feature of the different nanosized zinc oxide dispersed in the XNBR matrix have remarkable influences on the ultimate mechanical and dynamic properties of the rubber composites. Zinc oxide nanoparticles in aggregate form (130 nm to 2700 nm) were compounded with XNBR and the morphological investigations revealed that the zinc oxide with flake morphology produced the most interesting results. The outcome of the research by this group also suggests that the usage of zinc oxide could well be reduced upto ~ 40% if nanosized zinc oxide is used in the vulcanization recipe of di-ene rubber instead of microsized zinc oxide so far commonly practised in the industries. It is also realized in this work that the nanosized zinc oxide particles substantially increased the tensile strength of the vulcanizates as compared to the microsized zinc oxide particles (Fig. 2.8a). The enhancement in the mechanical properties of the rubber compounds with the increase of zinc oxide amount attributes to the increase in the ionic crosslink content in the elastomer network. Ionic clusters generated in such compounds are capable to mobilize to the surface of the zinc oxide particles which eventually accounts for the higher ability for stress relaxation, and as a result, enhancement in mechanical strength was obvious for the corresponding rubber vulcanizates.

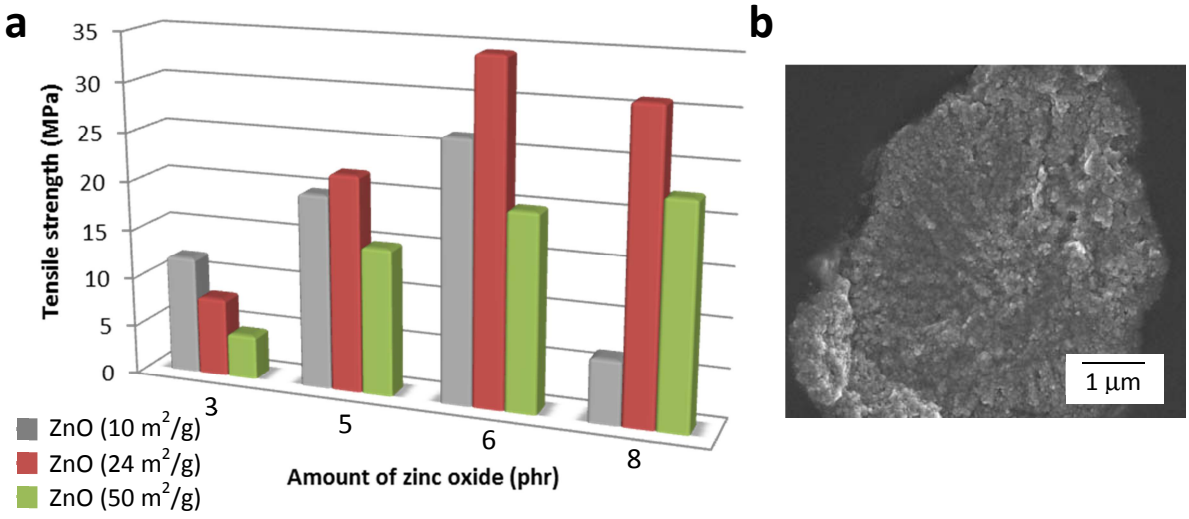

Fig. 2.8 (a) Mechanical properties of XNBR vulcanizates cured with nanosized zinc oxide, (b) SEM micrograph of XNBR vulcanizate cured with zinc oxide (surface area ~ 50 m^2/g) [64]

Nevertheless, the higher surface area of the zinc oxide nano particles (~ 50 m^2/g) leads to microsized agglomerate for the corresponding XNBR compound and needless to say, this morphological feature would influence the crosslinking nature of the vulcanizates to some degree.

Role of XNBR based ionomer is also explored in the lights of self-healing, a unique phenomenon mimicked from nature. Ionic association created between the zinc source and the polar elastomer matrix leads to microphase separation and such phenomenon is accountable for a thermally reversible network. The crosslinking network caused by the ionic association provides dynamic bonds in the system which generates self-healing nature in the compounds. Hohlbine *et al* [65] prepared a promising self-healing elastomer compound based on XNBR matrix which showed some remarkable mechanical, thermal and dynamic properties. The dynamic shear storage (G') and loss (G'') moduli are calculated using an oscillatory parallel plates rheometer of diameter 40 mm and a gap of 1.0 mm with a frequency sweep from 3.14 to 628 rad/s at 25 ºC with 2% strain level. In the Zn^{2+} based ionomer synthesized by Hohlbine *et al*, temperature-dependent dynamic mechanical study clearly demonstrates a positive shift of the crossover point towards higher frequencies at elevated temperature, whereas a shift of the ionic transition (revealed by a sharp increase of tan δ values) to higher temperatures with increasing frequency (Fig. 2.9a) was also evident.

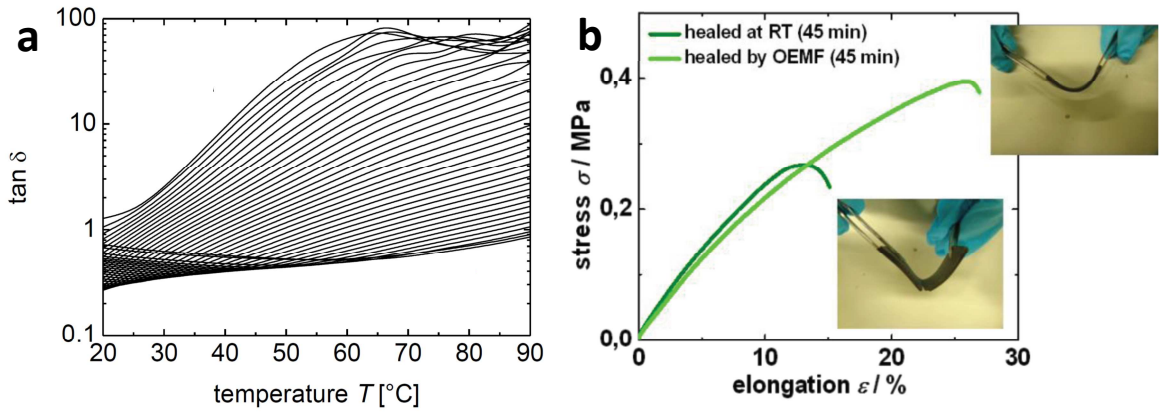

Fig. 2.9 (a) Dynamic mechanical behavior, (b) mechanical properties of healed at ambient conditions in presence or absence of magnetic field of Zn^{2+} based ionomer (RT= Room temperature, OEMF = Oscillating electromagnetic field) [65]

Influence of magnetic nanoparticles incorporated into the XNBR matrix is realized on the mechanical properties. The stress-strain plot, shown in Fig. 2.9b, suggests that approximately 100% recovery of the original elongation at break is possible to achieve for the Zn based XNBR ionomer healed at 55°C temperature.

Chapter 3

Experimental

3.1 Materials

3.1.1 Elastomers

In this study, apart from nitrile rubber (NBR), one modified form i.e., carboxylated nitrile buta di-ene rubber (XNBR) has been mostly used to explore various properties.

3.1.1.1 Acrylonitrile buta di-ene rubber (NBR)

Acrylonitrile buta di-ene rubber (NBR), popularly known as nitrile rubber is also used in this study. This grade of rubber selected is NBR Krynac 1846 F and kindly supplied by Lanxess, Germany. The specification of this grade of NBR is supplied in Table 3.1. The chemical structure of NBR is exhibited in Fig. 3.1.

Table 3.1 Various specification of NBR Krynac 1846 F

Properties	Value
Mooney viscosity ML (1+4) 100°C	46 ± 5
Acrylonitrile content (max, wt %)	18.5 ± 1.5
Volatile matter (max, wt %)	0.5
Specific gravity (g/cm^3)	1.01
Total ash (max, wt %)	0.7

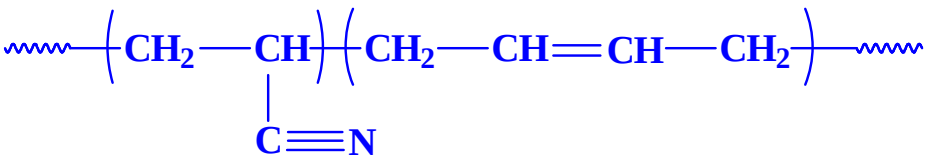

Fig. 3.1 Chemical structure of NBR

3.1.1.2 Carboxylated nitrile buta di-ene rubber (XNBR)

The elastomer used in this thesis work is mainly carboxylated nitrile buta di-ene rubber (XNBR). The grade used in this study is Krynac X 740 supplied by Lanxess, Germany. Various properties of XNBR are supplied in Table 3.2. The chemical structure of XNBR is exhibited in Fig. 3.2.

Table 3.2 Various specification of XNBR Krynac X 740

Properties	Value
Mooney viscosity ML (1+4) 100°C	38 ± 4
Acrylonitrile content (max, wt %)	26.5 ± 1.5
Carboxylic acid content (max, wt %)	7%
Volatile matter (max, wt %)	0.5
Specific gravity (g/cm^3)	0.99
Molecular weight (M_n) (g/mol)	1.7×10^5
Polydispersity index (M_w/M_n)	3.6

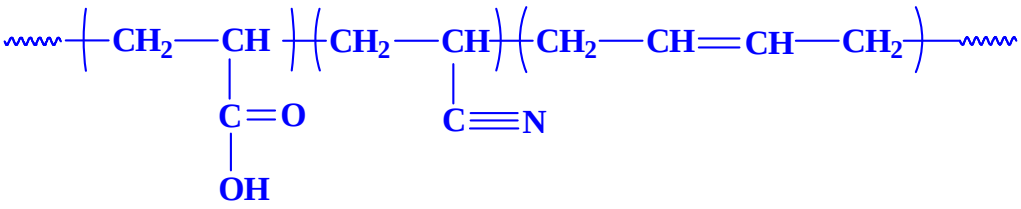

Fig. 3.2 Chemical structure of XNBR

3.1.2 Filler materials

3.1.2.1 Layered double hydroxides (LDH)

Layered double hydroxides, especially Zn-Al LDH used in this study were mainly of commercial sources. Small amount of Mg-Al LDH used for a specific part of the study was synthesized in the laboratory of IPF, Dresden. Unmodified Zn-Al LDH was supplied by Kisuma Chemicals BV, The Netherlands. The specifications of the commercially available LDH are supplied in Table 3.3.

Table 3.3 Specifications of unmodified Zn-Al LDH

Description	Unmodified Zn-Al LDH
Product trade name	Alcamizer P93
Manufacturer	Kisuma Chemicals, The Netherlands
Chemical formula	$Mg_{3.5}Zn_{0.5}Al_2(OH)_{12}CO_3.3H_2O$
Zn^{+2} / Al^{+3}	1:4
Loss on drying (105°C, 1 h)	0.3%
Specific gravity (g/ml)	2.3
BET surface area (m^2/g)	8
Average particle size (μm)	0.5

Unmodified Mg-Al LDH was synthesized in the laboratory by urea hydrolysis method. 0.5 M aqueous solution containing Al^{3+} and Mg^{2+} ions with the molar fraction Al^{3+}/ (Al^{3+} + Mg^{2+}) equal to 0.33 was prepared by dissolving $AlCl_3$ and $MgCl_2$ in distilled water. Solid urea was then added into this solution until the molar fraction urea/ (Mg^{2+} + Al^{3+}) reached 3.3. Next, the transparent solution was refluxed for 36 h. The white precipitate was then filtered, washed until chloride free and dried at 60 °C till constant weight.

3.1.3 Curing additives

Apart from Zn-Al LDH, other zinc sources are used in this study. Commercial grades of zinc oxide (purity ~ 99.5 %), was bought from ACROS Organics, Belgium whereas, zinc stearate (purity ~ 98%), and zinc chloride (purity ~ 99%) were bought from Sigma Aldrich. Stearic acid and sulfur both of general purpose grade were purchased from Fisher Scientific GmbH, Schwerte, Germany. The curing accelerator, tetramethyl thiuram disulfide (TMTD) (purity ~ 97%) was obtained from Lanxess, Germany.

3.2 Preparation of rubber composites

The rubber composites were prepared by mixing the raw rubbers with different filler materials and curing additives. Usually, incorporation of higher amounts of fillers or masterbatches are prepared in the internal mixer. The curing additives then are mixed in the two-roll mill.

Albeit, relatively lower amount of fillers are sometimes well managed to mix and homogenize in the two-roll mill.

3.2.1 Compounding

In rubber technology, compounding is defined by the process by which composition is obtained by adding an elastomer to other essential ingredients and blending to produce a homogeneous mixture or mix.

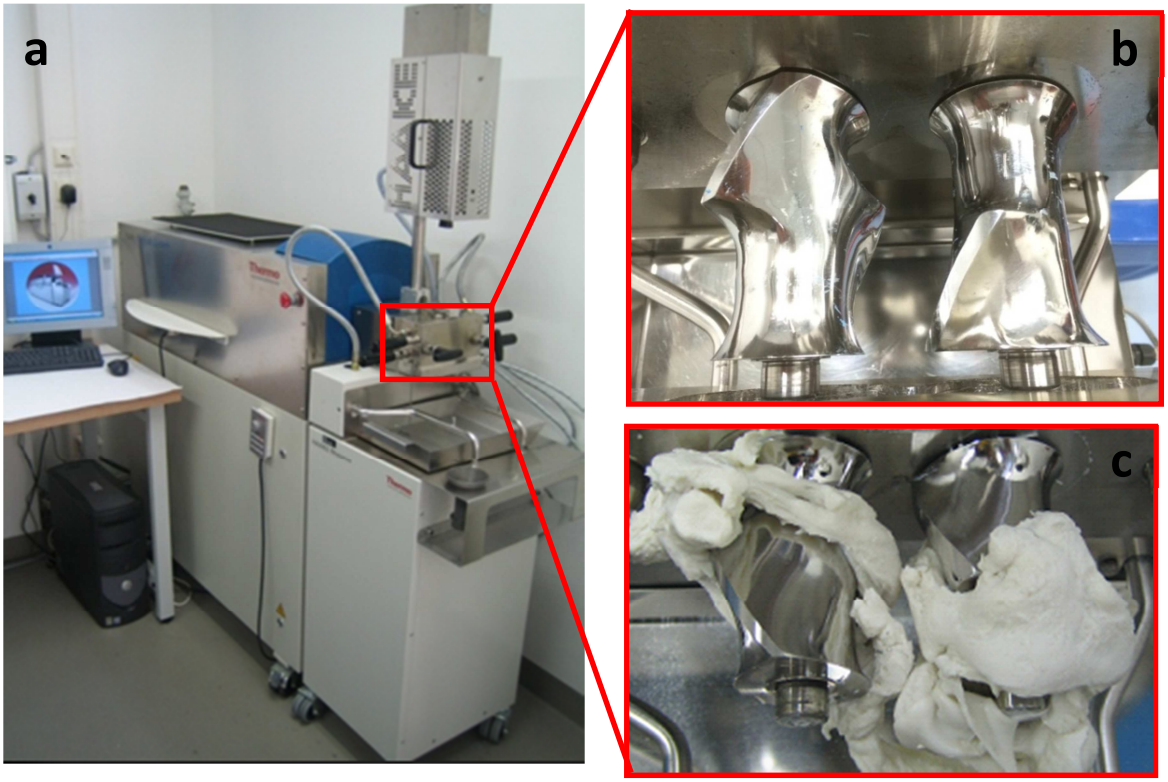

Fig. 3.3 (a) Haake internal mixer, (b) Banbury (tangential type) rotors, (c) rubber mixed by the rotors

3.2.1.1 Internal Mixer

Relatively larger amounts of fillers are incorporated into rubbers by internal mixer. Masterbatches are also prepared by using the same machine. A typical internal mixer, Haake Rheomix, Thermo Electron GmbH, Karlsruhe, Germany is exhibited in Fig. 3.3. Usually, for mixing rubber compounds, banubury types of rotors (Fig. 3.3b) are used. 40 phr and 100 phr of LDH material is incorporated into XNBR with the help of internal mixer. The raw XNBR and required amount of LDH (40 and 100 phr) were mixed at fixed rotor speed of 60 rpm and temperature of 70°C. The samples were mixed in the internal mixer for 15 min. Then the mass

was removed and allowed to cool at room temperature. The formulation of the corresponding rubber compounds are provided in Table 3.4.

Table 3.4 Formulations of XNBR – ZnO and XNBR – LDH composites

Sample designation	XNBR	Sulfur	TMTD	LDH	ZnO	Stearic acid
	(all in parts per hundred rubber)					
XNBR – 4 ZnO	100	0.5	1.0	0	4	1.0
XNBR – 4 LDH	100	0.5	1.0	4	0	1.0
XNBR – 10 LDH	100	0.5	1.0	10	0	1.0
XNBR – 40 LDH	100	0.5	1.0	40	0	1.0
XNBR – 100 LDH	100	0.5	1.0	100	0	1.0

Ionic elastomers formed by the compounding of XNBR with zinc oxide were further explored. Keeping the amount of zinc oxide fixed in each composite, zinc stearate was added in various concentrations. The specification of the commercial zinc stearate used in this study

Table 3.5 Formulations of XNBR-ZnO-zinc stearate compounds

Sample designation	XNBR	ZnO	Zinc stearate	Stearic acid
XNBR – 5 ZnO – 5 ZnSt	100	5	5	
XNBR – 5 ZnO – 10 ZnSt	100	5	10	
XNBR – 5 ZnO – 15 ZnSt	100	5	15	
XNBR – 5 ZnO – 20 ZnSt	100	5	20	
XNBR – 5 ZnO – 30 ZnSt	100	5	30	
XNBR – 5 ZnO – 40 ZnSt	100	5	40	
XNBR – 5 ZnO – 20 St.acid	100	5		20

Zinc stearate was purchased from Acros organics; M.W:632 g/mol, m.p ~ 118°C-128°C

is provided at the bottom of table 3.5. The details composition of the compounds based on XNBR, zinc oxide and zinc stearate was summarized in table 3.5. All the compounds were

prepared in the two roll mill using the friction ration 1:1.2 between the front and the back roll at 40°C with uniform mixing time (~ 12 min).

3.2.1.2 Two-roll mill

After the samples cooled down after taking out from the internal mixer, they were mixed and homogenized in an open two-roll mill (Polymix 110L, size: 203 x 102 mm^2, Servitec GmbH, Wustermark, Germany). A typical two-roll mill is exhibited in Fig. 3.4. The mixing was carried out at 40°C with the friction ration 1:1.2 between the front and the back roll using a 20

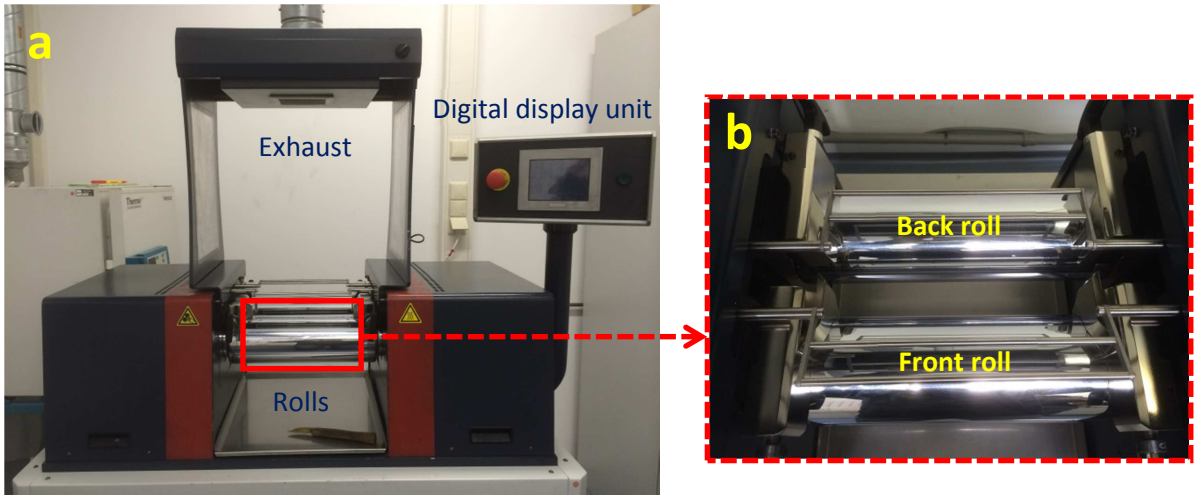

Fig. 3.4 (a) Two-roll laboratory mixing mill, (b) rolls

min compounding cycle. The nip gap between the two rolls was kept at approximately 0.30 mm to ease the processability and better capability of dispersion of the particles into rubber. Basically, the curing additives like zinc oxide and stearic acid, sulfur (wherever applicable), accelerator, were added sequentially to the compounds in the two-roll mill. The formulations of the rubber compounds only prepared with the help of two-roll mill are provided in Table 3.6.

3.2.2 Moulding

The rubber mass obtained after mixing was kept at room temperature for 24 h. Then required amount of sample was weighed (~ 30 g) and kept in the pre-heated mold. The thickness of the compression mold was 2 mm. A typical mold of the dimension of 12 cm x 11 cm x 0.2 cm is exhibited in Fig. 3.5a. The rubbers samples were molded and subsequently cured by a

compression moulding machine (Fortune Holland, Model TP 400) operated by an electrically heated hydraulic press with the optimum curing time (t_{90}). The curing temperature for the rubber samples is 160°C. After the moulding was over, the samples were kept at room temperature for 24 h and cooled down. The samples are now ready for the characterizations. A typical compression moulding machine is displayed in Fig. 3.5b.

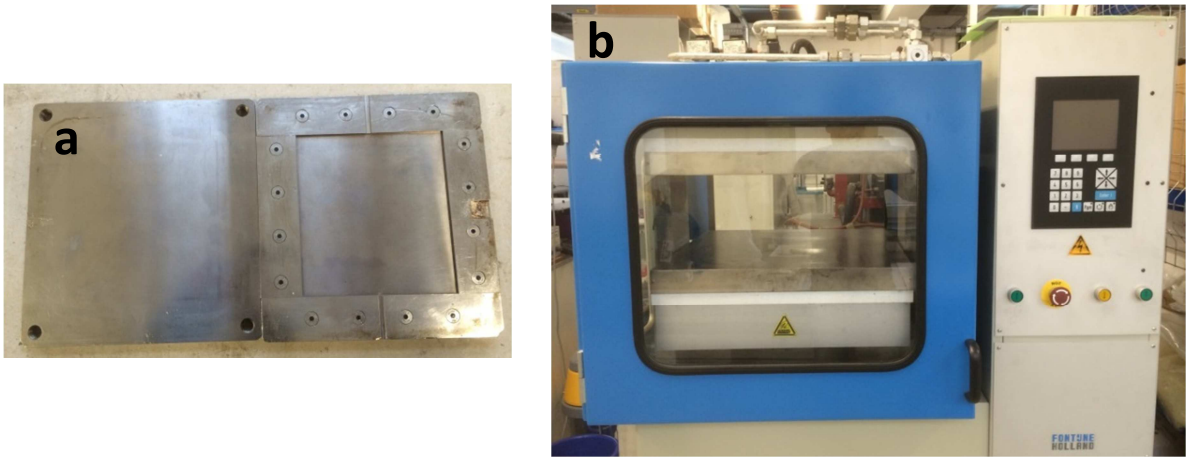

Fig. 3.5 (a) Compression mold (12 cm x 11 cm x 0.2 cm), (b) Compression moulding machine

3.3 Characterization

The rubber compounds prepared by the above processes now are ready to be characterized by the desired tools. The necessary characterization processes are described in the following sub sections.

3.3.1 Curing study

The rubbers compound obtained from two-rill mill post mixing were subjected to curing to determine their optimum curing times and torque-time behavior. Curing analysis was carried out in Scarabaeous SIS-V 50 displayed in Fig. 3.6 in isothermal time sweep mode for all the samples at 160°C for 60 min. In this procedure, an uncured mass (~ 5.5 g) from the compounded rubber was placed in a moving die rheometer (Scraeabaus SIS-V50) under isothermal conditions at 160 °C with a frequency of 1.67 Hz, and the generated torque was

Table 3.6 Formulations of XNBR composites prepared by different zinc compounds in two-roll mill

Sample designation	XNBR	ZnO	LDH	$ZnCl_2$	Sulfur	TMTD	Stearic acid
	(all in parts per hundred rubber)						
XNBR – 4 ZnO - S	100	4			0.5	1.0	2.0
XNBR – 20 ZnO - S	100	20			0.5	1.0	2.0
XNBR – 4 LDH - S	100		4		0.5	1.0	2.0
XNBR – 10 LDH - S	100		10		0.5	1.0	2.0
XNBR – 40 LDH - S	100		40		0.5	1.0	2.0
XNBR – 100 LDH - S	100		100		0.5	1.0	2.0
XNBR – 50 mmol ZnO*	100	4.05			0.5	1.0	2.0
XNBR – 50 mmol LDH*	100		7.25		0.5	1.0	2.0
XNBR – 4 ZnO	100	4					
XNBR – 20 ZnO	100	20					
XNBR – 20 LDH	100		20				
XNBR – 20 $ZnCl_2$	100			20			
XNBR – 4 LDH	100		4				
XNBR – 10 LDH	100		10				
XNBR – 40 LDH	100		40				
XNBR – 100 LDH	100		100				

**In these two compounds the zinc concentration was kept 50 mmol to maintain the amount of zinc at the same level.*

measured against time. From this torque−time curve, the optimum curing time (t_{90}) was calculated as the point at which the rheometric torque reached 90% of its ultimate value.

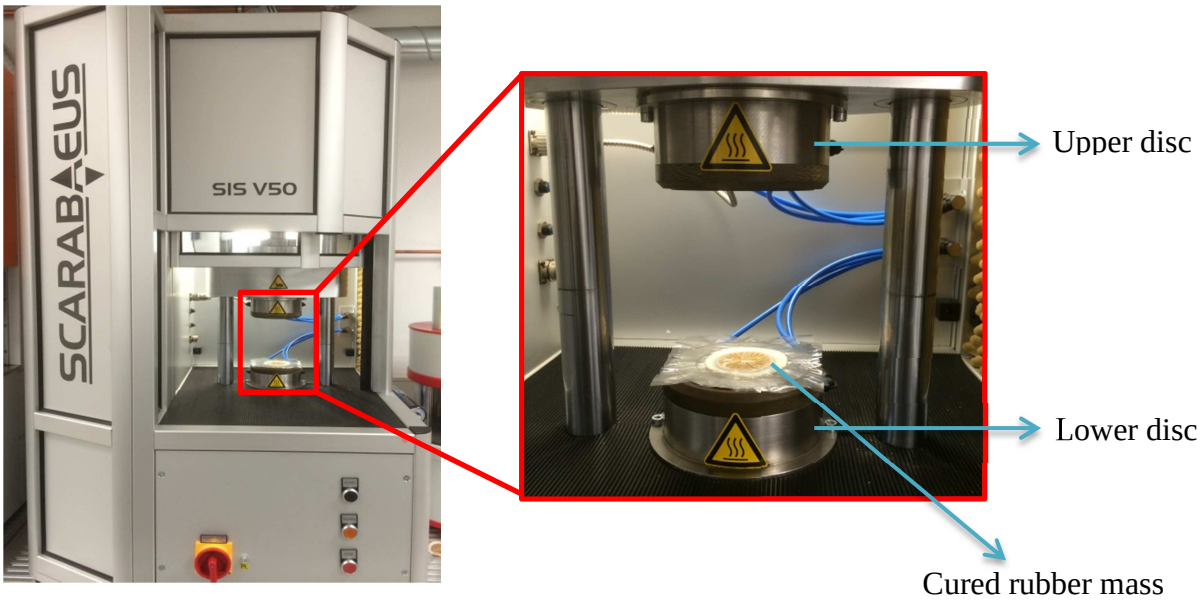

Fig. 3.6 Scarabaeus moving die rheometer

3.3.2 Fourier transform infrared analysis (FTIR)

The Fourier transform infrared (FT-IR) spectra of the samples were obtained using a Bruker Vertex 80 V spectrometer within the wavenumber range of 4000−400 cm^{-1} (Fig. 3.7). The experiment was carried out in the attenuated total reflection (ATR) mode. FTIR spectra at different temperatures were obtained using a heated golden gate in the ATR tool**.**

Fig. 3.7 Vertex 80v coupled with ATR-Golden Gate unit

3.3.3 Tensile test

Tensile tests have been performed with a Zwick 1456 (model 1456, Z010, Ulm Germany) with cross head speed 200 mm/min^{-1} (ISO 527) (Fig. 3.8). Dog-bone shaped samples (minimum 5 samples) were punched out from the rubber specimens to carry out the stress-strain test in tension mode.

Fig. 3.8 Universal tensile machine (UTM) Zwick 1456

3.3.4 Dynamic mechanical analysis (DMA)

Dynamic mechanical properties were measured using a dynamic mechanic thermic spectrometer (DMTS), GABO Eplexor 2000N, operating in tension mode. Therefore, vulcanized sheets were punched out into approximately 35 × 10 × 2 mm^3 rectangles. Storage modulus (E'), loss modulus (E''), and loss factor (tan δ) were recorded at a heating rate of 2 K/min at a test frequency of 10 Hz. Temperatures were swept as per requirement in this mode. Amplitude sweep tests were carried out on the same instrument as displayed in Fig. 3.9a in tension mode at room temperature. The frequency was maintained constant at 10 Hz whereas the static load was kept at 60% strain and the dynamic load was varied from 0.2 to 30 % strain. On the basis of combined temperature/frequency sweep measurements from −60 to +120 °C and 0.5 to 50 Hz, master curves for the frequency behavior of the tested materials were reconstructed, using the master curve software-module of the Eplexor-DMTS. In the mastering process, the measured frequency curves were horizontally shifted according to WLF theory for a reference temperature of 20 °C. Reverse temperature sweep analysis from +150 to −80 °C was performed with the same technique as the forward temperature sweep.

Test of heat build-up of the unaged samples was carried out in accordance with the specification DIN 53533 for the Goodrich flexometer test in the DMA machine (DMA, Eplexor 2000 N, Gabo Qualimeter, Ahlden, Germany). Tests were carried out in compression mode for 25 minutes (Fig. 3.9b). This experiment is carried out to determine the temperature rise at the center and the surface as well as the resistance to fatigue of the vulcanized rubber. A simple single piece, ten-cavity mold was used to make cylindrical rubber specimens having diameters of 17.8 mm and heights of 25.4 mm (DIN 53533-3) (Fig. 3.9c). After confirmation of the center point of the specimen, a small radial hole was drilled at the middle point to measure the amount of heat build-up at the center of the specimen. Very thin k-type

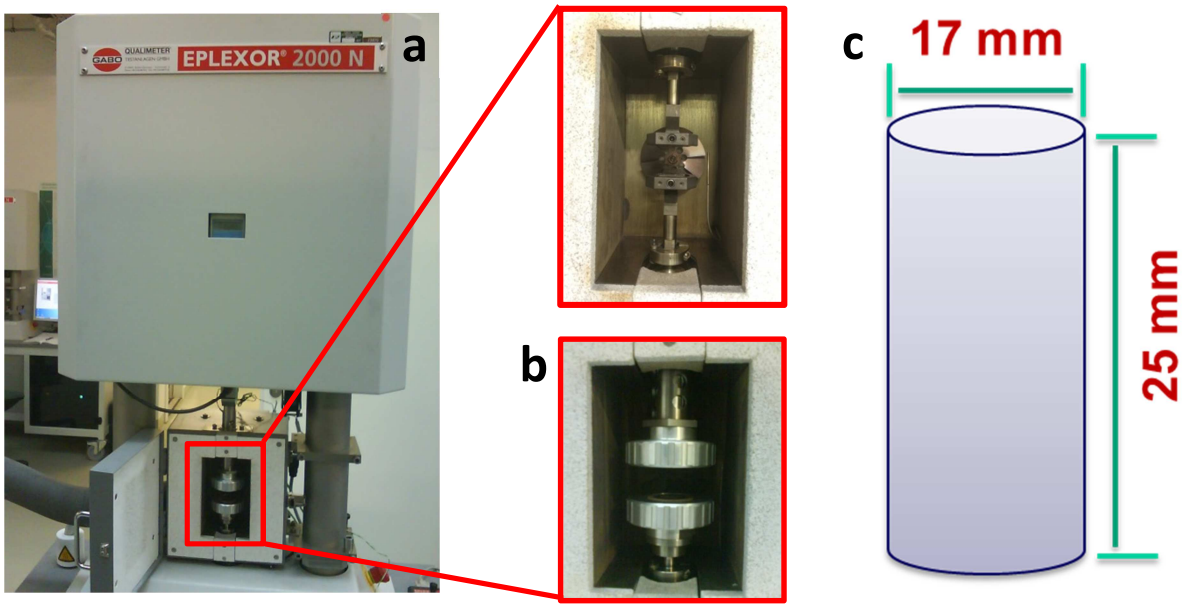

Fig. 3.9 (a) Dynamic mechanical analyzer (Eplexor 2000N), (b) compression mode for heat build-up test, (c) sample dimension for heat build-up test

thermocouples were embedded at the middle point in the cylindrical rubber block. Amount of heat build-up at the surfaces of the specimens were also measured with the help of the thermal sensors adhered to the both top and bottom surfaces of the cylindrical specimens. Compression set of the samples was also calculated from this test. The permanent compression set is defined by the change in height before and after 1 hour of testing of the specimen. The values are measured with the help of a caliper.

3.3.5 Thermal analysis (TGA and DSC)

Thermogravimetric analysis (TGA) was carried out using thermogravimetric analyser TGA Q 5000, TA instruments, USA (Fig. 3.10a). Samples were placed on a platinum pan and heated

in the temperature range 30–950 °C under nitrogen atmosphere at a heating rate of 10 K/min. At the end, heating was continued for half an hour in air for complete combustion of the polymers.

Differential scanning calorimetry (DSC) study was carried out for all the samples using Q1000 , TA Instruments, USA (Fig. 3.10b) coupled with an autosampler in the temperature range of −50 to +150 °C at the scanning rate of 10 K/min under nitrogen atmosphere.

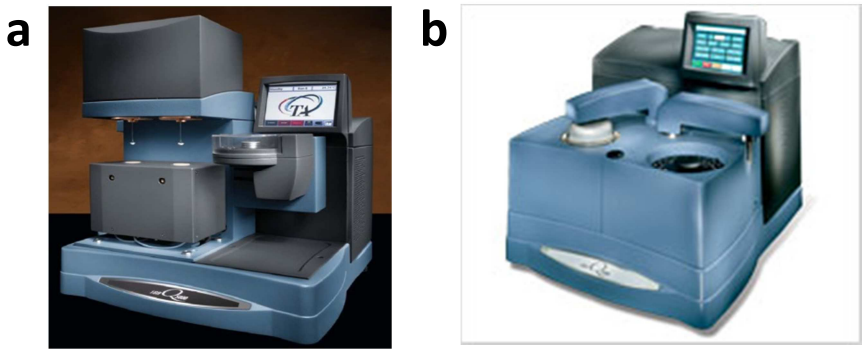

Fig. 3.10 (a) TGA Q 500 and (b) DSC Q 1000 by TA Instruments, USA

3.3.6 Thermo-oxidative aging

Thermo-oxidative aging was carried out with the test specimens (dumble shaped tensile test samples) in a hot air oven (HERAEUS, Thermo electron corporation, Langenselbold, Germany) at two different temperatures of 80 °C and 100 °C (ASTM D1349) with different aging times of 24, 48, 72 and 96 h. (ASTM D573). Resistance to thermal ageing was measured for the samples. To do so, standard PN-88/C-04207 was followed. In this method, the samples were exposed to the circulating hot air at the temperature of 70 °C for 100 h.
The coefficient of thermal ageing was then calculated using the eqn 3.1:

$$S = \frac{[TS_f \times E_f]}{[TS_i \times E_i]} \qquad (3.1)$$

where, S is the coefficient of thermal ageing, TS_f is the tensile strength after thermal aging, E_f is the elongation at break after thermal ageing, TS_i is the tensile strength before thermal ageing and E_i is the elongation at break before thermal ageing. Fig. 3.11 displays the hot air oven used for aging studies.

Fig. 3.11 Hot air oven and its inside view

3.3.7 Morphological analyses (XRD, SEM and TEM)

X-ray diffraction (XRD): X-ray diffraction (XRD) technique is employed to attain crystallographic informations about the lattice structures of the zinc based compounds used in the study. The experiments were executed in the small angle range, which was extended to the intermediate angular range. The measurements were carried out with a Panalytical Empyrean multipurpose diffractometer (XRD 3003 θ/θ, Seifert-FPM Freiberg/Sa.: GE Sensing & Inspection Technologies GmbH) (Fig. 3.12). The wavelength of the X-ray was 1.54 Å (Cu Kα radiation). The samples were scanned in 2θ between 0 and 5° with step size 0.01 deg min^{-1} and Δt = 3 s. Bragg's law gives opportunity to calculate the parameters about the crystal structure:

$$2dsin\theta = n\lambda \qquad (3.2)$$

where λ is the wavelength, n is an integer, θ is the angle between incident beam and planes, d is the distance between crystal lattice planes.

Scanning electron microscopy (SEM): The morphologies of the samples were observed with a field emission scanning electron microscope (SEM; Zeiss Ultra Plus, Carl Zeiss Microscopy GmbH, Jena, Germany) (Fig. 3.13a) equipped with an energy-dispersive X-ray spectrometer (EDX; Quad XFlash 5060, Bruker Corporation, Billerica, MA). Rubber specimens were cut into small square shapes. Prior to the experiment, all the rubber specimens were gold sputtered and inserted into SEM chamber.

Fig. 3.12 XRD 3003 T/T diffractometer

Transmission electron microscopy (TEM): Microscopic structures in more detail were observed using high-resolution transmission electron microscopy (TEM; Libra 200 with integrated Ω-type energy filter Carl Zeiss Microscopy GmbH, Jena, Germany) (Fig. 3.13b). Ultra-thin sections of the rubber specimens were prepared by ultramicrotomy (Reichert Ultracut S, Leica, Austria) (UCT) at -130 °C with a thickness of a section 100 nm. The energy filter was used for electron energy-loss spectroscopy (EELS) and elemental mapping by energy-filtered imaging (EFTEM) at the corresponding ionization edges of selected elements.

3.3.8 Cross-link density measurement (Swelling method)

Elastomers crosslinked above their gel points usually absorbs solvents and subsequently swells without dissolving. Swelling process carries on until the retractive forces in the extended molecular strands in the network balance the forces responsible for swelling the

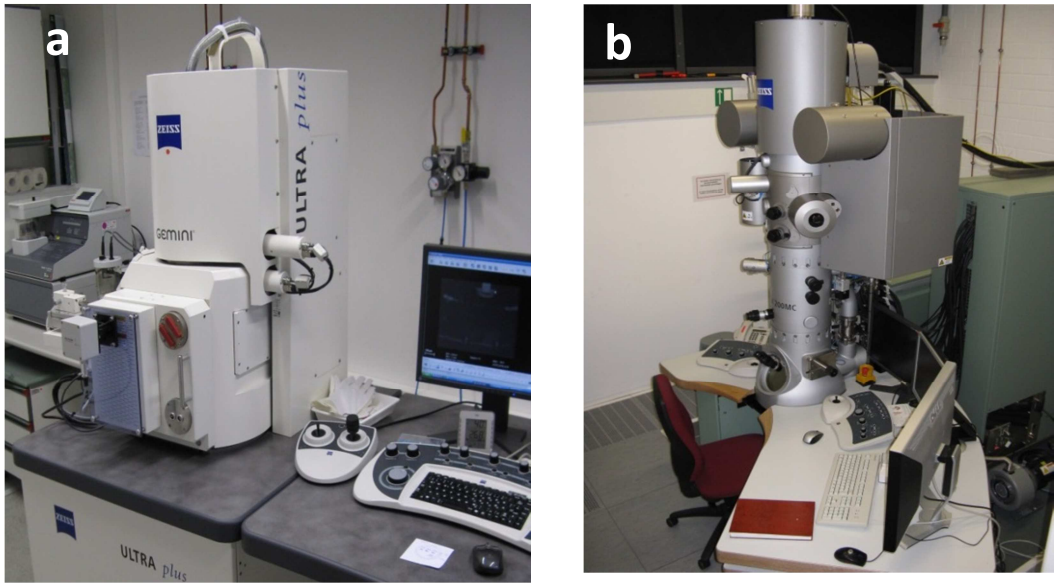

Fig. 3.13 (a) Zeiss ultra plus SEM machine, (b) Libra 200 TEM machine

network. The rubber samples, according to ASTM D 6814−02 standard, are swollen in a solvent with the knowledge of the polymer – solvent interaction parameter. Toluene is used in this study. The solvent chosen for this characterization was of reagent grade purity. Pre-weighed rubber specimens are swollen for 24 h at room temperature. The solvent is replaced with fresh solvent from time to time during this test. After swelling, the solvent is wiped off quickly from the surface of the specimens using a clean blotting paper. The samples then are dried at 70 ± 2 °C in a forced-ventilating air oven for around 16 ± 1 h until constant weight. The samples were next allowed to cool down to room temperature using a desiccator and weights were taken. The volume fraction of rubber in the swollen gel (V_r) was calculated from the following equation which is based the simple additive rule of volumes as follows:

$$V_r = \frac{(D-FH)/\rho_r}{\frac{D-FH}{\rho_r}+A_0/\rho_s} \quad (3.3)$$

where H = initial weight of the test specimen; D = deswollen weight of the test specimen (until constant weight); F = weight fraction of the insoluble components, such as fillers; A_0 = weight of the absorbed solvent (A_0 = immediate weight – H); ρ_r = density of the rubber; ρ_s = density of the solvent.

At swelling equilibrium condition the classical Flory−Rehner [66] equation (affine network) is given by:

$$-[\ln(1-V_r)+V_r+\chi V_r^2] = \frac{\rho_r}{M_c}V_s(V_r^{\frac{1}{3}}-\frac{2V_r}{f}) \quad (3.4)$$

where f is crosslinking functionality. However, a more adequate swollen network can be represented in the following way after consideration of phantom network model:

$$-[\ln(1-V_r)+V_r+\chi V_r^2] = \frac{\rho_r}{M_c}V_s(1-\tfrac{2}{f})V_r^{1/3} \quad (3.5)$$

If the crosslinking functionality is considered to be tetra functional ($f = 4$) then the apparent crosslinking density (ν_c) can be expressed in the following way

$$\nu_c = \frac{1}{2M_c} = -\frac{\ln(1-V_r)+V_r+\chi V_r^2}{V_s\rho_r\left(V_r^{\frac{1}{3}}-\frac{V_r}{2}\right)} \quad (3.6)$$

where V_r is the volume fraction of the polymer in the swollen specimen, χ is the Flory-Huggins polymer solvent interaction parameter, M_c is the molecular weight between crosslinks, and V_s is the molar volume of the solvent.

The Huggins parameter (χ) of XNBR-toluene system is given by the following equation [67]:

$$\chi = 0.487 + 0.228V_r \quad (3.7)$$

The content of ionic crosslinks (Δv) was calculated from the following equation:

$$\Delta v = \frac{v_c - v_A}{v_t} 100\% \quad (3.8)$$

v_t is the total crosslink density. v_A is the crosslink density determined for samples treated with ammonia vapor using the Huggins elastomer-solvent interaction parameter, described by the following equation [68]:

$$\chi = 0.487 + 0.320V_r \quad (3.9)$$

3.3.9 Flame retardancy test

The flame retardancy of the elastomer composites was quantified using cone calorimeter (FTT = Fire Testing Technology) (Fig. 3.14) following the standard procedures described in ISO 5660:2002 (without the use of 'frame and grid'). Milligrams amount of square shapes specimens of dimension of 100mm x 100 mm x 3mm were irradiated at a heat flux of 35

Fig. 3.14 Dual Cone Calorimeter (FTT)

kW/m^2, corresponding to a mild fire scenario. Many important fire retardant parameters like heat release rate (HRR), total heat release (THR), mass loss rate (MLR), and time to ignition (TTI), and so on were estimated by this method. Amongst these parameters, TTI is used to determine the influence on ignitability and can be directly estimated from the onset on an HRR curve. The exhaust flow was set at 24 liter per second.

3.3.10 Tear fatigue analysis

Tear fatigue analysis apart from tensile test falls under a very common and popular technique to assess the mechanical performance of a rubber specimen. Substantial evidences are there to establish that the fracture of rubber is mostly initiated from the imperfections existing or introduced into the materials. These imperfections later become the suitable source of crack growth under applied load of variable amplitudes. The branch dealing with such behavior of polymer specimens is commonly known as fracture mechanics. Tear- fatigue analysis of the rubber specimens was carried out in Instron Electroplus E 1000 electrodynamic tensile

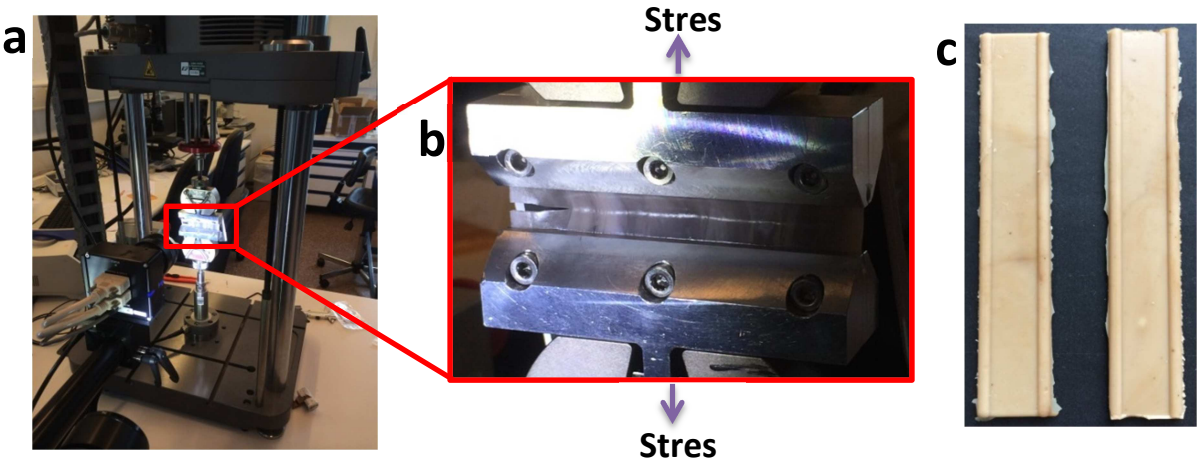

Fig. 3.15 (a) Instron Electroplus E 1000 electrodynamic tensile machine, (b) notched pure-shear test rubber specimen is under test, (c) standard pure-shear test specimen (30 cm x 4 cm x 0.2 cm)

machine (Fig. 3.15a). The fundamental principle on which the fracture mechanics approach is established is the energy required to propagate the crack in the specimen. Griffith [69] introduced the idea when he postulated that a crack in a glassy material would grow if the elastic energy released there became larger than the surface free energy of the surfaces thus originated. For rubber samples, the energy loss in the crack tip is considered to be larger than in the bulk. The energy required to propagate the crack is mostly governed by the rubber

itself, even though it may surplus the available thermodynamic surface free energy. The elastic energy termed as tearing energy (G) is defined by the energy released per unit area of crack surface growth, and given by eqn 3.10

$$G = -\left(\frac{\partial W}{\partial A}\right)_l \qquad (3.10)$$

Where W is the total elastic energy stored in the sample, A is the area of one fracture surface of the crack in the sample and l is the length of the specimen, G is the tearing energy. G is often termed 'strain energy release rate' or 'fracture energy' as well. Rivlin-Thomas [70] later introduced the tearing energy for rubber materials in the form of both single edge notch tensile (SENT) and pure-shear test specimens based on energy balance mechanism. Pure shear specimens have certain advantage over SENT specimens in regards of independence of the current crack length. The pure-shear test which is used in this study for the determination of the tearing energy is exhibited in Fig. 3.15b. The tearing energy according to Rivlin-Thomas for pure-shear test specimens of rubber can be written as eqn. 3.11

$$G = l_0 U \qquad (3.11)$$

Where l_0 is the unstrained (original) length of the test specimens between the grips and U is

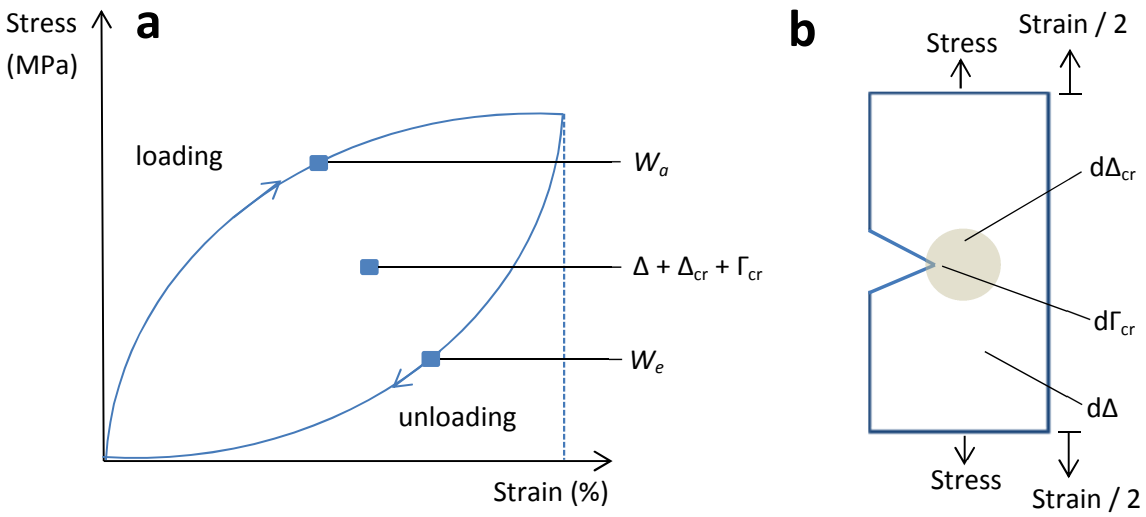

Fig. 3.16 Energy profile diagram of a notched rubber specimen during loading and unloading processes in the (a) stress-strain plot, (b) infinitesimal variation of energy during crack propagation of the rubber sample as well as the variation of external loading. Here, W_a = external work, W_e = internally stored elastic strain energy, Δ = dissipated energy in the body of the specimen, Δ_{cr} = energy dissipated in the dissipative process zone around the crack tip and Γ = energy leading to infinitesimal crack growth of the newly produced crack face area

the strain energy density in the pure shear region of the rubber specimen. Usually, the value of U can be estimated from the stress-strain plot of the corresponding samples. Fig. 3.16 illustrates the energy contribution for the loading and unloading plots of an inelastic rubber specimen initially notched before the test. The inelastic process zone subjected to uniaxial tension is also depicted in the same figure. It is realized after careful consideration with experimental results and data evaluation that the dissipation of energy in the inelastic material, especially into the process zone plays a significantly role in crack growth resistance.

For filled and highly reinforced systems, the dissipation of energy in the plastic process zone at the tip of the crack along with the rest of the area of the rubber specimen contributes simultaneously prior to the crack propagation [71]. Over the years, numerical methods have been evolved to successfully compute and interpret the crack resistance behavior of the materials under study. Materials force method is one such method used to understand the inelastic behavior of the specimens [71].

In principal, the propagation of micro-crack proceeds during strain at lower tearing energy and could initially commence with the high dynamic deformation of the specimen having considerable elastic modulus compared to the deformed elastomeric part. This phenomenon could be realized when a rolling tire comes into contact of the surface of the road. Post the loading in the time order of milliseconds, the deformation becomes stronger and consequently the strained rubber zone relaxes. This mechanism is known to be repeating in the frequency of real mechanical dynamic loading. The crack propagation in the rubber part follows the applied process described herewith and eventually is characterized by the crack growth rate.

From the practical point of view, tire treads while exposed to complex dynamic, cyclic loading and unloading conditions on road go through a higher magnitude of abrasion. Because of the uneven road surfaces, tire treads could not make perfect contact with the road and therefore, the tire tread-road contact area forms a small part of the nominal footprint contact area. Large deformation results as a consequence and fracture starts induced by micro-crack initiation in the tire treads.

Chapter 4

Results and discussions

4.1 Evidence for an in-situ developed polymer phase in carboxylated nitrile rubber

The reaction of different metal sources with unsaturated carboxylated nitrile rubber yields ionomers. The ionomers produced this way have been characterized by their unique dynamic properties. Unusual appearance of a high temperature transition in the dynamic mechanical spectra for only zinc oxide neutralized ionomer sample provides a vast opportunity to research in details to understand the fundamental phenomenon involved with this. A number of literatures [72-75] claim that the presence of a high-temperature transition due to relaxation in the dynamic mechanical analysis spectra is attributed to the restricted mobility of polymer chains in ionic clusters. Some investigations [62, 76-77] have highlighted the effect of a plasticizer in the form of base like NH_3 on ionic crosslinking of XNBR. A study [78] by Hara *et al* reveals that some plasticizers can even function as a 'dual' plasticizer, not only collapsing the ionic aggregates in the ionomer but also decreasing the T_g of the matrix material. Mandal *et al* [16] showed that plasticizers can be grouped into two types: backbone plasticizers, which preferably plasticizes the nonpolar hydrocarbon part of the chains, and ionic plasticizers, which preferentially affect the ionic clusters.

But it is much to our surprise that besides the concept of cluster formation by the ionic groups, no other explanations of higher mechanical properties have been proposed. Some literatures from inorganic and crystallographic journals [79-85] exist in which bivalent metallic ions, like zinc, are coordinated with different types of organic molecules with carboxylic groups, resulting in octa-, hexa- or tetra-coordinated geometries as well as their distorted forms. A simple bivalent zinc (II) carboxylate with empirical formula $Zn(carboxylate)_2$ was considered, and different polymeric forms of the compounds were explored. Owing to the tetrahedral geometry of the coordination complex in syn-syn and/or syn-anti configuration (Fig. 4.1), the polymer chains form a three-dimensional network. The polymeric structures largely depend on the conditions of polymer formation, in which zinc is allowed to react with different carboxylate ions. For example, when zinc salts of 2-

chlorobenzoic acid are prepared in acetone solution, two different polymers are produced: one is formed with syn-syn bridges, and the other with triply-bridged $Zn_2(carboxylate)^{3+}$ units

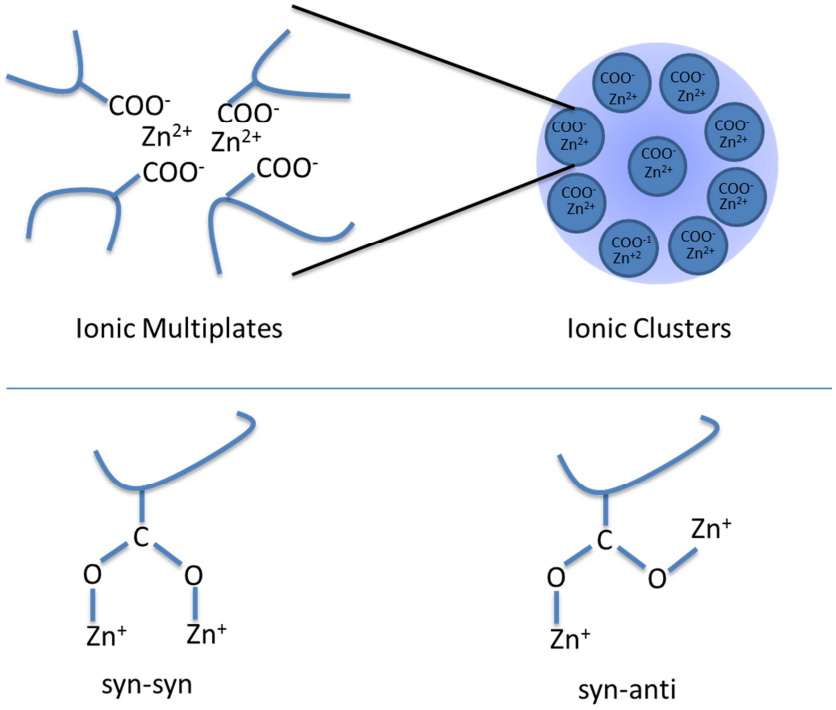

Fig. 4.1.1 Graphical presentation of the hierarchal microstructure of ionic clusters of ZnO-cured XNBR (above) and different configurational structures of zinc carboxylate polymers (below)

linked together by syn-anti carboxylates (Fig. 4.1.1). In spite of a relatively larger magnitude of research on this particular topic, some fundamental questions are still unanswered. These include: why do the inorganic monovalent ions not form cluster despite their interaction with the functional groups of polymers? Why some zinc-containing compounds, such as layered double hydroxide and zinc chloride, can not form ionic clusters in spite of being used as ionic cross-linkers? To unfold the mystery underlying with the mechanism of ionic crosslinking, the present study is carried out to exploring the role of zinc ions in different chemical environments in the crosslinking and microstructure of the polymer matrix and its effect on the high-temperature relaxation behavior of XNBR.

4.1.1 Curing study and kinetics

Three different types of zinc reactants, ZnO, $ZnCl_2$ and Zn-Al layered double hydroxides are used to elucidate the mechanistic pathways involved with XNBR. The XNBR used in this

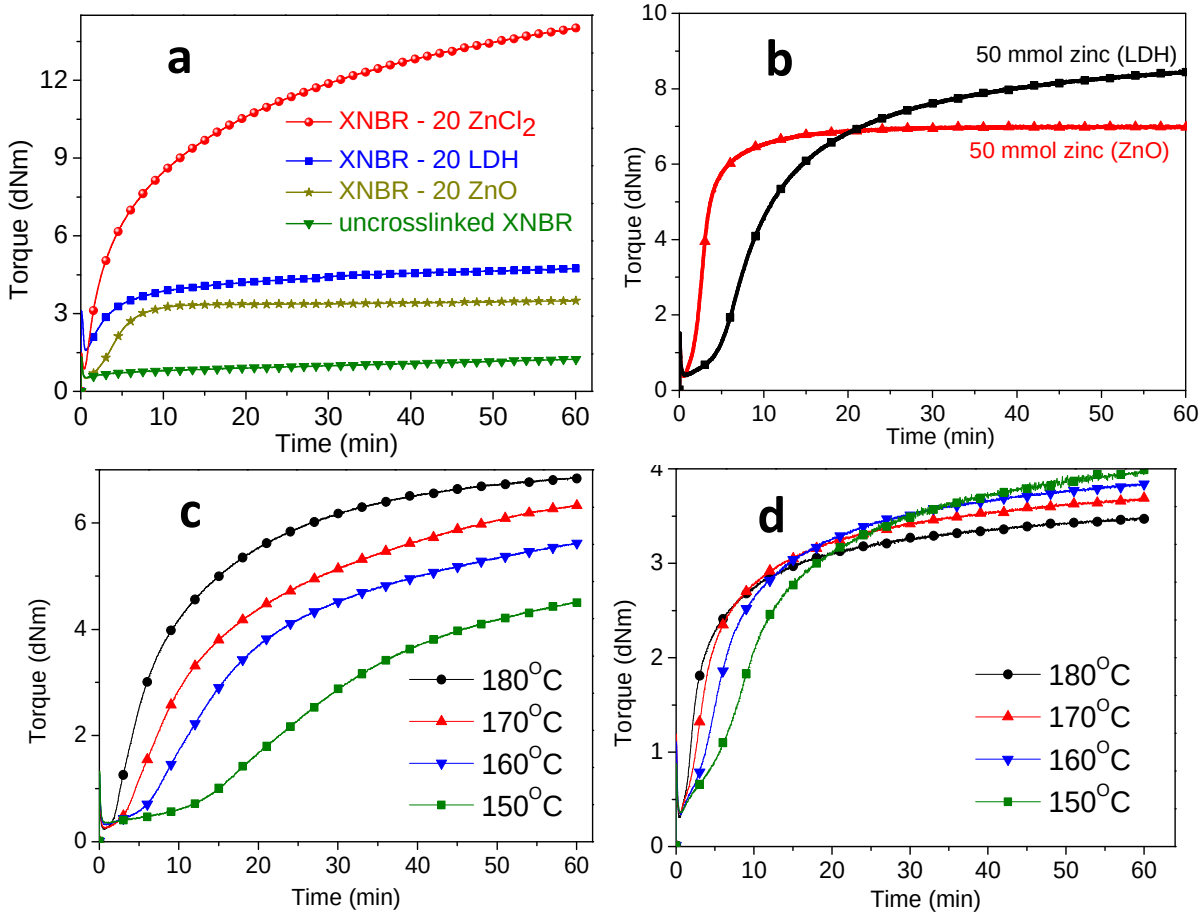

Fig. 4.1.2 Torque vs. time plot determined at 160 °C for 1 h: (a) in the presence of zinc compounds (without sulfur additives), (b) 50 mmol zinc compounds (cured at 160 °C), (c) 4 phr Zn-Al LDH and (d) 4 phr ZnO. The compounds in b, c, and d contain sulfur curatives

study contains 7% carboxylic groups by weight. Sufficient amount of different zinc-containing compounds was incorporated into XNBR to obtain the maximum number of interactions with the carboxylic groups of XNBR. The rheometric results illustrate (Fig. 4.1.2a) that the torque (elastic modulus) of all zinc-containing compounds increases over time, which is attributed to the chemical interactions between the zinc salts and carboxylic groups of the polymer, resulting in a cross-linked network. It is worthy to mention that the $ZnCl_2$-containing compounds showed the highest torque value compared to the rest of the compounds due to its higher crosslinking efficiency. Zinc has the tendency to form several co-ordination complexes with different ligands. Most likely, different zinc-containing compounds (in this investigation) form coordination complexes that ultimately results in a crosslinked network structure in the elastomers. To compare these only zinc compounds based curing system (sulfur less) with classical sulfur-based curing systems, another set of reference experiments were conducted with a conventional dose of zinc compounds (see table 3.7)

Usually 3-5 phr (parts per hundred parts of rubber by wt.) zinc oxide is considered to be the standard dose used in the sulfur formulation of rubber compounds. It is noticed from the rheometric data of XNBR cured with either ZnO or LDH at equivalent concentrations of zinc ions (Fig. 4.1.2b) that the absolute torque value of the LDH-cured compound is higher than the ZnO containing compound after one hour of experimental time. In these two different compounds, two simultaneous mechanistic pathways could be visualized in case of sulfur and zinc carboxylate crosslinking. Substantial level of curing was noticed, but the natures of the curing curves are somewhat different from each other. At the end of one hour curing time, the higher torque arising from LDH indicates its stronger crosslinking efficiency compared with that of ZnO. Furthermore, in an attempt to draw certain conclusions about the efficient curing system offered by ZnO and LDH in sulfur-based systems, curing kinetics were studied. The extent of cure or degree of crosslinking (α) was estimated from the torque-time plots at different temperatures, 150, 160, 170 and 180 °C, to understand the curing processes of ZnO and LDH (Fig. 4.1.2c and d).

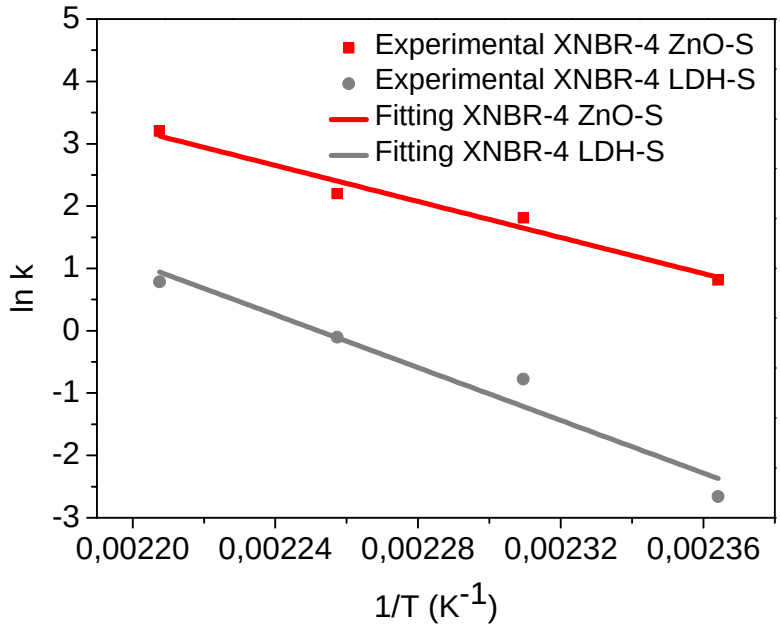

Fig. 4.1.3 Arrhenius type plot of ln K versus 1/T for calculating kinetic parameters of samples XNBR-4 ZnO–S and XNBR–4 LDH – S

The extent of cure at time t is expressed as the following expression (eqn 4.1):

$$\alpha = \frac{M_t - M_0}{M_h - M_0} \qquad (4.1)$$

where M_o, M_t, and M_h are torque values at time zero, after a given time of curing and at the end of crosslinking, respectively. For the rubber compounds, isothermal vulcanization kinetics is usually characterized by two general model equations, namely the n^{th}-order and

autocatalytic model equations. The former kinetics model, which is reckoned to be the simplest model equation to describe the overall curing process, is expressed as eqn. (4.2):

$$\frac{d\alpha}{dt} = k(T)(1-\alpha)^n \qquad (4.2)$$

where n is the reaction order and k denotes the temperature-dependent rate constant. The nth-order kinetic equation is based upon the expectation that the maximum reaction rate occurs at the very initial stage of the reaction. The latter equation, the autocatalytic kinetic model equation, expresses that the maximum reaction rate at any point after t = 0. Hence, this model equation has been employed in the current study for the investigation of curing behavior of XNBR composites. The autocatalytic model equation described elaborately in previous literatures [23, 52] can be expressed as follows (eqn 4.3):

$$\frac{d\alpha}{dt} = k(T)\alpha^m(1-\alpha)^n \qquad (4.3)$$

where K is the rate constant dependent on temperature and m and n are the orders of reactions, which also depend on reaction temperature. The values of K, m and n are calculated

Table 4.1.1 Kinetic parameters and activation energy of XNBR with 4 phr ZnO and 4 phr Zn-Al LDH cured at different temperatures (T_c = curing temperature)

Sample	T_C (°C)	K	A	b	E_a (kJ/mole)
XNBR–4 ZnO–S	150	4.35459	2.56621	3.56944	144.68
	160	6.11029	2.26404	3.95149	
	170	9.01778	2.15507	4.19612	
	180	24.61358	2.30211	5.14938	
XNBR–4 LDH–S	150	0.07085	0.46597	0.82555	211.60
	160	0.46003	1.21586	2.2567	
	170	2.19491	1.51684	4.27098	
	180	0.90963	0.94316	2.92888	

through non-linear multiple regression analysis of the experimental data. The function K (T) in both equations (8) and (9) is related to activation energy, provided by the Arrhenius equation.

$$K = Ae^{-E_a/RT} \qquad (4.4)$$

or

$$lnK = lnA - \frac{E_a}{RT} \qquad (4.5)$$

Kinetic parameters of the vulcanization reactions of two different rubber composites were calculated from the data obtained from the rheometer and are provided in Table 2. The slope of the straight line in the plot of ln K versus 1/T gives the activation energies for these two different rubber composites (Fig. 4.1.3). Based on the activation energies (E_a) listed in table 4.1.1 of two different rubber composites, ZnO has lower activation energy than LDH. It is noteworthy to mention that lower value of activation energy indicates the ease of the crosslinking process. However, with Zn-Al LDH, the ultimate torque increased with temperature, but, for ZnO, it remains constant. Therefore, the crosslinking rate for the compound with LDH is slower but ultimately enhanced the degree of crosslinking of XNBR.

4.1.2 Fourier transform infrared (FTIR) spectroscopy – study of chemical interaction

In the previous section, it was proved that the curing efficiency of all the zinc containing compounds was substantially satisfactory without the presence of any classical curing aid like sulfur or peroxide. Ionic crosslinking is established into the compounds through the special type of co-ordination reactions between the zinc metal and the carboxylic functionality present in the XNBR molecule. FTIR studies of the zinc-cured XNBR composites were conducted to gain insight about the formation of different types of co-ordination complexes. To understand the chemical reaction of the zinc curing process, the formulation of XNBR and 20 phr of zinc-containing compounds were considered without any other extra ingredients. In the IR spectrum (Fig. 4.1.4), various vibrational modes are observed: the peak at 2237 cm^{-1} could be assigned to the -CN groups of the acrylonitrile part of the XNBR chains. The characteristic peaks arising from the carboxylic groups -COOH are found at 1697 and 1727 cm^{-1}(Fig. 4.1.5a and Fig. 4.1.5b). The appearance of the former peak at 1697 cm^{-1} in the spectrum ascribes to the stretching vibration of the C=O bond, present in the carboxylic group along the hydrocarbon backbone of the XNBR structure [85], producing a carboxylic acid dimer local structure. The peak at 1727 cm^{-1} is associated with the -C=O stretching vibration of free carboxylic groups. After the incorporation of ZnO, these two peaks are shifted to a position at 1587 cm^{-1} and 1539 cm^{-1} which are associated with tetra-coordinated and hexa-coordinated zinc carboxylate structures (Fig. 4.1.5c and Fig. 4.1.5d) [71-73, 84] respectively. The shifting of these two strong bands directly supports the formation of ionic crosslinking of XNBR with ZnO. This shifting has been observed for all samples cured with different zinc-containing inorganic compounds, indicating the formation of zinc-carboxylate crosslinking

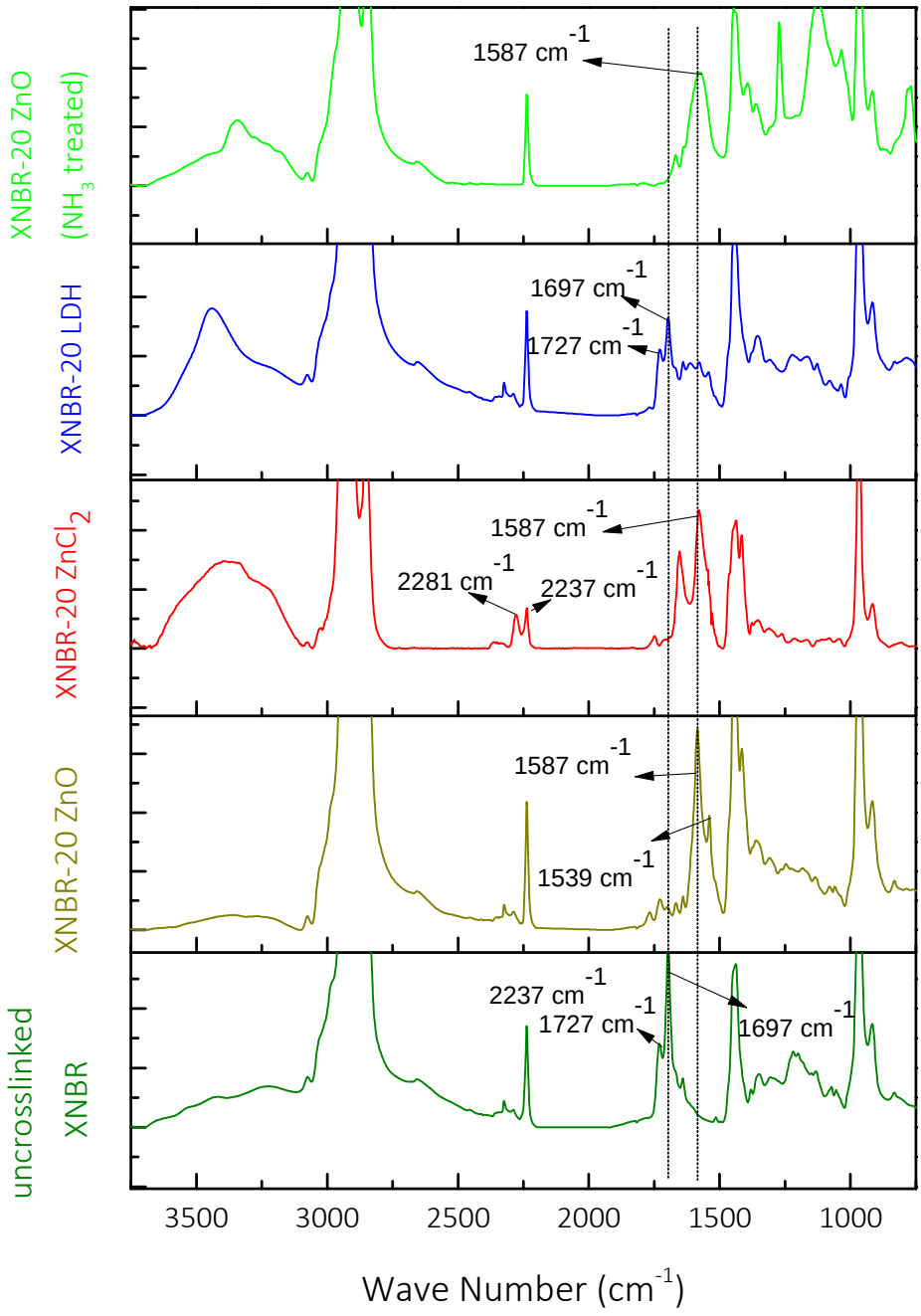

Fig. 4.1.4 FTIR spectra of uncrosslinked XNBR, XNBR compounds crosslinked with different zinc compounds and NH_3 treated XNBR – ZnO compound

structures. Additionally, for the Zn Al-LDH-cured composites, the intensities of the peaks at 1697 and 1727 cm^{-1} for free carboxylic groups are weakened significantly. The vibrational mode of the -C=O group in raw XNBR was somehow affected by interaction with metal oxides present in the layered crystal structure of LDH. A broad peak at 3438 cm^{-1} was found in addition due to the presence of water molecules in the LDH structure. Another interesting fact is that the stretching frequency at 2237 cm^{-1} originated from the acrylonitrile groups of XNBR (cured with $ZnCl_2$) is found to be partially shifted to a higher wave number of 2281 cm^{-1}. This observation can be noticed only in the sample of XNBR treated with zinc chloride.

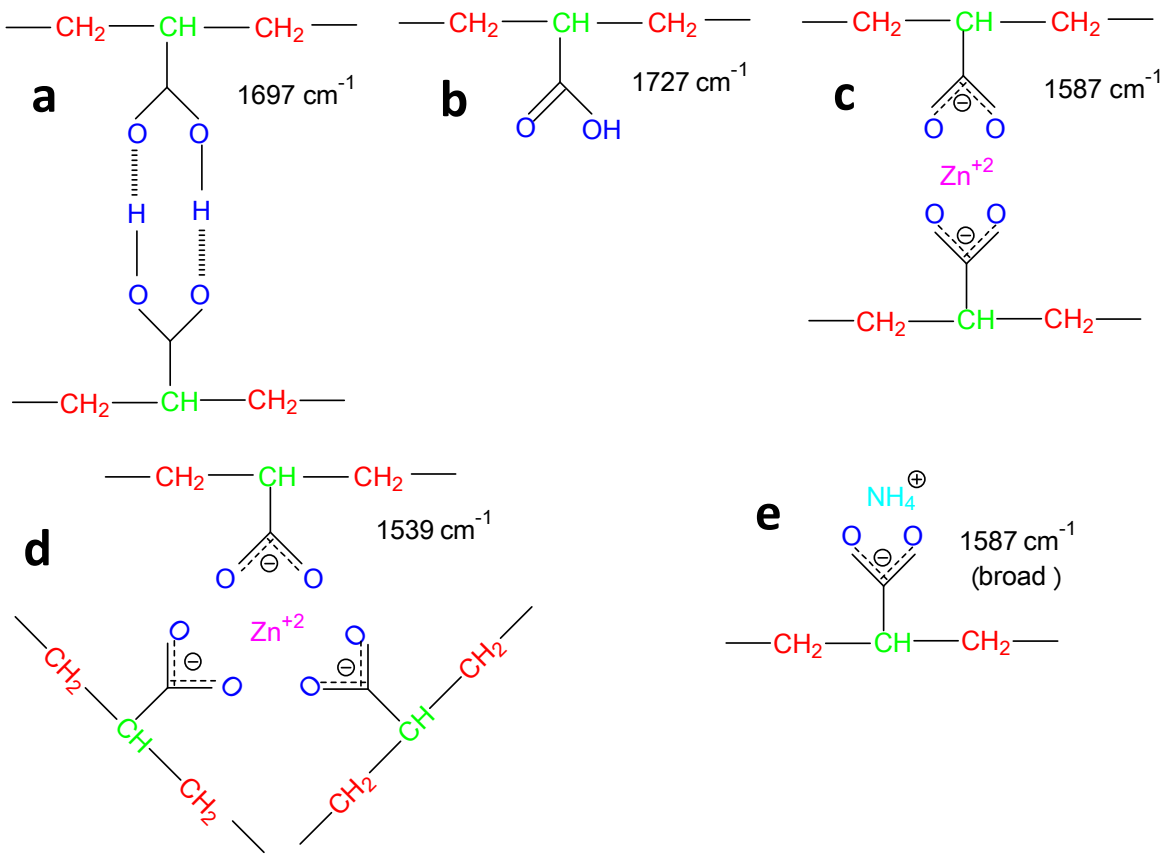

Fig. 4.1.5 Several chemical microstructures of the carboxylic groups of carboxylated nitrile rubber and its various co-ordination complexes, a) carbonyl stretching of hydrogen-bonded acid dimer (1697 cm^{-1}), b) carbonyl stretching of monocarboxylic acid (1727 cm^{-1}), c) tetra- and d) hexa-coordinated zinc carboxylated structure, e) carboxylic ammonium salt

This change reveals partial participation of acrylonitrile groups in a co-ordination-type reaction with $ZnCl_2$ [86]. The zinc ions from zinc chloride in this case, perhaps form a certain kind of inorganic zinc complex supported by the free electron of the nitrogen atom from the acrylonitrile group of the XNBR side chain. To gain more insight on the co-ordination complex formed between ZnO and the carboxylic groups, the sample of XNBR cured with ZnO was treated with saturated ammonia vapor. Post ammonia treatment, the structure of the coordination complex will be rearranged by the participation of ammonia molecules in the co-ordination geometry. After this treatment, the C=O stretching frequency at 1539 cm^{-1} disappears, and the peak at 1587 cm^{-1} becomes broader (Fig. 4.1.5e). This change could be attributed to the formation of a different coordinated compound.

Significantly, the existence of a typical peak at 1539 cm^{-1} (missing or very weak in other zinc compounds) in the ZnO-carboxylate complex is a clear indication of a co-ordination complex that can behave like an additional polymer in the XNBR matrix by showing a high-

temperature tan δ peak. It is reported by Coleman *et al* [85] that the peak at 1539 cm^{-1} indicates a complex with octahedral geometry (coordination number six) and the peak at 1587

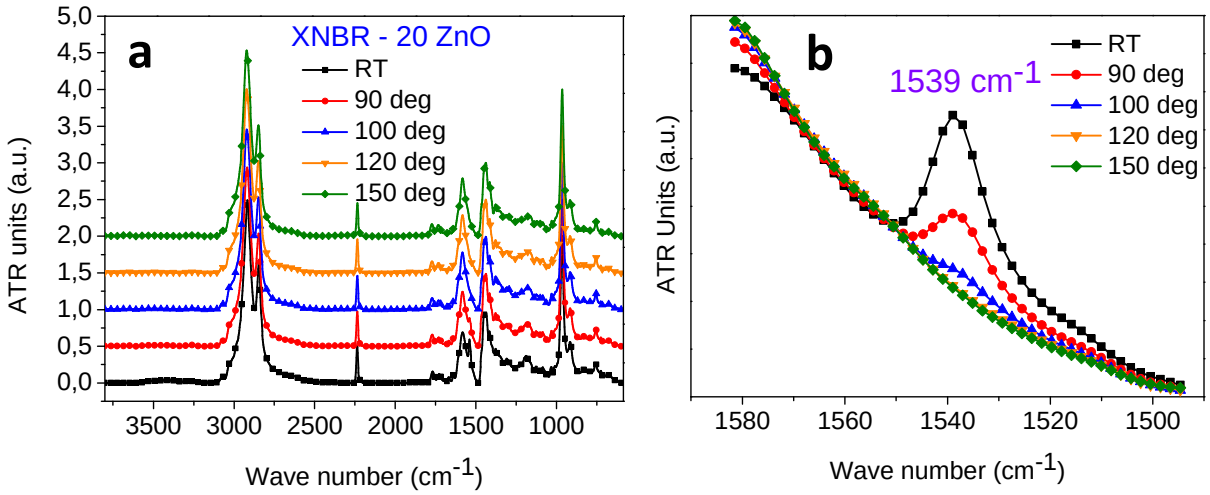

Fig. 4.1.6 (a) Effect of temperature on the FTIR spectra of ZnO-treated XNBR, (b) enlarged portion near the peak at 1539 cm^{-1} from the left side figure

cm^{-1} indicates the formation of tetrahedral geometry with co-ordination number four. It is also reported [79, 87-88] that hexa-coordinated complexes easily form a "*zinc-carboxylate polymer*" by a special arrangement of the syn- and anti-configurations, whereas the formation of a polymeric network by tetra-coordinated complexes is limited. Additionally, the sample was further analyzed through the temperature-dependent FTIR spectroscopy and the correspondent spectra are exhibited in Fig. 4.1.6. Thermal reversibility of the peak at 1539 cm^{-1} was obviously realized when it appears during heating and subsequently tends to re-appear after cooling. Therefore, the reversible transition of the peak corresponds to the alteration or destruction of the hexa-coordinated complex during heating and reordering of the structure after cooling.

4.1.3 Dynamic mechanical analysis

Ionic elastomers are unique and different from other classically crosslinked systems by the virtue of consisting typical dynamic mechanical spectra. Fig. 4.1.7 demonstrates the loss tangent (tan δ) from dynamic mechanical analysis measured under temperature sweep conditions. From the plot of tan δ vs. temperature (Fig. 4.1.7a), it is easily noticed that only the ZnO-vulcanized compound has two clear transitions, visible as two peaks: one at a low temperature (2.7 °C), corresponding to the glass transition of the macromolecular chains (XNBR molecule), and another in the rubbery plateau region at high temperature (82 °C). It is surprisingly observed that despite of presence of the same metal atoms in the structures, this high-temperature peak is absent when XNBR is cured by other Zn-containing salts, such as

$ZnCl_2$ and Zn-Al LDH (Fig. 4.1.7b). The reaction of different zinc salts with carboxylated nitrile rubber does not always necessarily produce the zinc carboxylate linkage as seen in the FTIR study. Therefore, it can be concluded that the formation of ionic linkages or coordination complexes could not always contribute to a high-temperature mechanical relaxation. Additional factors are also responsible for the unique high temperature

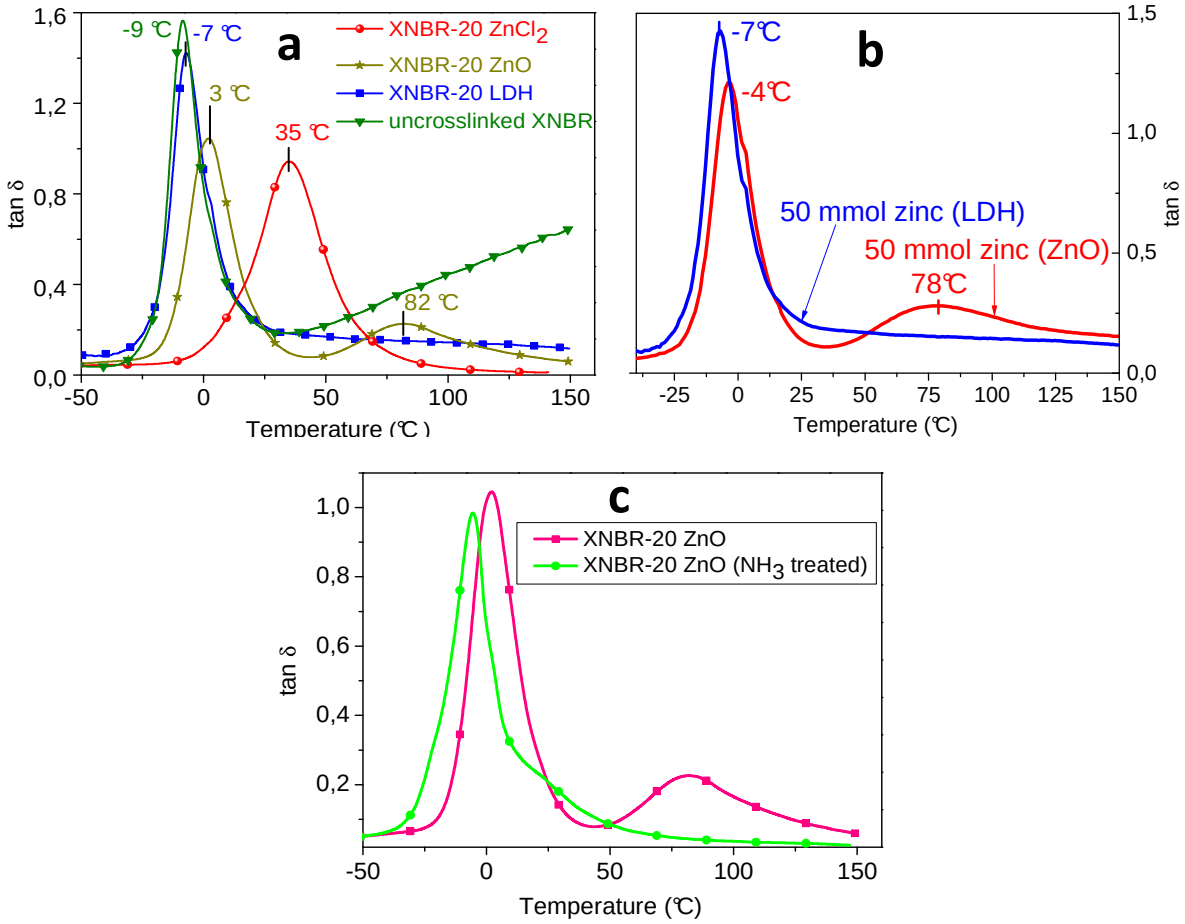

Fig. 4.1.7 Dynamic mechanical spectra (tangent loss vs. temperature plot) of a) XNBR with different zinc compounds, b) XNBR cured with ZnO and LDH (50 mmol zinc equivalent) and c) untreated and NH_3-treated XNBR-ZnO composites (all the rubber samples shown here are sulfur free)

phenomenon. One such factor is obviously the formation of ionic cluster [74, 89-90] at elevated temperature. But, still a specific ambiguity over this issue remains unsolved. This is: why does ZnO form clusters while $ZnCl_2$ does not, although the coordination efficiency of $ZnCl_2$ is higher than that of ZnO? A few literatures [91-92] are available in which a decrease or disappearance of the high-temperature transition peak after treatment with NH_3 solution was observed; also, in the current study, disappearance of that high-temperature peak after ammonia treatment of the ZnO cross-linked rubber sample was noticed (Fig. 4.1.7c). The chemical interaction responsible for this effect has already been discussed in the FTIR

analysis in the subsection 4.1.2. Usual explanation that can be found in the literature is that treatment with NH_3 forms a coordinated bond with the zinc ions of zinc carboxylate salts [86, 93] or can even solvate the carboxylic ions [94-95], resulting in either a decrease in the

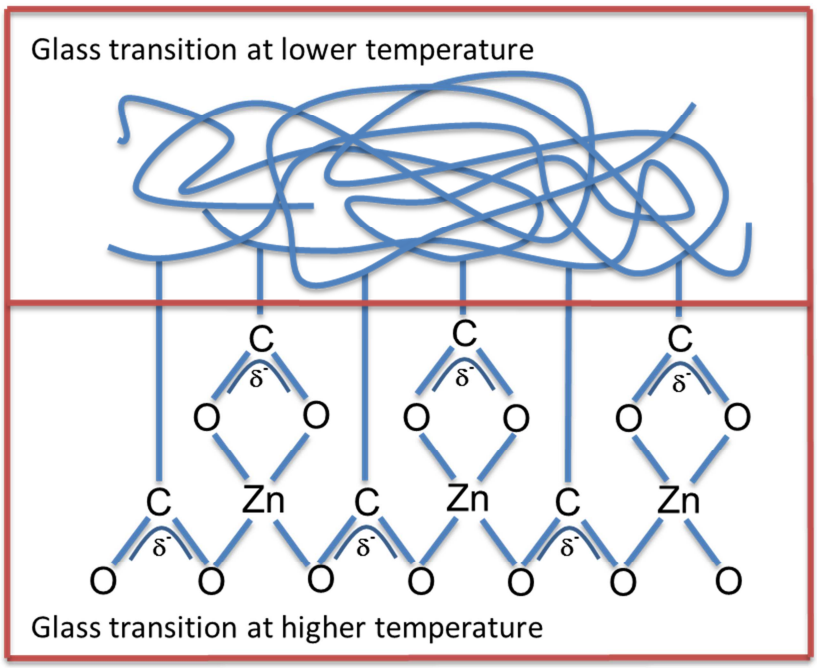

Fig. 4.1.8 Zinc and carboxylic group interaction and in-situ formation of zinc polymer by co-ordination complexes

electrostatic interaction of the multiplets, inhibiting cluster formation, or even disappearance of the peak because of the formation of a different co-ordination complex [62] by the free electrons of nitrogen atoms that are present in ammonia molecules. Hence, the appearance or disappearance of the high-temperature peak is therefore largely governed by the microstructure of the co-ordination complex and cannot be explained only by cluster formation. In this context, a hypothesis is introduced to explain this high-temperature behavior. Only in the presence of ZnO, the carboxylate groups react with ZnO to form a three-dimensional polymeric network (Fig. 4.1.6), by the formation of a special co-ordination complex. This additional cross-linked network is established as a new polymer phase ("*zinc-carboxylate polymer*") having its own glass transition temperature. For the rest of the zinc compounds ($ZnCl_2$, Zn Al LDH), the coordination complexes are formed, but the complexes are not further coordinated to produce a discrete polymeric network structure.

Fig. 4.1.7 illustrates a very sharp glass transition for the uncrosslinked elastomer, which is broadened for ZnO- and $ZnCl_2$-cured compounds. The glass transition temperature of the $ZnCl_2$ cross-linked sample was found to be higher than that of a ZnO-cured compound. The

crosslinking reaction occurred due to formation of an acid anhydride [96] while pressing the sample for 30 min (t_{90}) at 160 °C in the compression moulding machine. In case of conventionally cured (in the presence of sulfur) systems, two peaks were also noticed for ZnO-cured compounds: one broad peak at +78 °C and another at -7 °C (Fig. 4.1.7b). The low-temperature peak is attributed to the glass transition temperature of XNBR [86], and the high

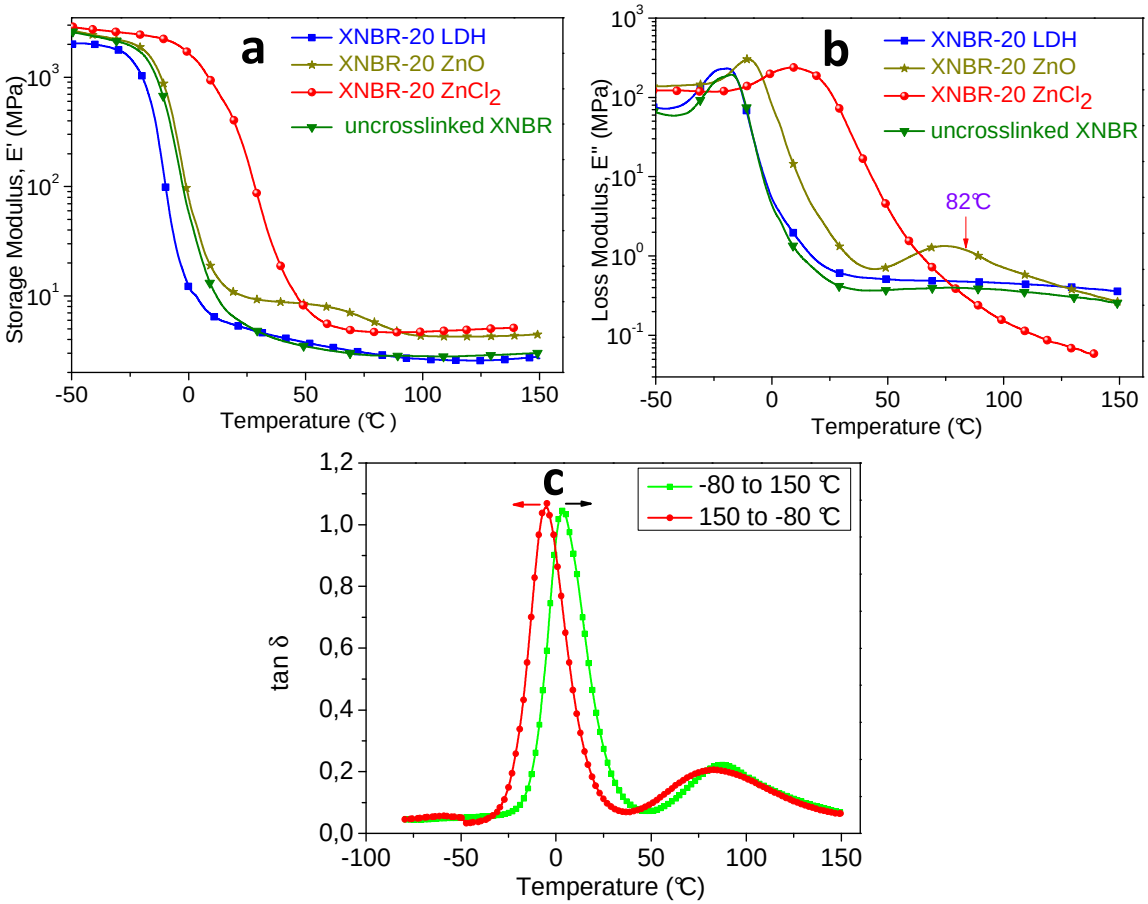

Fig. 4.1.9 Temperature dependence of (a) Storage modulus, (b) Loss modulus of various zinc-containing XNBR composites, (c) Temperature sweep plot in heating and cooling modes (-80 to 150 ° C and 150 to -80 ° C) of XNBR-20 ZnO composite

temperature peak is perhaps due to an in-situ developed zinc-containing polymer phase, as also observed in sulfur less ZnO cross-linked systems. The sulfur molecule does not interfere with the formation "*zinc-carboxylate polymer*" phase. No additional high-temperature peak was observed for LDH-cured compounds, only a slight lowering of the glass transition temperature of XNBR was noticed. Fig. 4.1.9a suggests that all compounds exhibit a rubbery plateau region in the storage modulus (E') vs. temperature plots after the glass transition temperature. The plateau nature explains a well cross-linked character of the rubber matrix cured by different zinc salts. This data is in excellent agreement with the description provided in section 4.1.1.Particularly, in case of the ZnO-cured compound, this plateau is superimposed by a broad peak in the region of 50 to 100 °C. Also, in the loss modulus E'' vs. temperature

plot, the ZnO-cured sample shows a peak in this temperature range (Fig. 4.1.9b). The storage moduli at 100°C of $ZnCl_2$- and ZnO-cured compounds are higher than that of the Zn Al-LDH-cured sample suggesting either a reinforcement effect and/or higher crosslinking densities. The particle nature of ZnO could play a role in slight reinforcement effect; for the $ZnCl_2$ system, an extra coordination type of linkages of the acrylonitrile group present in the structure [97] could offer a higher degree of crosslinking that is reflected in the enhanced storage modulus of the compound. An additional crosslinking process by the nitrile groups, as described by Mou *et al* [97] could be responsible for the shift of the glass transition temperature towards higher temperature.

Reverse temperature sweep analysis, one scan during heating and another during cooling was carried out to obtain a better understanding about this second glass transition behavior. Fig. 4.1.9c shows the tan δ vs. temperature plot obtained from this experiment. Two distinct peaks, one due to the glass transition temperature of the main polymer (XNBR) and another due to the glass transition of the newly formed in-situ co-ordination polymers ("*zinc-carboxylate polymer*"), appear in both directions, proving the reversibility of the co-operative relaxation processes.

4.1.4 Morphology study

From the above studies, it was claimed that the high temperature transition behavior of the ionic elastomer produced by XNBR and ZnO is primarily because of formation of an extra polymer phase at high temperature. In-depth morphological analysis was carried out to investigate the relevance of this claim and establish the true mechanism involved with this phenomenon. Morphological experiments were accomplished by means of transmission electron microscopy and then supported with the help of X-ray diffraction findings. Fig.4.1.10 exhibits the TEM micrographs obtained from XNBR cured by different zinc compounds. Existence of solid particles was realized in ZnO- and LDH-cured matrices (Fig. 4.1.10a & 4.1.10b); however, due to its strong hygroscopic and deliquescent characteristics, $ZnCl_2$ (Fig. 4.1.10c) does not demonstrate the existence of any solid particles. Some portion of area of ZnO-cured XNBR matrix was randomly chosen and subsequently enlarged as shown in Fig. 4.1.7d. This arbitrarily chosen area looks homogeneous and resembles typical block co-polymer morphology. Information on local chemical composition was obtained by utilizing elemental mapping by energy- filtered TEM (Energy Filtered), EELS and EDX spectroscopy. Dohi *et al* [98] have already reported the details of this technique and its usefulness in

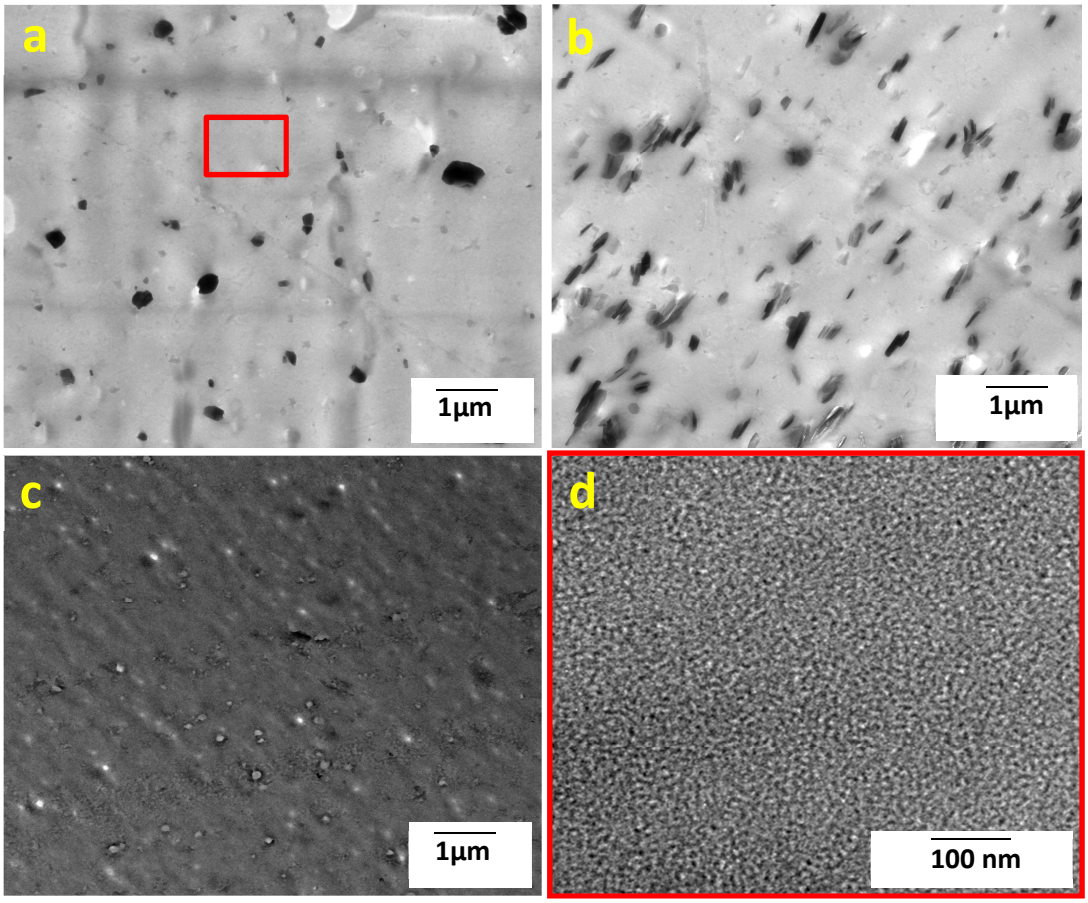

Fig. 4.1.10 Transmission electron micrographs for XNBR cured with a) ZnO, b) LDH, and c) $ZnCl_2$, (in each case the amount of zinc compound is 20 phr) and d) the enlarged portion (red box in a) of an area without any solid XNBR-20 ZnO composite particles

obtaining important information about the chemical structure of a polymer. To ascertain the presence of zinc qualitatively, some portion of the matrix elastomer was randomly chosen (red circles in Fig. 4.1.11) and inspected by the EELS technique in TEM. Furthermore, some randomly chosen area (red rectangles in Fig. 4.1.11) was inspected by the EDX technique in SEM as well. Dissimilarities between the intensities in the energy loss region corresponding to the L_{23} ionization edge in zinc (at 1030 eV) was noticed between the XNBR-ZnO, XNBR-LDH and XNBR-$ZnCl_2$ composites. Spectra obtained in this way clearly suggest that a significant amount of zinc is present in the XNBR matrix in case of both XNBR-ZnO and XNBR-$ZnCl_2$ (Fig. 4.1.11a & c), whereas the presence of zinc can hardly be detected in case of XNBR-LDH composite (Fig. 4.1.11b). Zinc chloride does not retain its crystallinity due to its deliquescent nature, unlike other zinc salts of interest. From the EELS and EDX spectra, therefore, it is obvious that zinc chloride has dissolved in the XNBR matrix to a quite significant extent. The EELS technique allows us to evaluate the localization of zinc in the

polymer matrix with a combination of different types of zinc-containing salts in a comprehensive manner.

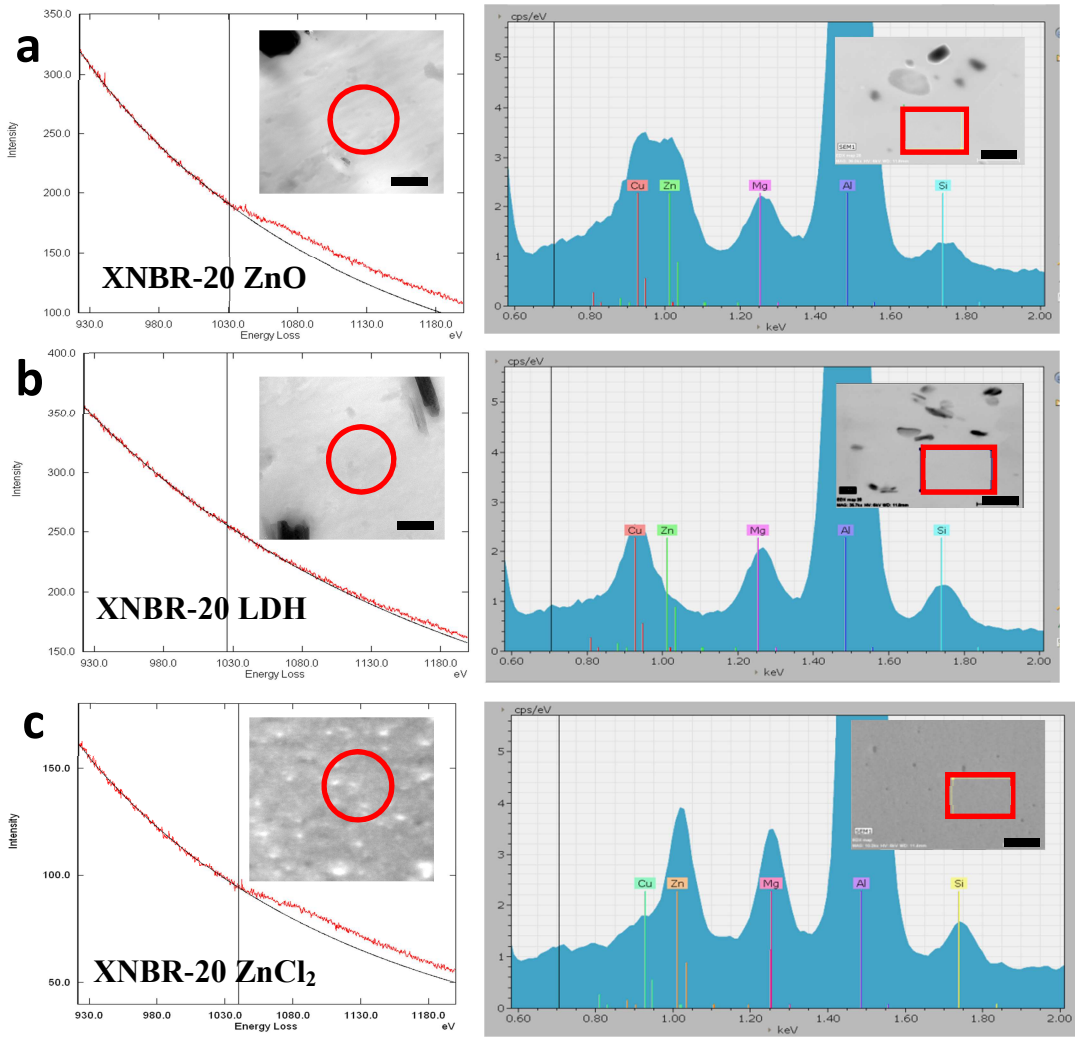

Fig. 4.1.11 EELS (in TEM) and EDX (in SEM) spectra of (a) XNBR-20 ZnO, (b) XNBR-20 LDH, (c) XNBR-20 $ZnCl_2$ composites. Left spectra correspond to EELS and right correspond to EDX. The insets show the marked areas from which the spectra were recorded. In the EELS spectra, the background (black line) is fitted to the region before the Zn-L_{23} ionization edge to highlight the varying content of zinc. The small shifts of the horizontal axis are due to experimental limitations and do not reflect any chemical shift. The peaks in EDX spectra corresponding to Si, Mg, Al, and Cu originate from the specimen holder and do not reflect the compositions of the specimens. (scale bar in TEM images: 200 nm, scale bar in SEM images: 1000 nm)

The dissolution of zinc chloride in the polymer matrix is the primary reason for the presence of zinc observed in EELS analysis. In contrast, ZnO has a strong solid-like presence in the XNBR matrix due to its crystallinity and simultaneously interacts with the carboxylic groups, resulting in a solubilization effect of zinc ions partially in the rubber matrix. This observation

strongly infers that the presence of zinc oxide in the matrix polymer facilitates the formation of the "*zinc-carboxylate polymer*", which is not the case for the other zinc compounds.

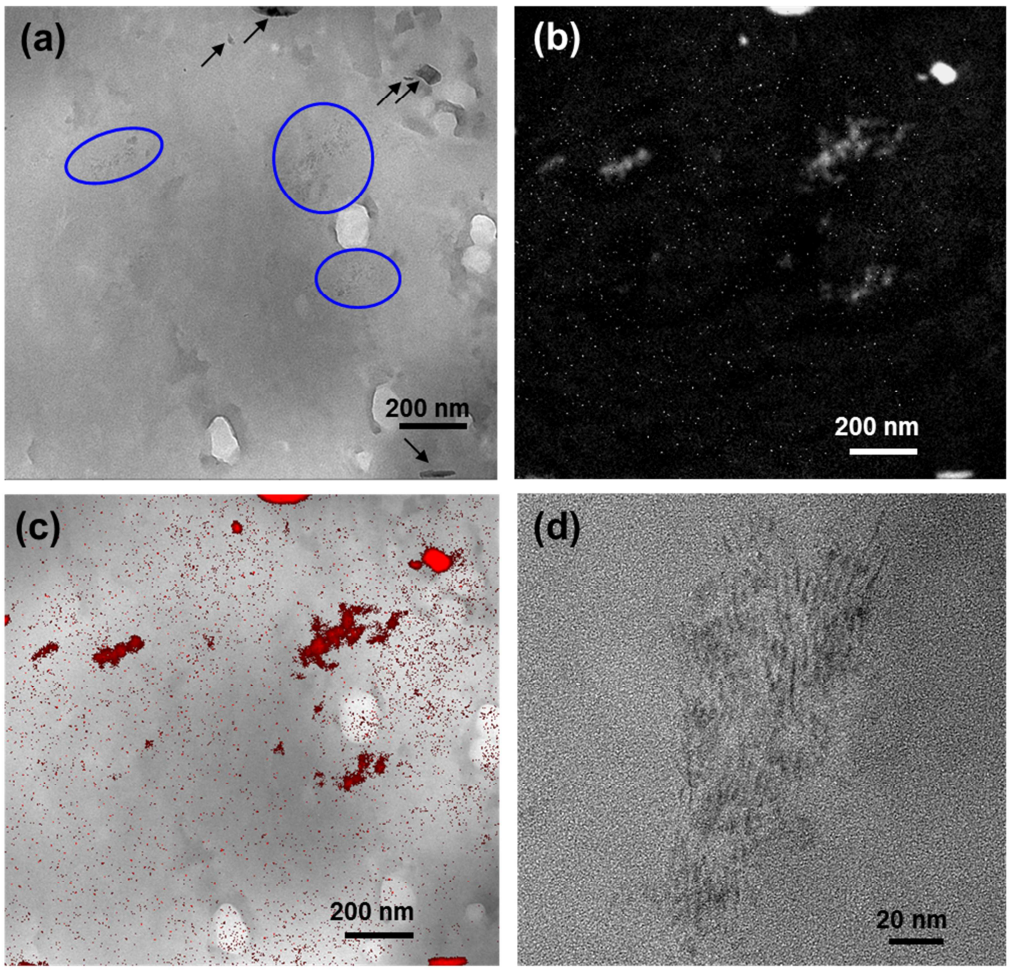

Fig. 4.1.12 (a) TEM image of XNBR-20 ZnO annealed with solvent THF, with solid ZnO particles marked with arrows. (b) Zn map derived from energy-filtered TEM images. (c) TEM image with overlying red-colored Zn map. The Zn-containing lamellar structures are hardly visible in (a) (blue ovals), but their presence is revealed in (b). (d) TEM image of a lamellar structure at high magnification

The presence of zinc in the XNBR matrix could be observed in the molecular distribution of the XNBR-ZnO composites, however, the existence of an in situ formed "*zinc-carboxylate polymer*" phase cannot be observed directly. To achieve a direct evidence of possible formation of an ionic "*zinc-carboxylate polymer*" either in phase-separated blend morphology or another kind of microstructure, the ZnO cross-linked samples were solvent annealed to enhance the structure formation for direct visualization in TEM studies. The samples were swelled in three different solvents (THF, toluene and dichloromethane) for 5 h at 70 °C and

then dried for 3 days. The high resolutionTEM micrographs of a tetrahydrofuran (THF)-treated sample (Fig. 4.1.12) clearly ascertain some regions of phase-separated lamellar morphology in short-range order, with a periodicity of the lamellae in the range of 3.5 - 4.5 nm (measured on several randomly selected regions). This observation leads us to conclude

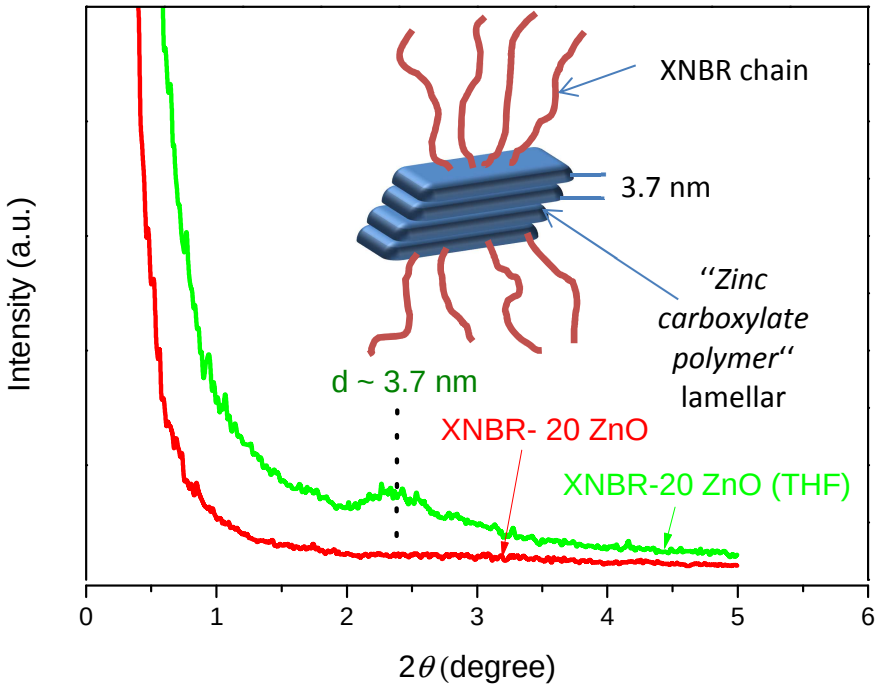

Fig. 4.1.13 XRD profiles of the original XNBR−ZnO and the same composite treated in tetrahydrofuran solvent. The inset shows the lamellar structure (periodicity ~ 3.7 nm) of the "*zinc-carboxylate polymer*"

about the formation of the "*zinc-carboxylate polymer*" evolving in-situ inside the XNBR matrix because of the ionic interaction between zinc from ZnO and carboxylic groups from XNBR, eventually yielding zinc carboxylate polymeric material. This type of phase-separated lamellar morphology was not at all visualized in the other two composites, XNBR-LDH and XNBR-$ZnCl_2$.

The short range order in the TEM micrographs could not provide us strong information about the periodicity of the lamellae. Therefore, the exact molecular order of the ionic phase of XNBR was examined using conventional X-ray diffraction (XRD) technique. A vulcanized rubber sample (ZnO cured XNBR) pre and post solvent-annealing were used in this study. Fig. 4.1.13 clearly illustrates that the sample of XNBR-20 ZnO after solvent annealing shows a very broad diffraction peak in the 2θ range of 2−3° with a corresponding domain length of 3.7 nm but, the same sample without solvent annealing does not exhibit such pattern. Both qualitative and quantitative informations were obtained suggesting about the formation of

certain kind of lamellar structure of the ionic phase inside the rubber (inset of Fig. 4.1.13. In most of the usual cases, the periodicity of a lamellar morphology of a block copolymer is

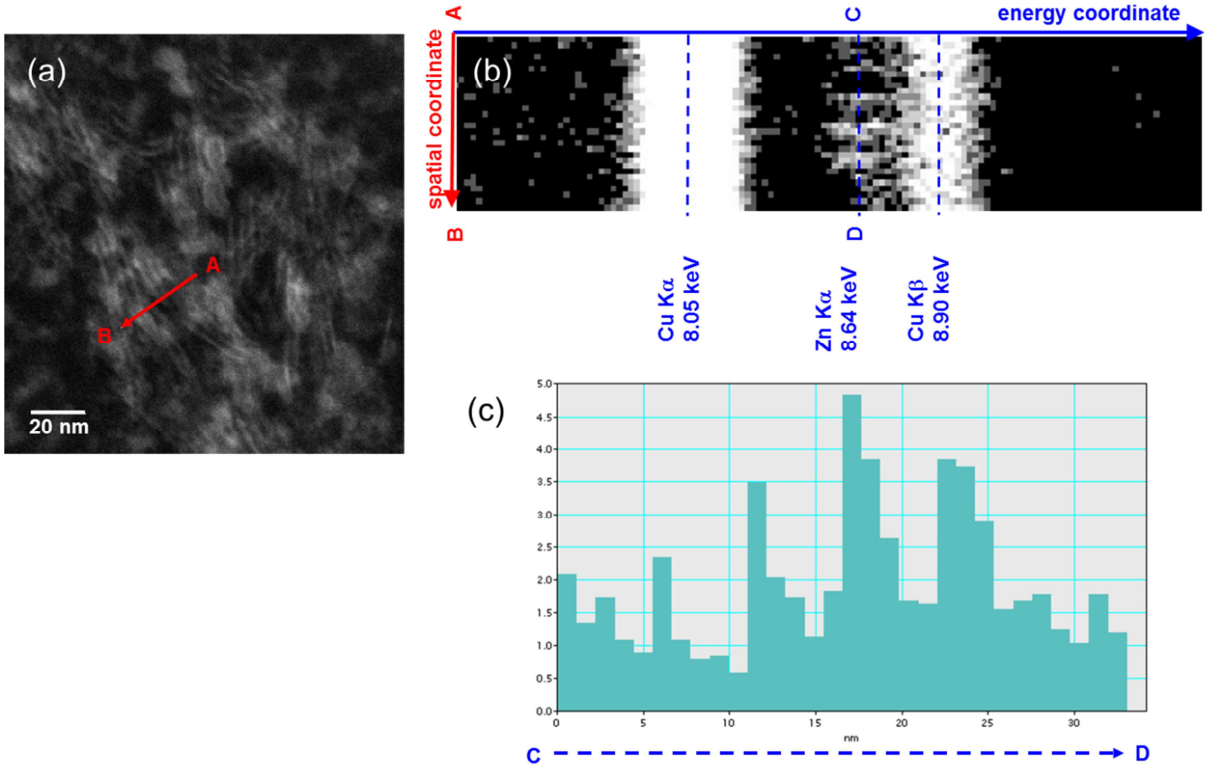

Fig. 4.1.14 (a) Scanning-TEM image of a lamellar structure in a ZnO-cured XNBR specimen (amount of ZnO is 20 phr). The EDX spectra were measured in 30 points along line A-B. (b) Thirty EDX spectra along line A-B displayed as a grey-level image in log scale. The periodic variation of Zn-K_α peak intensity along line C-D is clearly visible. (The Cu peaks originate from the specimen-supporting grid.) (c) Variation of Zn-K_α peak intensity (integrated from 8.58 to 8.78 keV) along line C-D, which reflects the periodic variation of zinc concentration along line A-B in (a)

larger than the value obtained in our case. As for example, poly (styrene-block-methyl methacrylate) under suitable conditions forms lamellar morphology with a lamellar thickness of ~50 nm which is nearly 14 times larger than the present case [99] .The thickness of the lamella of a block copolymer is primarily governed by the molecular weight and composition of the block. Here, zinc containing polymer is established in a cross-linked environment where the chain movements are restricted by the cross-links points resulting a finer layer thickness of the lamellar domain as visualized in the smaller viewing area in TEM images.

Moreover, the elemental distribution within the lamellar microstructure was qualitatively analyzed further by EDX line scans for zinc on the cross-section of the material (Fig. 4.1.14). The TEM cross-section micrograph in this study, ascertains about the periodic variation of the concentration of zinc ions across the lamellar structures in the material. This observation

ensures that the new polymer phase developed by the reaction between zinc oxide and XNBR is associated with higher concentration of zinc ions. The elemental distribution profiles along the cross section illustrated in Fig. 4.1.14 reveals a periodic variation of zinc concentration along the line A to B. Therefore, opportunity is there to hypothesize that the in-situ developed "*zinc-carboxylate polymer*" is immiscible with the acrylonitrile butadiene random copolymer chains and this incompatibility between the newly formed polymer and parent polymer develops a microphase-separated periodic structure of the polymer matrix. After solvent annealing of the rubber sample, the two types of the polymer chains are arranged in such a way that largely resembles typical block co-polymer morphology with similar block lengths.

4.1.5 Relaxation dynamics of different zinc compounds with XNBR

The primary reason for delayed elastic response in rubbery solids is internal friction between the molecular chains of the polymer (viscosity). With temperature, the small segments of the rubber molecule shift to new positions with a specific rate (φ) strongly controlled by random Brownian motion. The magnitude of φ increases with the elevation in temperature. Consequently, the energy dissipation as well as the internal viscosity decrease at elevated temperatures. Owing to the co-ordination chemistry involved with different types of zinc compounds, the resulting network structures usually show unclassical relaxation while subjected to mechanical deformation and heat. To investigate and understand this anomaly of behavior in the dynamic mechanical spectra of ionic elastomer formed with same matrix polymer but different types of zinc sources, dynamic-mechanical master curves were compiled using the time-temperature superposition principle in a broad frequency region. The dynamic mechanical spectra measured at different frequencies and temperatures were shifted with respect to the reference temperature (25 °C) according to the Williams-Landel-Ferry (WLF) equation:

$$\log\left[\frac{\varphi(T)}{\varphi(T_0)}\right] = \log a_T = \frac{-C_1(T-T_0)}{C_2+(T-T_0)} \qquad (4.6)$$

where a_T is the shift factor, C_1 and C_2 are the so-called WLF constants and T_0 is the reference temperature. This equation was based on the free volume theory that can also be derived from the Doolittle equation. If f_0 is the fractional free volume and α_f is the co-efficient of thermal expansion then C_1 and C_2 correspond to $B/2.303\, f_0$ and f_0/α_f respectively. Here, B is a constant used in the Doolittle equation and for suspension with hard

sphere particles its value is 0.57 [100]. In the present case, for simplicity, it is set equal to unity (B ~ 1). The above equation also could be expressed in VF (Vogel-Fulcher) form. If $C_1 = {\Delta E \cdot \log(e)}/{R \cdot (T_0 - T_{VF})}$ and $C_2 = T_0 T_{VF}$, then WLF can be reduced to VF form:

$$f = f_0 . e^{-\Delta E / R.(T - T_{VF})} \qquad (4.7)$$

.

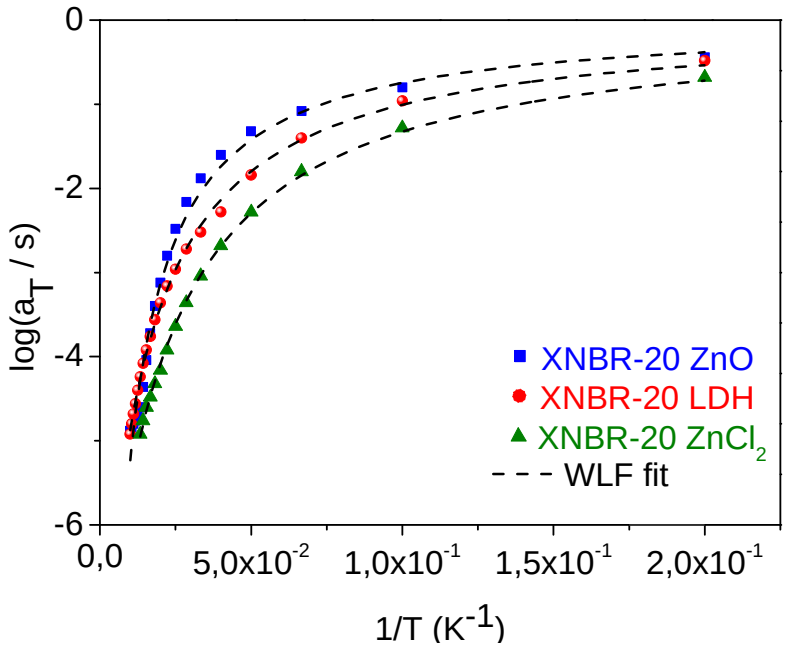

Fig. 4.1.15 Plot of frequency shift factor (a_T) vs. 1/T. The solid line shown in the graph is the best fit WLF equation to the a_T values for XNBR treated with different types of zinc compounds

where f_0 is the frequency when T→∞, ΔE is the activation energy when T→∞, T_{VF} is the Vogel-Fulcher temperature, and R is the gas constant. So by the evaluation of C_1 and C_2 values derived from WLF equation the three VFT parameters (T_{VF}, f_0, and ΔE) can be evaluated.

After fitting the WLF equation (Fig. 4.1.15), the values of various derived parameters obtained from the XNBR composites are listed in table 4.1.2. The C_1 and C_2 values of XNBR composites cured with Zn Al-LDH and $ZnCl_2$ are in a similar range, but the values are much higher for ZnO-cured rubber. The C_2 value of XNBR filled with $ZnCl_2$ is smaller than that of the ZnO system. The derived parameter from these WLF factors yielded the free volume at a comparable range, but the thermal expansion coefficient of ZnO-filled compounds is almost ≈ 5-8 times higher than those of the other two systems. However, the fractional free volume of ZnO-cured rubber is almost half those of the LDH- and $ZnCl_2$-based systems. The data

showed that Vogel - Fulcher temperature (TVF) is specific for final crosslinked materials and indicates the temperature at the relaxation times of the polymer in running cooperative relaxation processes converge to infinity. The calculated activation energy after fitting the equation was higher for ZnO-containing systems than those of other systems, which may be due to "*zinc-carboxylate polymer*" formation. In the master curves (Fig. 4.1.16), ZnO-cured XNBR sample shows two distinct relaxation processes, one at 10^{-3} Hz frequency and

Table 4.1.2 WLF and VFT parameters of various XNBR composites

Sample designation	C_1	C_2	f_0	α_f (K^{-1})	T_{VF} (K)	ΔE (kJ/mole)
XNBR – 20 ZnO	15.84	202.56	0.0274	1.4×10^{-4}	90.4	61.34
XNBR – 20 LDH	8.52	74.8	0.0510	6.8×10^{-4}	218.2	12.18
XNBR – 20 $ZnCl_2$	8.54	54.49	0.0508	9.3×10^{-4}	238.5	8.89

the other at 10^{3} Hz frequency in the tan δ vs. frequency plot. These two relaxation processes were already observed and discussed in the studies of temperature-dependent dynamic properties. In the rubber glass transition regime, a change of the slope is observed in the plot of storage modulus versus frequency (Fig. 4.1.16). The slope of the $ZnCl_2$-filled sample is $E' \propto f^{3/4}$, whereas, for ZnO- and LDH-filled materials, nearly identical values with a slope of $E' \propto f^{3/6}$ are observed. Stöckelhuber *et al* [101] also found similar changes of slope in a study of silica-filled solution styrene butadiene rubber (S-SBR) composites. In this report, the slope for unfilled rubber was $E' \propto f^{3/4}$, which exactly matches our $ZnCl_2$-filled rubber compounds. For silica-filled compounds, the value was $E' \propto f^{3/8}$, which is less steep than those of gum rubber compounds. According to Vilgis [102-103], such an effect is described as a restricted movement of the semi-flexible chain by adsorption or chemical linkage of chain segments. In our case, due to deliquescent nature of $ZnCl_2$, these samples are hypothesized to behave like unfilled composites, while ZnO and LDH show behavior typical of filled rubber composites. Most likely, $ZnCl_2$-cured composites do not exhibit a solid-like phase in the XNBR matrix; therefore, no hydrodynamic reinforcement is expected.

In contrast, because of their particle nature, LDH and ZnO can adsorb rubber chains on their surfaces and form an interphase between solid particles and polymer matrix. As far as the morphology of the XNBR matrix is concerned, no evidence of $ZnCl_2$ particles has been

observed. However, very small particles of LDH and ZnO with different size and shapes can be easily traced out. ZnO has high-temperature relaxation due to the formation of a zinc carboxylate polymer, resulting from zinc-carboxylate crosslinking but not owing to the chemical interaction on the surface of an individual ZnO particle itself.

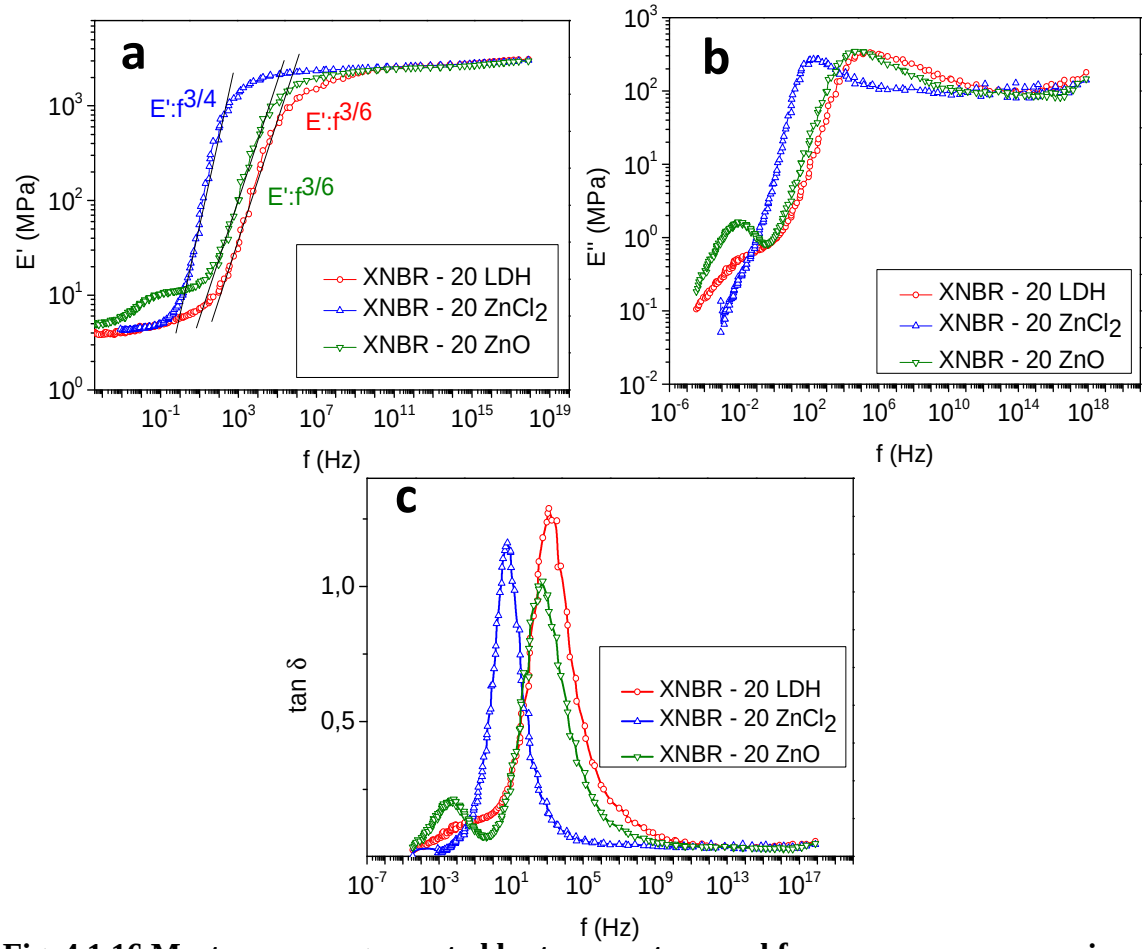

Fig. 4.1.16 Master curves generated by temperature and frequency sweep experiments for different XNBR composites. Dynamic a) storage modulus, b) loss modulus, and c) loss tangent are plotted against the frequency

4.2 Zinc containing LDH as a potential filler for carboxylated nitrile rubber

In the previous section, we discussed elaborately about the fundamental aspects of the ionomeric properties evolved from the of carboxylated nitrile rubber cured with different types of zinc salts. Different mechanistic pathways between the XNBR cured with zinc oxide and other sorts of zinc sources were thoroughly investigated and interpreted. Use of modified Zn Al LDH can reduce [104] the need for zinc oxide in sulfur vulcanization of the di-ene rubbers [10, 12], which is less toxic for aquatic species. The refinement of the structures of this clay material can be easily done in the laboratory as per the requirements of the ultimate properties of the nanocomposites. The cost of synthesis and modification of this nano clay is also relatively lower, and the ease of processability, greater. Furthermore, Zn Al LDH, by the

virtue of possessing zinc atom in the structure can effectively cure some rubbers to a very significant extent [10-12, 14, 42, 105]. Mechanical reinforcement is evidently realized in nitrile rubber compounds because of excellent state of dispersion of layered double hydroxide. Additionally, this inorganic clay material offers other smart properties like, optical properties [48], and flame retardancy [52, 56] in the rubber compounds as well. Rubber compounds made of LDH could be used in the production of green tires and they could be used to create tires with intelligent properties such as thermotropicity, without compromising the other fundamental properties. Therefore, the effects of layered double hydroxide (LDH) as multifunctional filler for rubber materials are explored in this section within the scope of the study.

4.2.1 Curing study

The rheometric characteristics of the rubber compounds based on XNBR and different amounts of LDH are demonstrated in Fig. 4.2.1. Firstly, it is quite obvious from Fig. 4.2.1 that in spite of being unmodified in nature (see table 3.5 for the composition of the corresponding rubber compounds), Zn-Al LDH can effectively cure the XNBR matrix significantly.

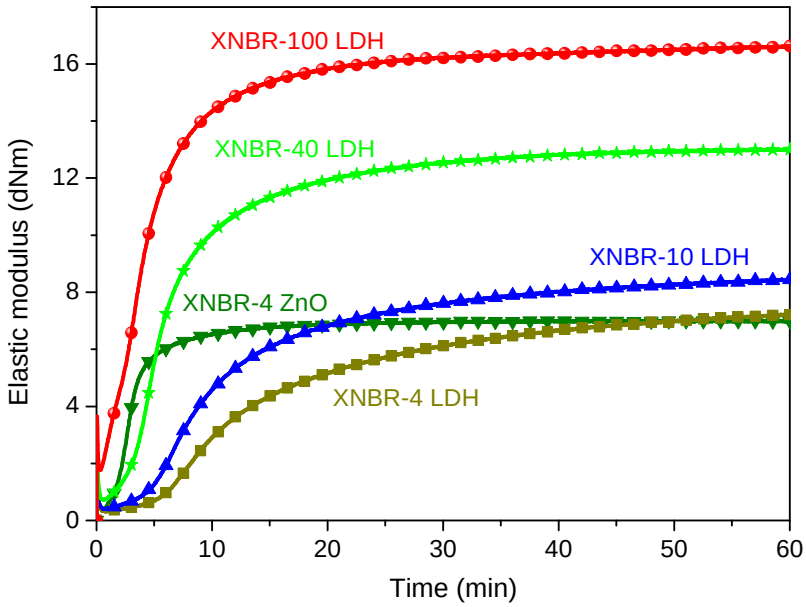

Fig. 4.2.1 Rheometric plots of the XNBR compounds cured with different amounts of LDH

Very small amount of ZnO and LDH (4 phr each) yielded almost same torque value in the curing curve. But, the development of the torque was slightly faster in case of ZnO than LDH. Unmodified clay varies the cure characteristics of the rubber to a significant extent as clear from the gradual increase in the elastic modulus values with the increase in LDH content in

the compounds. The enhancement in torque attributes to an excellent compatibility between the unmodified clay and polar rubber. Another important factor accounting for supreme vulcanizing characteristics of the compounds is the crosslinking density. Dual crosslinking reactions take place when XNBR is cured with Zn-Al LDH in the presence of sulfur additives; the ionic crosslinking between carboxylic group and zinc ions, the other one is covalent crosslinking through sulfidic linkages (mono-sulfidic, di-sulfidic or poly-sulfidic) between two unsaturated rubber chains. Since the zinc is present here in two different chemical structures, the mechanistic pathways of the vulcanization reaction would be different. Curing kinetics between these two types of zinc molecules with XNBR is discussed in details in section 4.1.1.

4.2.2 Swelling study (crosslink density determination)

In order to investigate the increasing trend of the rheometric torque of the XNBR compounds with the increased loading of LDH, swelling analysis was carried out. The crosslinking parameters according to Flory-Rehner equation are summarized in table 4.2.1. It is assumed that, with an increase in the amount of LDH, the zinc content of the compound is consequently increased; therefore, the covalent crosslinking activated by sulfur is also increased by the formation of active sulfurating complex [106-108] that eventually results in overall higher crosslinking density. Ionic crosslinking also takes place courtesy to the

Table 4.2.1 Crosslinking parameters (V_r = volume fraction of rubber, V_c = total crosslink density, V_A = covalent crosslink density and ΔV = % ionic crosslinking) of the XNBR composites

Samples	V_r (%)	$V_c \times 10^5$ (mol /cm^3)	$V_A \times 10^5$ (mol /cm^3)	Ionic crosslinking (ΔV) (%)
XNBR – 4 ZnO	0.3169	7.25	4.98	31.3
XNBR – 4 LDH	0.2798	4.87	3.31	32.1
XNBR – 10 LDH	0.3027	6.26	4.27	31.7
XNBR – 40 LDH	0.3247	7.87	5.41	31.2
XNBR – 100 LDH	0.3344	8.68	5.99	30.9

interaction between the zinc atoms of LDH and the carboxylic functional group of XNBR molecule. Treatment with saturated ammonia vapour neutralizes the ionic crosslinking. Therefore, the ammonia-treated sample can be utilized to estimate only the crosslinking degree formed by sulfur bridges. By subtraction of these values from the overall crosslinking degree, the ionic crosslinking degree can be estimated. Interestingly, the percentage ionic crosslinking calculated for different XNBR composites are nearly identical: 31 ± 1%. . This finding indicates that the degree of ionic crosslinking depends on the total available carboxylic groups present in the XNBR polymer chain backbone.

4.2.3 Fourier transform infrared (FTIR) spectroscopy

The chemical interaction between the two different types of zinc molecules, zinc oxide and Zn-Al LDH has been discussed in details in section 4.1.2. For an intensive understanding about the chemical interaction between XNBR and LDH and subsequently correlate with the physical properties of the corresponding composites, a rubber compound was prepared in which Zn-Al LDH was replaced with Mg -Al LDH (same amount). Other mixing ingredients and their amounts were kept fixed. Fig. 4.2.2 clearly reveals that the characteristic peaks at 1727 cm^{-1} and 1697 cm^{-1} attributing to the -C=O stretching vibration of free carboxylic group in uncrosslinked XNBR are also found in case of composites cured with Zn-Al LDH as well as Mg-Al LDH but with lower intensities. These peaks quite expectedly disappear in the XNBR – ZnO compound due to the formation of zinc carboxylate complex (peaks at 1535

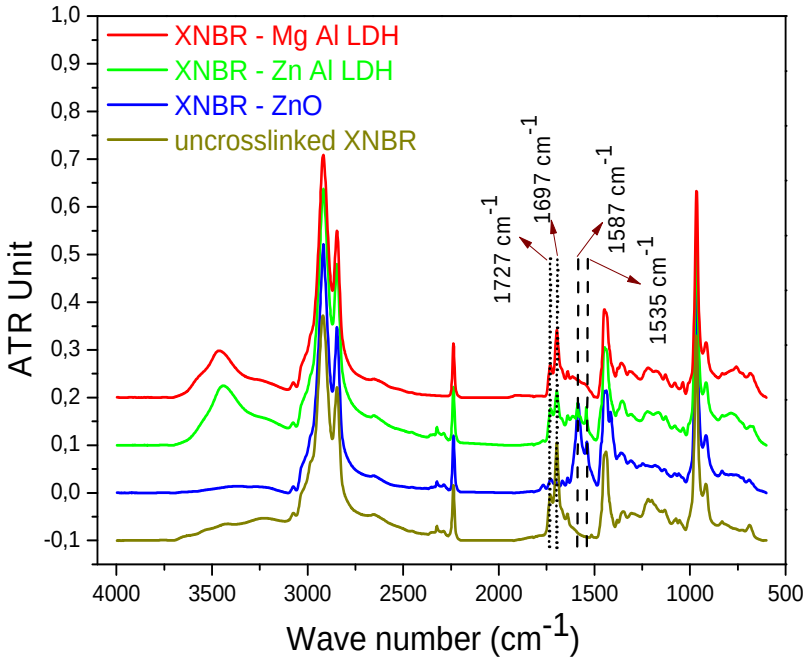

Fig. 4.2.2 FTIR spectra of the uncrosslinked XNBR and its compounds

cm^{-1} and 1587 cm^{-1}) with different stoichiometric configurations (syn-syn and syn-anti). In the FTIR spectra of the XNBR – Mg-Al LDH sample, no such strong interaction of the carboxylic group of XNBR and LDH particles has been observed. This suggests that the chemical interaction between Zn-Al LDH and XNBR is compatible in nature and therefore allows the LDH particles to be dispersed very nicely in the XNBR matrix. The situation could be compared with a rubber system filled with silica along with a silica coupling agent where a direct chemical interaction is established between silica and rubber chains.

4.2.4 Morphological analysis

The state of dispersion of high amount of LDH (40 and 100 phr) in XNBR matrix was investigated by transmission electron microscopy technique. Fig. 4.2.3 illustrates that in spite of large amount of clay material incorporated into the rubber, no tendency of agglomeration was evident. The LDH particles show a typical stacked compact structure and are not in intercalated or exfoliated form Most of the particles are well dispersed even at 100 phr loading, and do not tend to form a filler network. This phenomenon is very unusual with highly filled systems. Uniform and homogeneous dispersion of the unmodified LDH particles along with a chemical coupling with the rubber chains account for improved curing behavior of the composite. Moreover, lack of agglomerate formation in the composite could pave the way towards mechanical reinforcement induced by higher amount of LDH.

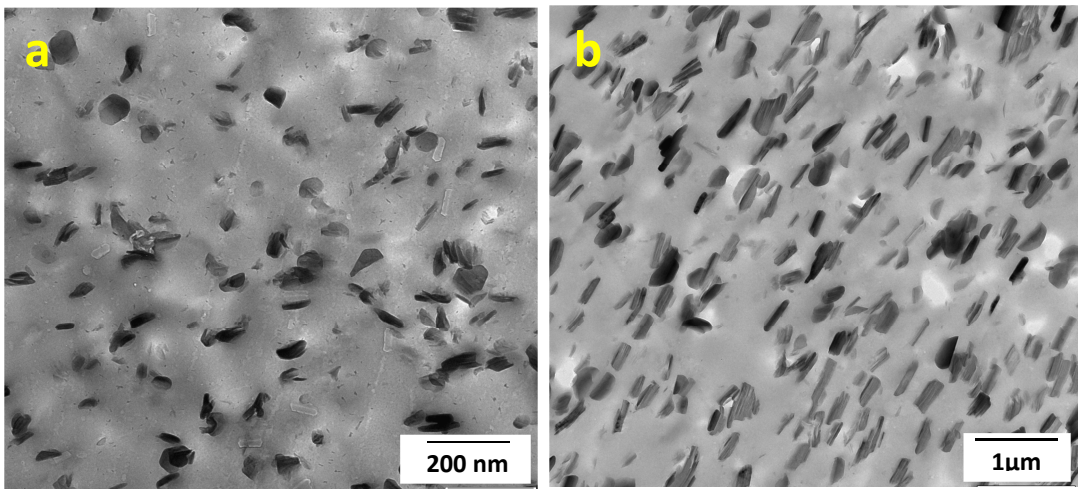

Fig. 4.2.3 TEM micrographs of (a) XNBR – 40 LDH and (b) XNBR – 100 LDH composites

4.2.5 Dynamic mechanical analysis

There was clearly no direct trace of filler-filler interaction in the highly loaded rubber samples in the TEM micrograph. Furthermore, amplitude sweep analysis was carried out in the dynamic mechanical apparatus to offer more evidence supporting this statement. Comparative analysis was done between XNBR – Zn -Al LDH and XNBR – Mg -Al LDH composites in order to check and interpret the nature of rubber – filler and filler – filler interactions between the fillers comprised of two different metal atoms. It should be noted here that the density of Zn-Al LDH and Mg-Al LDH were almost similar which make the composites with same

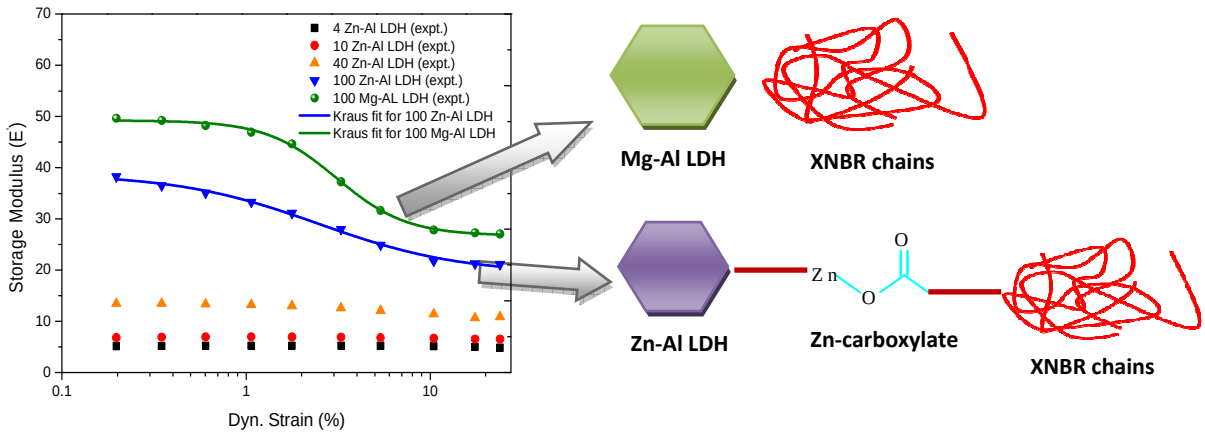

Fig. 4.2.4 Amplitude sweep data of XNBR-LDH composites, storage modulus (E') values fitted according to the Kraus model. A schematic corresponds to different types of interaction between XNBR and LDH

volume fraction of the fillers. The amount of Zn-Al LDH and Mg-Al LDH mixed with XNBR for this study is 100 phr. For this purpose a phenomenological model, namely, Kraus model [109] was employed. This model elucidates a quantitative idea about the agglomeration-deagglomeration mechanism [110]. The so-called Kraus eqn. in terms of storage modulus (E') is provided as follows:

$$\frac{E'(\gamma)-E'_{\infty}}{E'_{0}-E'_{\infty}}=\frac{1}{1+\left(\frac{\gamma}{\gamma_c}\right)^{2m}} \qquad (4.8)$$

Where, $E'_{\infty}=E'(\gamma_0)$ for very large strain; $E'_{0}=E'(\gamma_0)$ for very low strain; γ_c = characteristic shear strain amplitude termed as critical strain; $E'_{0}-E'_{\infty}$ = quantitative measure of the Payne effect determined from the amplitude sweep plot; m = constant which is related to specific fractal dimensions of the fractal agglomerate structures. m is mainly a geometric quantity of the filler network and its agglomerates. Report suggests that the constants γ_c and m are

completely independent of the matrix polymer, the state of the dispersion of the filler in polymer matrix and the type of filler [109]. The magnitude of critical strain (γ_c) largely depends on the nature of the filler-filler networks. Stronger is the bond, more strain is necessary to break the network. It is estimated that γ_c obtained from Zn-Al LDH (γ_c = 2.48) is

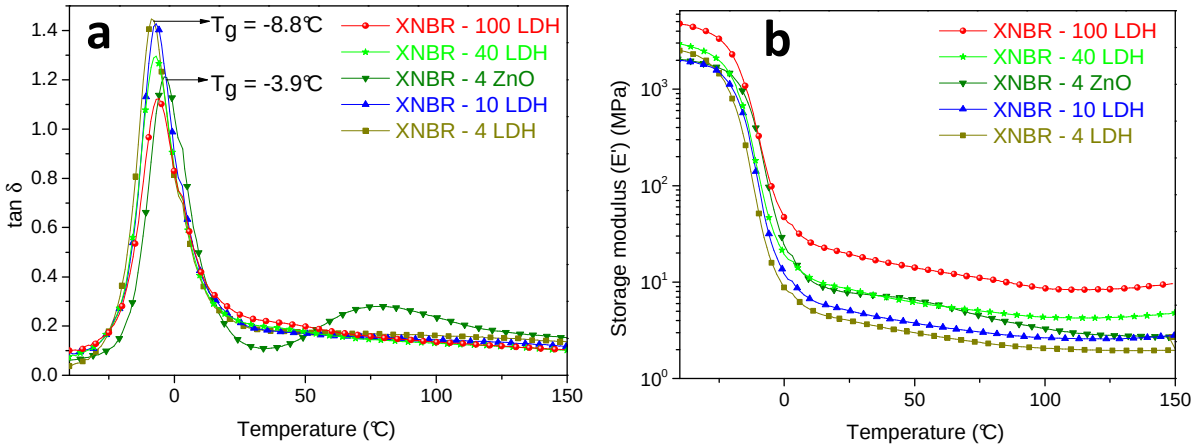

Fig. 4.2.5 Dynamic mechanical spectra of XNBR based composites, (a) tan δ vs. temperature and (b) storage modulus (E') vs. temperature

smaller than Mg-Al LDH (γ_c = 3.10) indicating more strong filler-filler network of LDH particles comprised with Mg and Al (Fig. 4.2.4). Absence of zinc metal atom in Mg-Al LDH do not contribute to any direct coupling between the filler particles with the rubber chains whereas zinc ions present in the Zn-Al LDH crystals interact with the carboxylic group of the rubber chains and more rubber filler interactions are established at the expense of filler-filler interactions. Fig. 4.2.5 exhibits the temperature sweep plot obtained from DMA analysis. XNBR compound mixed with 4 phr LDH shows slightly lower T_g (-8.8 °C) compared to XNBR mixed with 4 phr ZnO (-3.9 °C) (Fig. 4.2.5a). A more rigid network structure formed due to higher crosslink density of XNBR-ZnO compound leads to the shifting of the glass transition temperature to higher temperature in comparison with XNBR-LDH compound (see table 4.2.1 for the respective crosslink density values). Marginal decrease in the peak heights of tan δ was noticed for the XNBR compounds filled with higher amounts of LDH. Furthermore, the storage modulus in the rubbery plateau region is also observed to gradually increase with the higher loading of LDH (Fig. 4.2.5b). Therefore, the enhancement of mechanical strength of the rubber vulcanizates is confirmed as the filler (LDH) loading is increased indicating the significance of the effect of rubber–filler reinforcement at higher loading of LDH. Appearance of an additional peak in the range of 50 °C to 110 °C for XNBR – ZnO compound is discussed in details in the section 4.1.

4.2.6 Mechanical properties

The tensile properties of XNBR/LDH composites under uniaxial stress are demonstrated in Fig. 4.2.6. It is quite apparent that uncrosslinked XNBR has inferior mechanical properties due to lack of network formation. However, the pristine XNBR rubber is highly stretchable

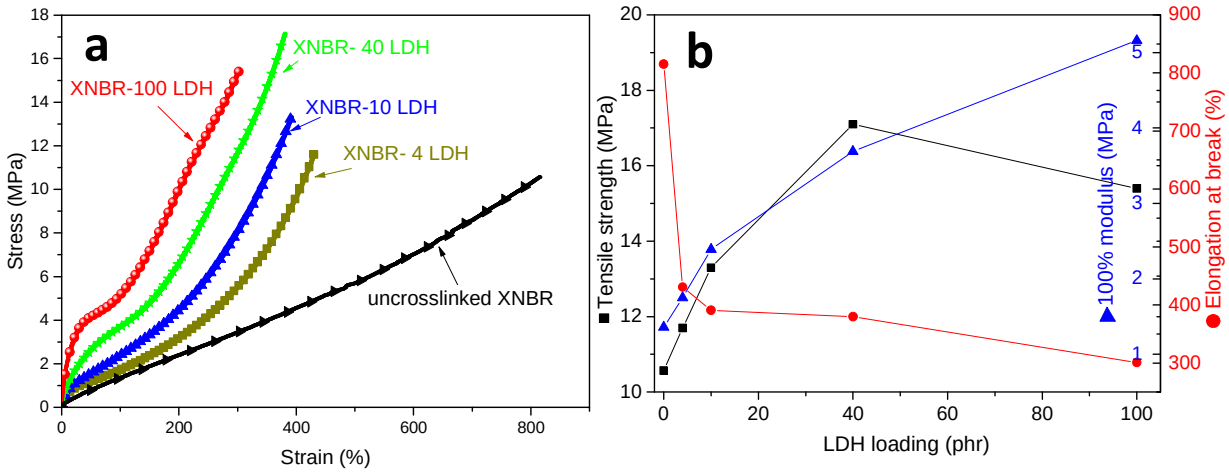

Fig. 4.2.6 (a) Stress-strain plots of the uncrosslinked XNBR and XNBR-LDH composites, (b) variation of mechanical properties for different loadings of LDH in XNBR

(up to ~ 800%). The composites filled with LDH have much improved mechanical properties in the form of stresses at 100%, 200% strains and tensile strength as compared to XNBR gum compound. It is believed that the incorporation of LDH in XNBR matrix imparts reinforcement due to the hydrodynamic effect [46] and the interfacial interaction between the XNBR matrix and LDH particles [44, 46, 53]. Quite expectedly, the elongations at break values are observed to decrease with the increase of 100% modulus values. It can also be found that the tensile strength of the composite increases up to a certain loading (40 phr) of LDH and then drops. The incorporation of the LDH in the rubber matrix restrains the free mobility of the polymer chains through the formation of chemical bonding between them [46], enhancing thereby the stiffness of the composites. The increase in tensile strength and 100% modulus suggests that the composite is strengthened and toughened simultaneously by increasing the concentration of LDH.

4.2.7 Thermal analysis

Thermogravimetric analysis (TGA) analysis provides fruitful informations about the thermal stability of composites and potential char formation capability of the filler material. Thermograms displayed in Fig. 4.2.7 clearly reveal that the onset degradation temperature is

higher in case of LDH mixed XNBR composites than the pristine LDH. A clear trend of increasing % char residue amount was noticed for higher loading of LDH in XNBR. The thermal stability of the composites did not improve by a greater margin with the variation of the loading of LDH material. The thermal decomposition of the uncrosslinked XNBR (gum)

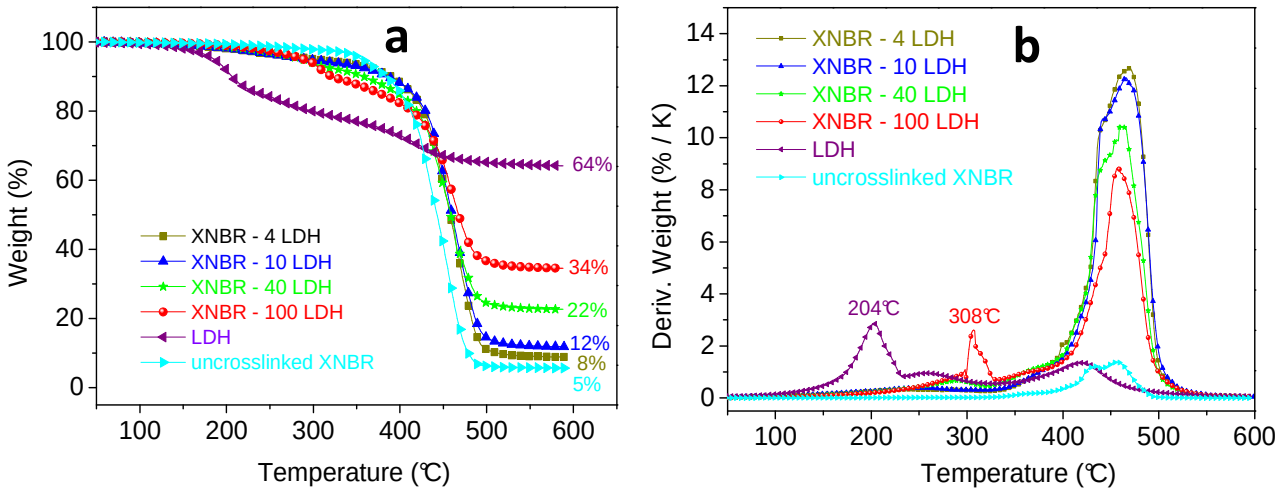

Fig. 4.2.7 (a) Thermogravimetric analysis (TGA) and (b) differential thermal gravimetric (DTG) plots of pristine LDH, uncrosslinked XNBR and its composites

characterized by the major weight loss in the temperature range of 400-500 °C (about 90 % weight loss occurs at this temperature region). In the differential thermogram, this region is demonstrated as a relatively broader decomposition peak ranging from 425 °C to 490 °C. At this temperature range, oxidative degradation of the hydrocarbon chains of the XNBR polymer takes place. For pristine LDH (unmodified form) two-stage decomposition process takes place. At low temperature (around 204 °C) interlayer water is desorbed [95] and a corresponding peak is generated (Fig. 4.2.7b); whereas, at the higher temperature decomposition (250–450 °C) occurs due to the loss of interlayer carbonate and dehydroxylation of the metal hydroxide layer [110] present in the interlayer spacing of the LDH structure (see section 2.1.1.1). Presence of an extra peak around 308 °C is realized from the DTG plot shown in Fig. 4.2.7b for XNBR – 100 LDH. This peak is attributed to the partial loss of water molecules intercalated into the layers of the said composite [111]. It is therefore clearly understood that in case of the highest loaded (100 phr LDH) composite specimen, maximum amount of water molecules are accommodated. The presence of more volume of water molecules for XNBR – 100 LDH facilitates the flame retardancy behaviour which will be discussed elaborately in the following sub-section.

4.2.8 Flame retardancy test

The flame retardancy of the XNBR-LDH rubber composites was interpreted in terms of its heat release properties (like, heat release rate, i.e., HRR and its maximum, i.e., PHRR and total heat released, i.e., THR). To measure these properties, cone calorimeter was used as a universal approach to ranking and comparing the fire behaviours of materials to predict the behaviour of materials in a real fire [112]. A very significant parameter monitored during this test is heat release rate (HRR) that is calculated from the amount of oxygen consumed during combustion based on the principle described by Huggett [113]. The results obtained from HRR provide informations regarding the size of the fire and how fast it grows. Fig. 4.2.8a illustrates that the addition and subsequent increase in the LDH loadings in XNBR not only substantially reduces the peak heat release rate (PHRR) but also increasingly flattens the HRR curve to a significant extent. Primary reason behind this behaviour is decreasing burning rate

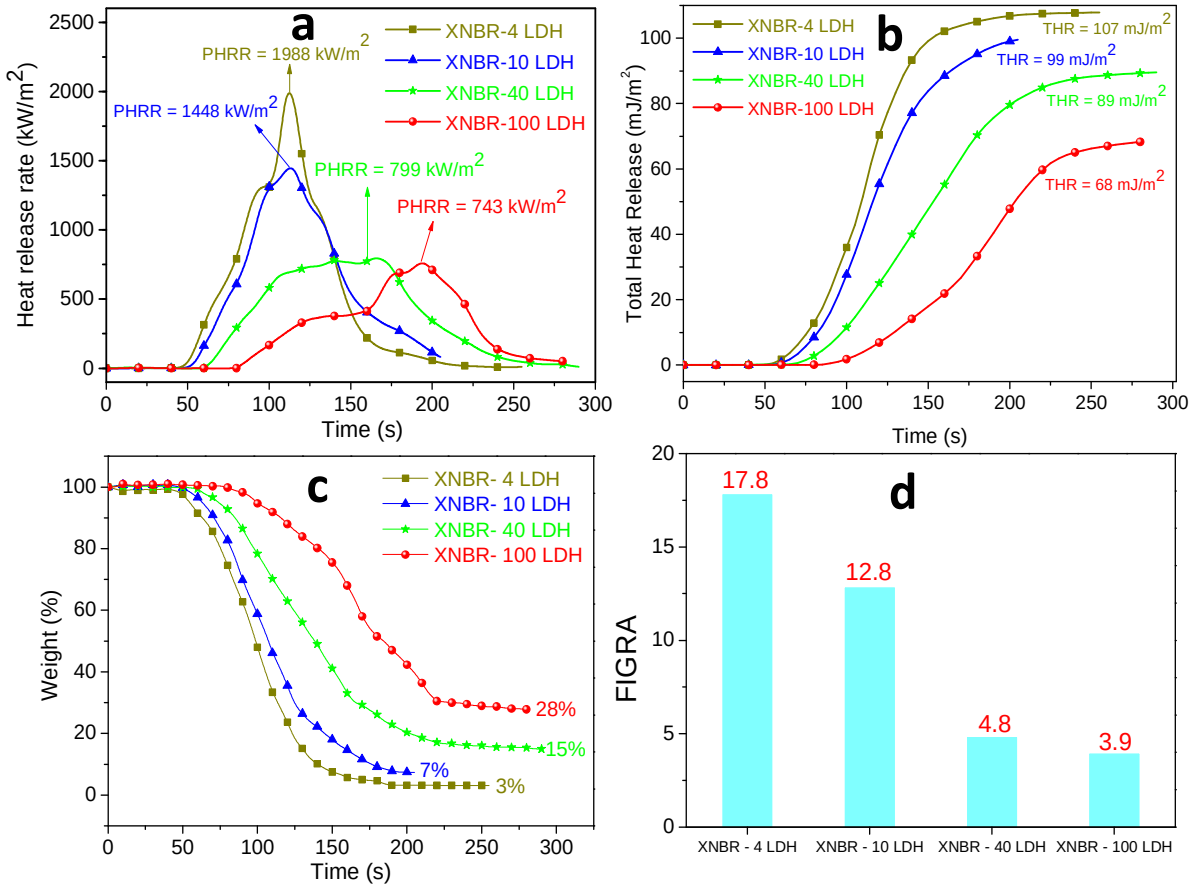

Fig. 4.2.8 Comparison of (a) Heat Release Rate (HRR), (b) Total Heat Released (THR) and (c) mass loss estimated from cone calorimeter and (d) Fire Growth Rate (FIGRA) between all the XNBR-LDH composites

of the materials with increasing LDH concentration. XNBR mixed with only 4 phr of LDH gives the peak heat release rate value of 1988 kW/m^2, however, at higher loading of LDH i.e.,

40 phr and 100 phr, PHRR is almost lowered by the margin of 2.5 times and the ultimate value reaches approximately 800 kW/m^2.

Another important parameter is total heat released (THR) which indicates how intensified the fire is. After the ignition of the test materials, THR steadily increases with burning time and attains a steady state before the flameout occurs. Fig. 4.2.8b exhibits that the THR, over the first one minute after application of an external heat flux, is progressively reduced with increasing LDH loading in XNBR. At 3 min after the application of external heat flux, the THR value is reduced in the highly loaded (40 and 100 phr) LDH samples than the XNBR -4 LDH nanocomposite sample. The corresponding values of THR for XNBR-40 LDH and XNBR-100 LDH samples after 3 min of the ignition reach 70 and 33 mJ / m^2 respectively in comparison to the value of 105 mJ / m^2 obtained from the XNBR-4 LDH sample. THR is often considered as the measure of the propensity to sustain long duration fire. Therefore, in principle, an efficient flame retardant should reduce THR considerably when incorporated into a polymer. In this regard, LDH materials emerge as a much more potential candidate than the layered silicates as flame retardants. LDH takes part actively in the combustion process through endothermic decomposition acting as a heat sink and significantly reduces the THR value during combustion. LDH participates actively in the combustion process through endothermic decomposition, acting as a heat sink and significantly reducing the THR value during combustion. Combined presence of intercalated water molecules to stabilize the whole

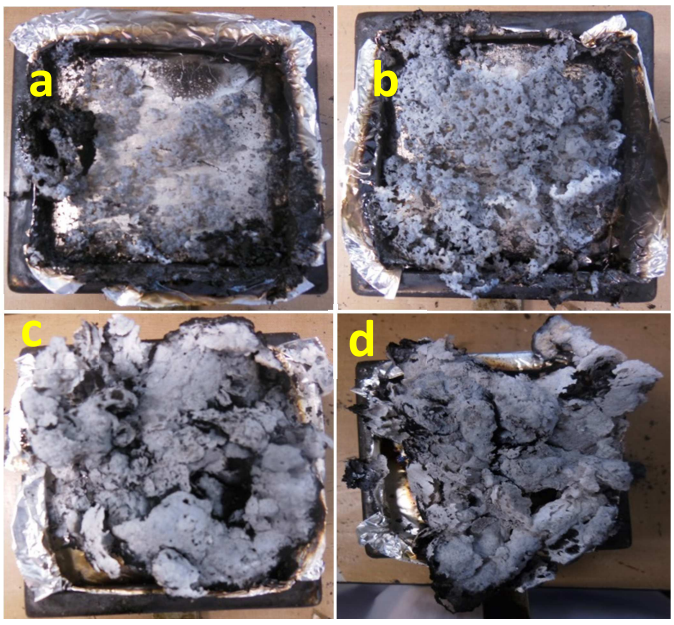

Fig. 4.2.9 Digital photographs of the samples burnt in cone calorimeter; (a) XNBR – 4 LDH, (b) XNBR – 10 LDH, (c) XNBR - 40 LDH and (d) XNBR - 100 LDH

structure of the layered double hydroxide and the metal hydroxides layers primarily accounts for the endothermic decomposition [114, 115]. The results displayed in Fig. 4.2.8a and b based on heat release rate (HRR) and total heat released (THR) are in fine accordance with the % weight loss of the corresponding rubber samples displayed in Fig. 4.2.8c.

In the burning test, XNBR mixed with less amount of LDH (XNBR – 4 LDH) burns comparatively faster after ignition with a very small amount of residue left (3 wt%). Higher loading of LDH in the matrix significantly improves the burning behaviour. The amount of char residue left after burning for the 40 and 100 phr LDH filled XNBR composites are 15 wt% and 28 wt% respectively.

Fire growth rate, abbreviated as FIGRA is generally computed by dividing peak heat release (PHRR) value by time to peak heat release (TTPH). FIGRA offers a quantitative estimation of both the spread rate and the size of fire. The FIGRA index has been regarded as a good parameter to reveal the contribution to fire growth of materials. FIGRA values of all the XNBR-LDH composites are displayed in Fig. 4.2.8d. Lower value of FIGRA attributes to better cone calorimeter performance and the results in Fig. 4.2.8d exhibits that the XNBR-100 LDH has the weakest fire risk in the cone calorimeter which has very significant coincidence with the data in PHRR results. Digital photographs of the char residues left after the cone calorimeter test are shown in Fig. 4.2.9. These images clearly suggests that the amount of char residue left after the cone calorimetry experiment is more in case of highly loaded sample in comparison to the lower amount of LDH mixed rubber composites and henceforth corroborates excellently with the results of the mass loss of the composites as displayed in Fig. 4.2.8c. The basic reason for the substantial improvement of the burning behaviour is attributed to the formation of consolidated and thick char layer that would restrict the effective transfer of gas and volatiles through the surface, and therefore preventing further burning of the samples. In conclusions, compounding with relatively higher amount of LDH yields novel and green flame retardant elastomer composites. Thus, usage of toxic and economically dangerous flame retardant chemicals could be avoided to produce the essential fire retardant commodities like, electrical cables, wires, conduits etc. for our day to day use.

Layered double hydroxides based rubber compounds exhibit excellent resistance against thermo-oxidative aging by the virtue of retention of the mechanical properties. These compounds also show lower heat build-up measured by DMA. Both these properties are featured in Appendix A.

4.3 Development of thermo-responsive rubber compounds

Many applied materials like metal alloys and solid-state polymers consist of multiple phases. Their properties depend crucially on their internal phase-structures, i.e. the fraction and local distribution of the phases, their composition and their molecular configuration. Chemical aspects influence the mechanical properties while mechanical load couples back to chemistry. The goal of this part is to understand the structure-property relation of the molecularly integrated but phase separated structure of XNBR. In order to have a compatible phase with zinc carboxylate linkages in XNBR we have used zinc stearate with similar type of chemical linkage. The chemical microstructures of the semi-crystalline thermoplastics, for example, isotactic polypropylenes can be usually tuned according to the end use. Likewise, the thermo-responsive rubbers produced by introducing selective ingredients during compounding could also be explored by altering their mechanical and dynamic properties with the effect of external stimulations like heat. XNBR compounds ionically crosslinked by zinc oxide was further pursued to enhance the flow processability and mechanical strength as well. A suitable polar additive like zinc stearate was incorporated in varied amounts to the mixture of XNBR and zinc oxide. Zinc stearate acts as 'ionolyzer' and hence generally called as 'zinc soap'. As a consequence, the dynamic mechanical properties could be reversed in case of these rubber compounds at higher temperature facilitating melt processing [32]. Zinc stearate is not reported to effectively crosslink XNBR as compared to zinc oxide [116] but, by the virtue of its strong crystalline nature, it enhances the mechanical properties like , stress-strain, tear strength, hardness etc. of the final rubber compound. More significantly, due to the melting nature of the zinc stearate molecule at relatively high temperature, a switching behavior in dynamic mechanical behavior is observed which might pave the way to design various engineered rubber products according to the particular requirements.

4.3.1 Curing study

Fig. 4.3.1 exhibits the MDR rheographs for the rubber compounds cured at 160 °C for 1h. XNBR-ZnO sample shows the highest value of rheometric torque compared to all other samples incorporated with zinc stearate. The formulation of zinc carboxylate ionic linkage in the corresponding rubber compound of XNBR-ZnO is mainly responsible for the higher elastic modulus. Addition of zinc stearate shows the tendency of decreasing elastic modulus in the rheographs. As the amount of zinc stearate increases, the torque values decreases accordingly. It seems that addition of 40 phr zinc stearate in the compounds inhibits the ionic

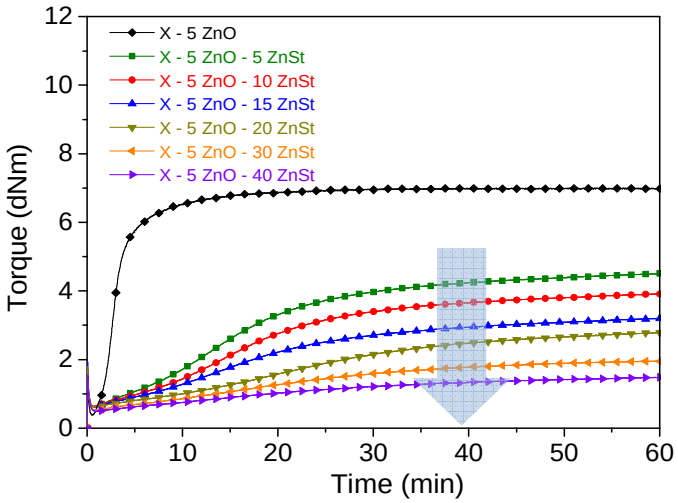

Fig. 4.3.1 Torque-time plot of the zinc stearate based XNBR compounds. The arrow downwards signifies the gradual decrease of the torque values for highly filled zinc stearate samples

crosslinking reaction but, in the mechanical properties study (discussed later) it was confirmed that the compounds was also crosslinked as expected. The melting temperature of the commercial zinc stearate used in this current study is ~ 118 °C – 128 °C. While curing at higher temperature i.e., at 160 °C , the zinc stearate particles melt inside the rubber matrix and therefore the ionic domains are solvated by a significant degree. The presence of higher amount of zinc stearate causes more dissolution at higher temperature and hence the torque values are reduced further. The melting phenomenon of zinc stearate at higher temperature is

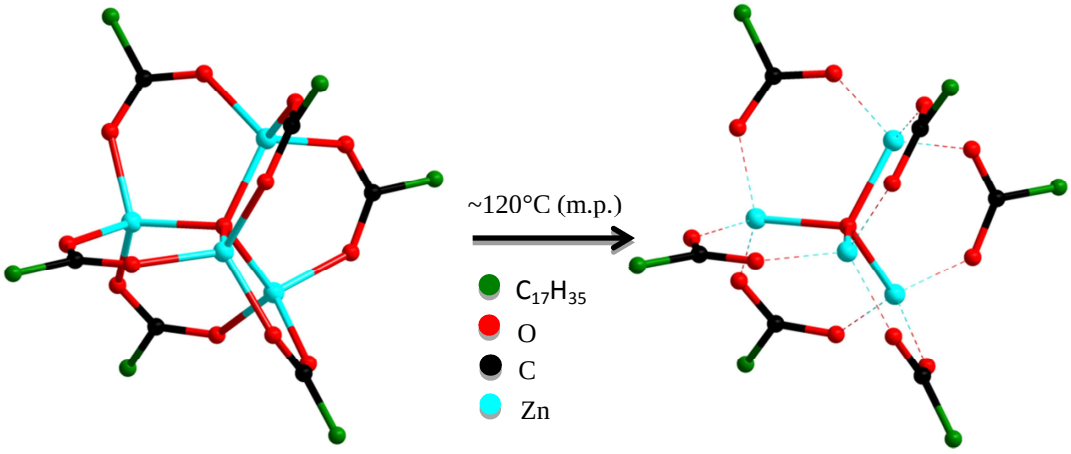

Fig. 4.3.2 Schematic representation of the melting behavior of zinc stearate. Above the melting point, the weak ionic bond between Zn^{2+} and COO^- breaks and destabilizes the whole structure

demonstrated in Fig. 4.3.2. The bulky alkyl group ($C_{17}H_{35}$) is represented as the green dot and this group is attached with the carbon atom (black dot) of the –COO group. Enough evidences were found by DSC or IR study claiming that the alkyl chains in the zinc stearate structure at ambient temperature normally show all-trans conformation and the co-ordination bond between –COO and zinc cation was bridging bidentate type [117]. But, at higher temperature, due to the melting, zinc stearate undergoes a structural change as depicted in Fig. 4.3.2. At 120°C temperature, the physical bond (red and blue bonds) between Zn^{2+} and COO^- caused by the ionic association breaks and therefore the whole molecule of zinc stearate shows liquid-like behavior. This phenomenon influences the elastic modulus of the rubber compounds mixed with zinc stearate and as a consequence, the elastic modulus values drops gradually.

4.3.2 Morphology study

Interesting observations were found out from the TEM micrographs of the zinc stearate filled samples as exhibited in Fig. 4.3.3. Some distinct islands with tiny black particles can be found, which are finely dispersed inside the island (Fig. 4.3.3a and b). Several such islands are found to exist in the microstructure. Black (dark) and white (bright) regions co-existing in the microstructures attribute to the impurities (additives mixed during production) present in the raw rubber. No tendency of formulation of agglomerates by the tiny nanoparticles was noticed in the rubber specimens. The size of the islands is approximately 1 μm. The size of the tiny black particles deposited in these islands lies in the range of 5-8 nm. Hence, these islands comprising of the nanoparticles are designated as '*micro-islands'*. Apart from the special island like morphology, lamellar structures are also present in the specimens as displayed in Fig. 4.3.3c and d. The origin of the lamellar structure in the corresponding compounds has already been discussed in details in the section 4.1.4 in the chapter 4.1. Formation of "*zinc-carboxylate polymer*" [14] due to the ionic interaction between the zinc atom the carboxylic group of XNBR is primarily responsible for the phase separated lamellar morphology. Zinc stearate particles on the other hand also consist of carboxylic group. Based on the morphological features, it can be hypothesized that zinc oxide particles predominantly participates in the crosslinking of the carboxylated nitrile rubber whereas the zinc stearate particles prefer to be attracted to the ionic part in the microstructure. The zinc stearate particles driven by their crystalline nature could not correlate with amorphous structure of the random co-polymer and therefore form numerous *'micro-islands'* in the structure. The *'micro-islands'* eventually behave like filler materials and provide the necessary reinforcement to the rubber compounds by opposing external deformations. In order to probe

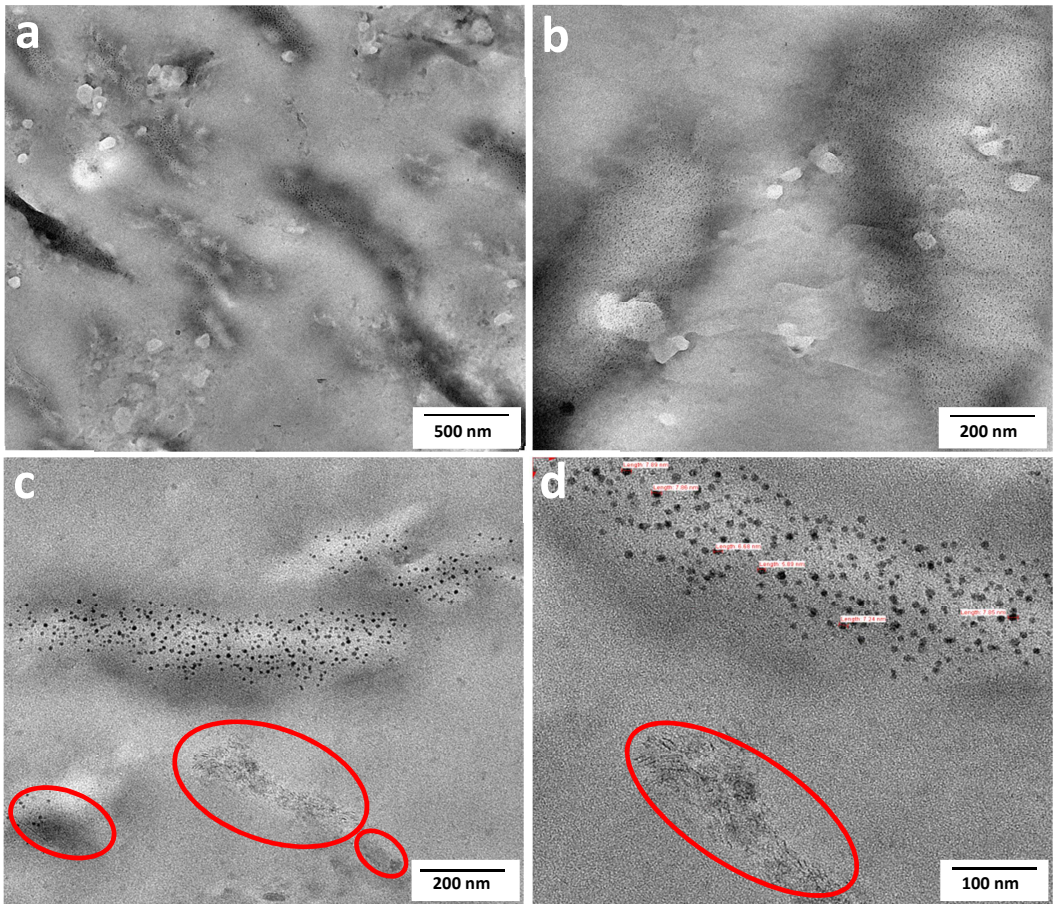

Fig. 4.3.3 TEM images of (a) X-5 ZnO-30 ZnSt , (b) X-5 ZnO-40 ZnSt, (c) and (d) magnified portions of the X-5 ZnO-40 ZnSt. Several '*micro-islands*' comprising of nano crystals of zinc stearate particles are observed in the specimens. Red circles represent the lamellar morphology of the zinc carboxylate ionomer produced in-situ in the structure as depicted in Fig. 4.1.9d

the crystalline *'micro-islands'* more intensively, morphological features were investigated of the quenched X-5 ZnO-40 ZnSt samples. The rubber specimens with 2 mm thickness were

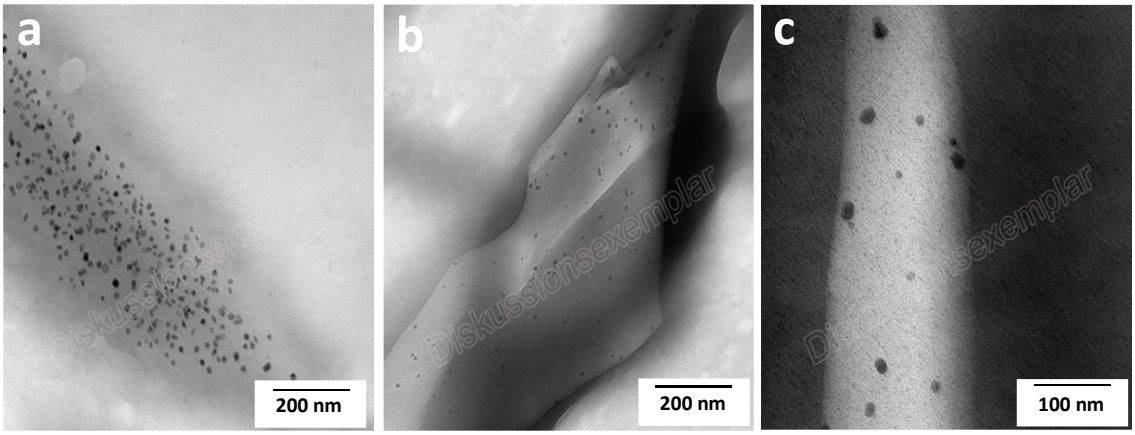

Fig. 4.3.4 TEM images of X-5 ZnO-40 ZnSt sample (a) unquenched and (b), (c) after quenching

annealed at 150 °C for 5 min and then quenched in ice water. The difference in the morphology between the samples unquenched and after quenching is exhibited in Fig. 4.3.4. As expected, the faster cooling did not allow the molten zinc stearate particles nucleate faster while quenching. As a consequence, the population density of black nanoparticles in the *'micro-islands'* significantly dropped post quenching operation. Due to lack of time to crystallize, the quenched samples would certainly deteriorate in mechanical properties as compared to the slowly cooled samples.

4.3.3 Fourier transform infrared (FTIR) spectroscopy

Fig. 4.3.5 shows the ATR - FTIR spectra of the XNBR compounds mixed with zinc stearate and zinc oxide. Comparison is basically made between the IR spectra of uncrosslinked XNBR, XNBR-ZnO, XNBR-ZnO-zinc stearate and XNBR-ZnO-stearic acid compounds. FTIR spectra were measured in the spectroscopic range of 4000 to 600 cm^{-1}. Fig. 4.3.3.a represents the most significant regions of the wave frequency of 1625 to 1350 cm^{-1}. This particular area was of much significance in the IR spectra and hence intensively explored. Band arising at 1539 cm^{-1} attributes to the hexa coordinated chemical structure configuration of zinc carboxylate ionic salt and the band at 1587 cm^{-1} is due to the tetra coordinated form of the same salt [14]. It is observed in Fig. 4.3.5a that the intensities of the former band in case of 40 phr zinc stearate mixed sample after proper normalization in the spectra is relatively higher compared to the lower amount of zinc stearate mixed samples.

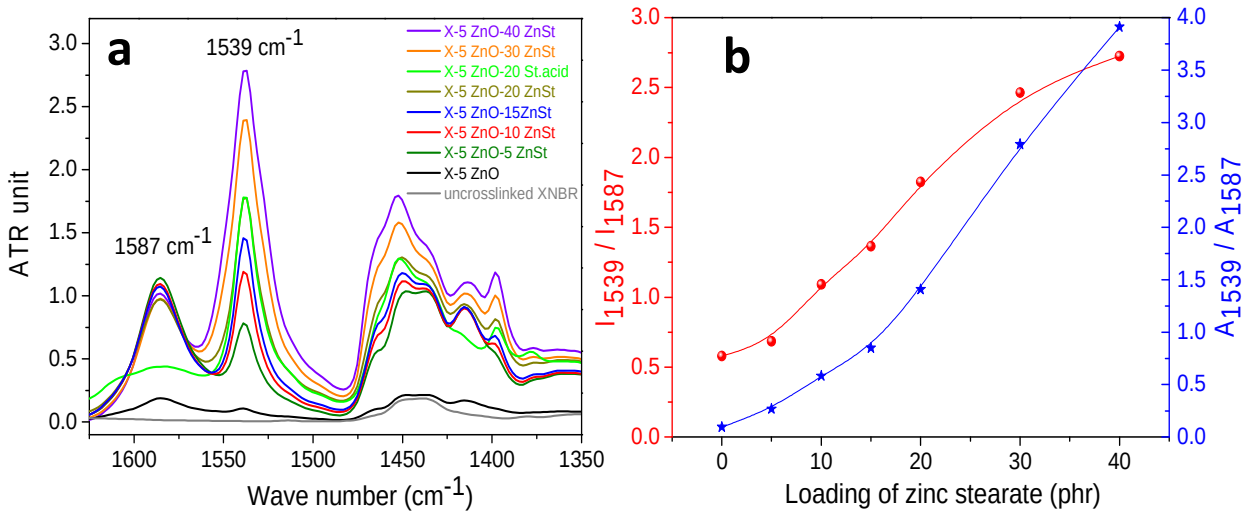

Fig. 4.3.5 IR spectra of (a) all the samples of uncrosslinked XNBR and crosslinked XNBR compounds in the range 1625-1350 cm^{-1}, (b) relative intensity and area between the peaks 1539 & 1587 cm^{-1} of the zinc stearate mixed samples ('I' is intensity and 'A' is area under the curves)

The peak intensities of XNBR-5 ZnO-20 ZnSt. and XNBR-5 ZnO-20 St. acid at this particular wave number are identical. However, in case of the later compound, the peak intensity at 1587 cm^{-1} decreases substantially compared to the former compound. This observation consequently allows us to conclude that the carboxylic groups of the XNBR as compared to the stearate particles are much more active in the crosslinking process with the zinc. Additionally, it is evident from Fig. 4.3.5a that the peak intensities at 1587 cm^{-1} for all the compounds with different zinc stearate concentration are more or less same. Formation of the polymeric structure produced by the interaction of ZnO and the carboxylic group of the host polymer gives rise to the corresponding stereo chemical configuration i.e., the tetra coordinated zinc carboxylate ionomer [14, 118].On the other hand, the hexa coordinated ionomeric structure [65] is predominantly formed due to the carboxylate group from stearate part of zinc stearate. The intensities of the band at 1539 cm^{-1} therefore increases gradually with the increase in the amount of zinc stearate. Furthermore, Fig. 4.3.5b clearly illustrates the effect of loading of zinc stearate in XNBR compounds on the relative intensities and areas of the peaks 1539 cm^{-1} and 1587 cm^{-1}. Based on the calculation of the relative areas of the two bands, certain hints were obtained that the threshold of interaction is 15 phr and beyond this concentration, formation of hexa coordinated ionomeric structures increased. This phenomenon also indirectly supports that the physical interaction between the zinc stearate and the zinc-carboxylate crosslinkage of XNBR may be responsible for mechanical reinforcement for the said compound. Peaks appearing at the positions of 1453 and 1398 cm^{-1} are assigned to $–CH_2$ bending vibration of the methylene scissoring band and asymmetrical and symmetrical stretching vibrations of the $–COO^-$ group respectively [119-121].

4.3.4 Differential scanning calorimetry (DSC)

Fig. 4.3.6 exhibits the DSC thermograms of the zinc stearate powder and the elastomer compounds made of XNBR, zinc oxide and zinc stearate. It is observed from the plot in Fig. 4.3.6a, that the glass transition temperatures of the elastomer compounds are mostly unaltered except the specimen mixed with excess amount of stearic acid. Higher amount of stearic acid helps lubricate the polymer chains and hence the glass to rubber transition takes place at relatively lower temperature. With the addition of zinc stearate in the XNBR and zinc oxide systems, although the glass transition temperature does not change much, but an extra transition at higher temperature is observed. Evolution of the peaks at the temperature range of 97°C to 106°C for the zinc stearate mixed samples does not resemble to any melting-like behavior but rather glass transition-like behavior attributing to the development of ionic

elastomer for such compositions [14] which is already supported by infra-red spectroscopy analysis discussed in section 4.3.3.

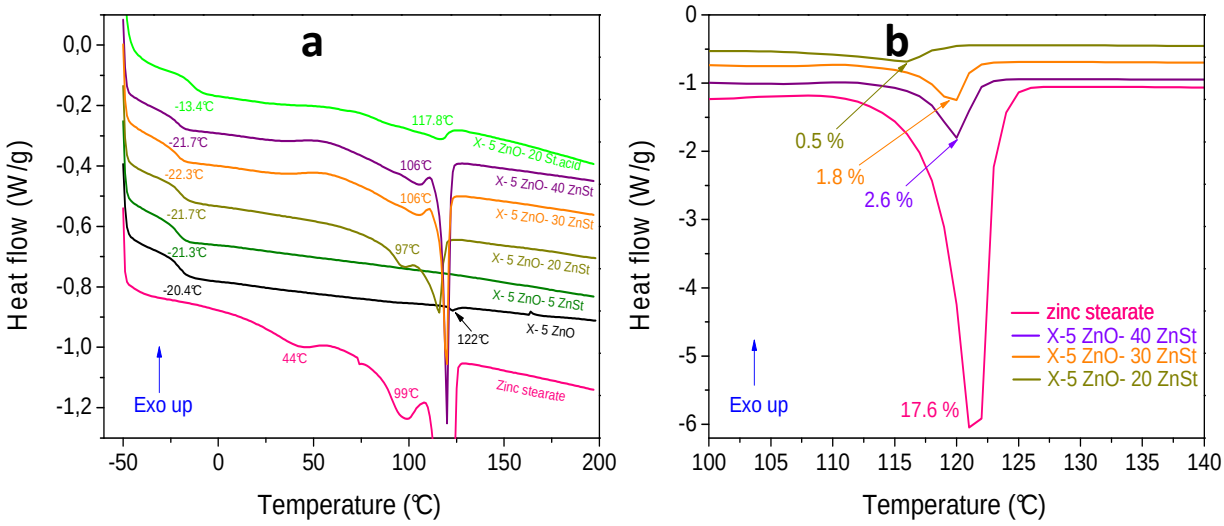

Fig. 4.3.6 (a) DSC thermograms of the zinc stearate powder, X-5 ZnO, X-5 ZnO-20 stearic acid and X-ZnO-zinc stearate samples, (b) the melting peaks with the corresponding % crystallinity of the zinc stearate powder and zinc stearate mixed XNBR compounds (calculated from the area under the melting curve)

Above the melting point, pure zinc stearate powder and the elastomer compounds prepared with this powder show typical melting thermograms. The % crystallinity values, calculated from the area under the melting peaks are provided in Fig. 4.3.6b. As the amount of zinc stearate increased in the elastomer compounds, the % crystallinity also increased to some extent. This phenomenon could impart certain degree of crystallinity to the rubbers and therefore reinforce the matrix.

4.3.5 Dynamic mechanical analysis (DMA)

Dynamic mechanical analysis was carried out to study the thermo-responsive nature of the zinc stearate mixed rubber compounds on mechanical properties. The samples were scanned from -100 °C to +150 °C with a constant frequency (10 Hz) in the normal temperate sweep mode in the DMA apparatus. Fig. 4.3.7a displays the influence of zinc stearate on the storage modulus (elastic part) as a function of temperature. In the rubbery region, from 0 °C to 125 °C, the modulus value of all the zinc stearate mixed compounds are substantially higher than the zinc stearate free sample i.e., XNBR-ZnO. Furthermore, the modulus values show the tendency to gradually increase with the increase in the zinc stearate concentration up to a certain temperature (~ 125 °C). Beyond this temperature, the modulus values drop

significantly in the similar order due to the melting of zinc stearate inside the rubber compounds. This phenomenon clearly indicates that below the melting point, zinc stearate reinforces the ionic elastomer system to a significant degree but reverses the effect at higher temperature. Such remarkable improvement in storage modulus values is attributed to the strong interaction between zinc stearate and ionic elastomer as suggested by the IR spectra. More conclusive evidences about the mechanical reinforcing behavior of zinc stearate were obtained from the tan δ vs. temperature plot as exhibited in Fig. 4.3.7b and c. Approximately 37% drop in the tan δ peak height along with slight broadening of the highly loaded rubber compound (40 phr zinc stearate) with respect to the reference sample of XNBR-ZnO, manifests the reinforcing ability of zinc stearate. In addition, the glass transition temperature (T_g) of the 40 phr zinc stearate loaded XNBR compound shifts towards higher temperature by a small margin (~3 °C) in comparison to the T_g of the reference sample (Fig. 4.3.7c). This phenomenon is perhaps attributed to the enhanced crosslink density of the zinc stearate mixed

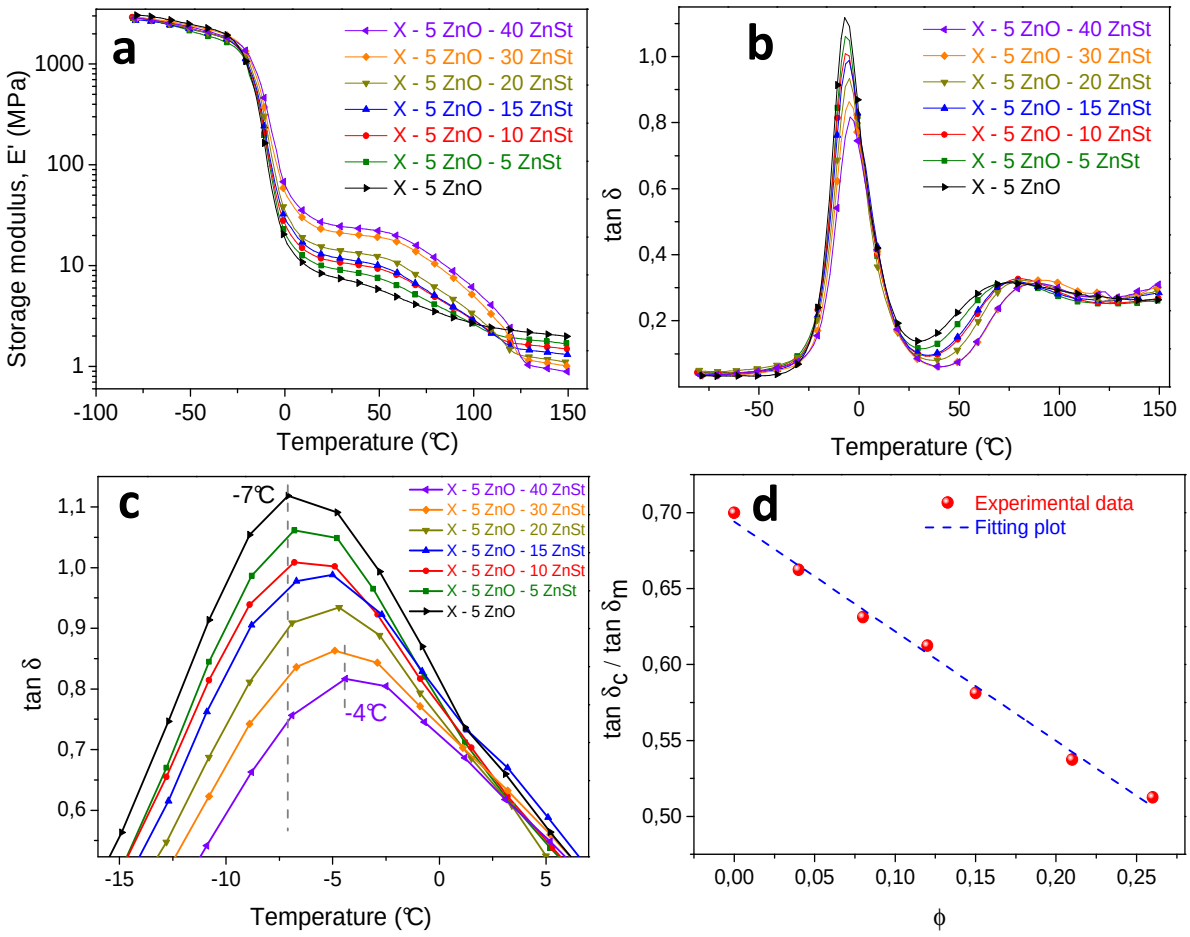

Fig. 4.3.7 a) Storage modulus, b) loss modulus c) loss tangent δ as a function of temperature of the rubber compounds temperature (magnified from Fig.c), and d) tan δ vs. volume fraction of filler

samples due to the better state of dispersion of the zinc soap. Moreover, all the samples demonstrate an additional relaxation at high temperature (Fig. 4.3.7c) owing to the formation of '*zinc carboxylate polymer*' phase formed through ionic association. A quantitative and phenomenological relationship could be established based on the relative loss tangents of the samples mixed with and without zinc stearate as follows:

$$\frac{\tan\delta_{ZS}}{\tan\delta} = 1 - B\phi \qquad (4.9)$$

Where, $\tan\delta_{ZS}$ = loss tangent maximum of the samples mixed with zinc stearate, $\tan\delta$ = loss tangent maximum of the sample without zinc stearate, ϕ = the volume fraction of zinc stearate in the rubber compounds and B = a phenomenological interaction parameter which is also called as matrix dependent coefficient [122,123]. The negative slope obtained from Fig. 4.3.5c by using eqn .4.9 represents the effective interaction between the ionic elastomer and zinc stearate [118,123].

4.3.6 Mechanical test (Stress-strain analysis)

The strength enhancement of the ionic elastomers by the presence of zinc stearate is realized by the stress-strain plot (Fig. 4.3.8) of the corresponding compounds. It is apparent that the ionic elastomer comprising of XNBR and zinc oxide, shows some improvement in the tensile properties with addition of relatively lower amount of zinc stearate i.e., 5-15 phr. But addition of more amount of zinc stearate enhances the tensile strength and stress (at 50%, 100%, 200% and 300% strain) substantially. This phenomenon can be explained in accordance to the morphological evidences obtained in TEM micrographs. The tiny nano-crystals (~ 5-6 nm) of zinc stearate particles deposited in the *micro-islands* provide the necessary reinforcement to the rubber nanocomposite. The nano-crystalline zinc stearate particles hinder the external deformation and henceforth act like ideal filler material. A typical percolation is observed after the threshold loading of 15 phr of zinc stearate into the rubber compounds. Two distinct slopes were noticed while fitting the stress at 200% strain values and elastic modulus values at relatively lower strain (~ 2%) with a linear plot. In both the cases, the slopes tend to increase by some margin after 15 phr loading of zinc stearate. This phenomenon clearly indicates that higher amounts of zinc stearate e.g., 20, 30 and 40 phr substantially reinforce the rubbers by introducing more crystalline particle nature into the matrix. It is well known that in contrary to the metals, the elasticity of rubbers is driven by entropy instead of energy. A rubber

specimen, while going deformation by stretching, the chain segments assume fewer conformations and therefore the entropy associated with them reduced significantly but the

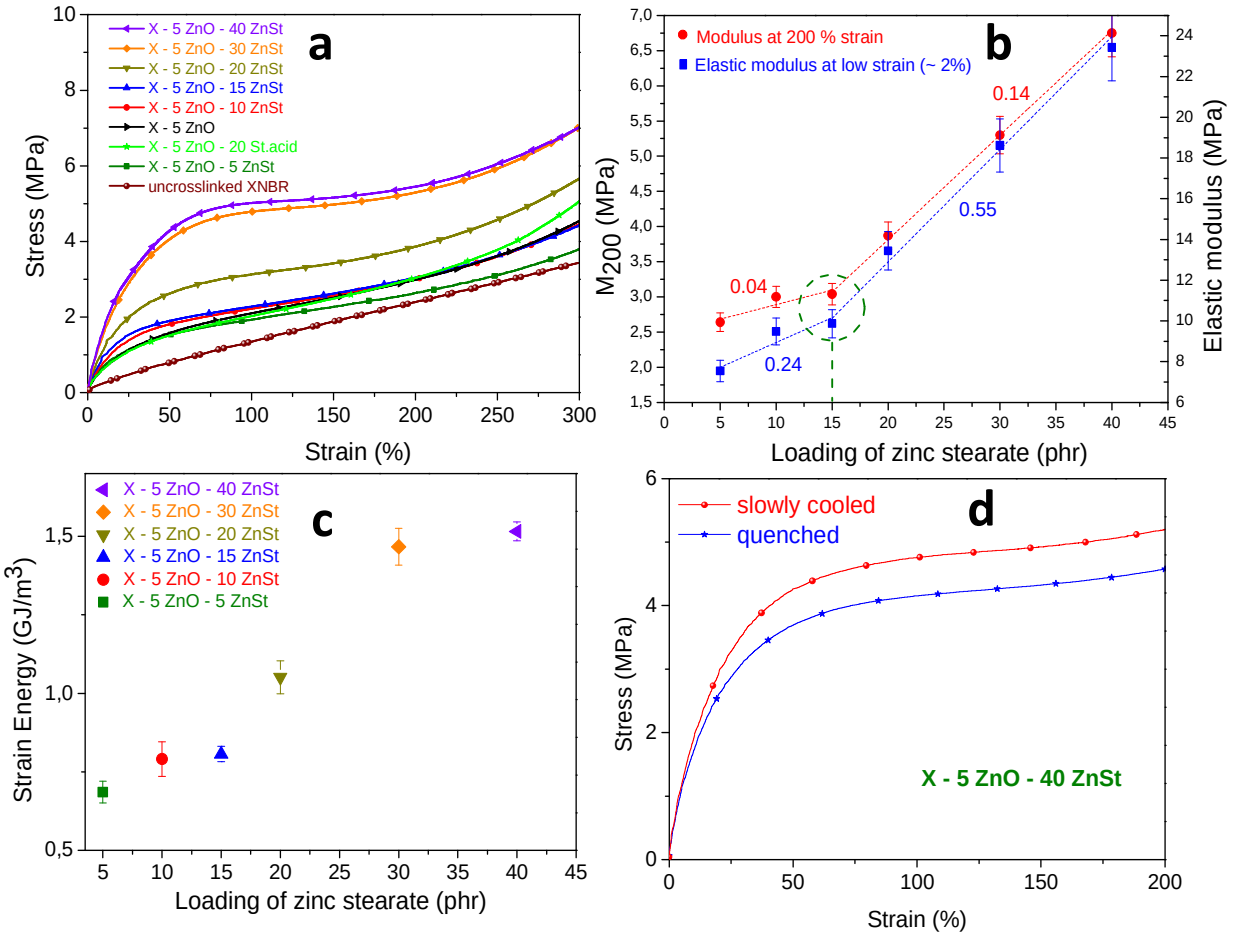

Fig. 4.3.8 Mechanical properties of the XNBR and zinc stearate based compounds. (a) stress-strain plots, (b) change in 100% modulus and elastic modulus with respect to the loading of zinc stearate, (c) strain energy density (toughness) plots and (d) effect of quenching on the stress-strain property of X-5 ZnO-40 ZnSt compound

free energy increases. The enhancement of free energy is subsequently balanced by the work done externally on the rubber [124-126]. At constant temperature, the free energy is equal to the work done on the system externally which is nothing but the elastic strain energy of the specimen. The strain energy density is directly related to the stress. The derivative of the former with respect to the displacement produces the stress (σ) in the simplest manner as described by the Neo-Hookean eqn. [127] as follows

$$\sigma = NRT\left(\lambda - \frac{1}{\lambda^2}\right) \qquad (4.10)$$

Fig. 4.3.8c shows the influence of toughness or strain energy density plot of the corresponding compounds with the loading of zinc stearate. The values for toughness have been obtained

from the area under the stress-strain plots as displayed in Fig. 4.3.8a. A constant tendency of increase in the toughness is noticed for the compounds while increasing the amount of zinc stearate. This result signifies the reinforcement nature of the zinc stearate filled rubbers. The effect of quenching on the mechanical properties of the X-5 ZnO- 40 ZnSt was also investigated. Fig. 4.3.8d indicates that the corresponding sample when quenched gave inferior mechanical property as compared to the slowly cooled (1K/min) sample. This result expectedly suggests that the nano-crystals of zinc stearate could not grow in the fast cooled specimen whereas in the slowly cooled specimens, the crystals obtained sufficient time to grow. Increase of the stress values by almost ~ 1 MPa at 50%, 100%, 150% and 200% strain in the slowly cooled specimens compared to the quenched specimen could lead a significant commercial interest.

4.3.7 Tear fatigue analysis

Fracture mechanical behavior of the zinc stearate filled composites was carried out to explicit the crack growth behavior of the said samples. Pure shear specimens were prepared (as discussed in detail in section 3.3.10) for all the rubber compounds. The crack growth rate, designated as *da/dn* obtained from each sample was subsequently plotted against the tearing energy, designated as *T* using a log-log scale. The results of the zinc stearate filled samples

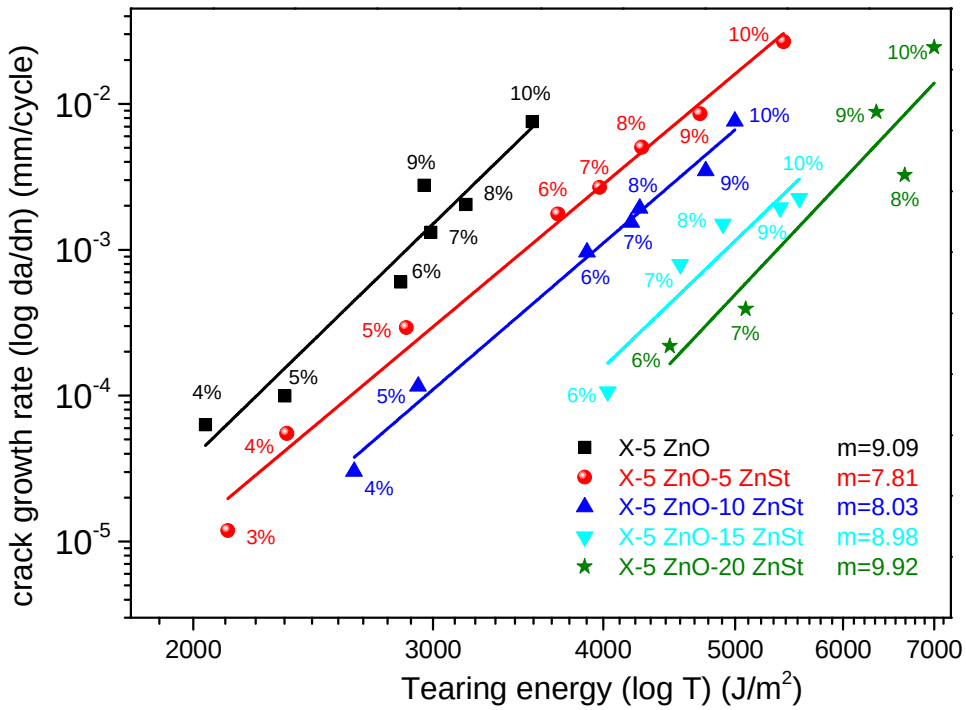

Fig. 4.3.9 Paris plot for the XNBR-ZnO-ZnSt based compounds obtained from tear fatigue analysis. The strain amplitude varies between Ɛmax = 3% …. 10%

were compared with the reference sample, X-5 ZnO. As demonstrated in Fig. 4.3.9 linear fits can be obtained by plotting crack growth rate vs. tearing energy and therefore it is quite obvious to say that power law equation is followed in each case. The relation between stable crack growth rate and tearing energy follows the Paris-Erdogan power law (with exponent *m*) which is written as $da/dn = T^m$ where da/dn is the crack growth rate and T is the tearing energy. In Fig. 4.3.9, the influence of loading of zinc stearate in XNBR on crack growth rate becomes apparent. It was clearly observed that the fatigue crack growth rate at a given tearing energy decreases significantly with an increase in the loading of zinc stearate, whereas, the crack growth rate exponent termed as *m* slightly increases with the higher amount of zinc stearate filled in the rubber specimens [128]. Enhancement of the tear strength in the compounds irrespective of the zinc stearate loading induces the enhanced crack growth rate. Moreover, at the integration of more loading of zinc stearate, the tear resistance becomes superior. Presence of '*micro-islands*' comprised of nano-crystalline zinc stearate particles provide the reinforcement to the corresponding compounds and hence the fracture mechanical properties of the samples are improved. A higher crack growth resistance is also known if the rubber is reinforced with fillers like carbon black or silica [129-132]. Therefore, we conclude that in lights of the crack resistance behavior the zinc stearate containing XNBR compounds, despite of containing no filler particles, behaves like a filled rubber composite.

4.4 Exploration of the role of $ZnCl_2$ in NBR compounds

In the earlier sections different aspects regarding the effect of different zinc compounds on the curing behavior and its subsequent effects on thermal, mechanical, dynamic mechanical, fracture mechanical properties of carboxyl modified nitrile rubber are discussed. In most of these cases, crosslinkings have been mostly induced either by ionic association between the zinc atom and the carboxyl functionality of XNBR or covalent crosslinking caused by the network formation between the sulfur bridges and the unsaturation present in the host polymer. Study on the elastomers crosslinked by co-ordination reaction between nitrile groups of nitrile rubber and different metal salts of Zn^{2+}, Cd^{2+}, Cu^{2+}, La^{2+} is also an interesting topic of research. Being recognized as a d^{10} metal ion, Zn^{2+} cation is the most popular choice for generating co-ordination network especially with nitrile based rubbers. The typical nature of the reversibility of the bonds formed by zinc complexes offers the metal ions and ligands to dissociate or rearrange in such a way that an effective network structure is formed within the compound [133]. The primary objective of this study is to explore various properties obtained

by the physical mixing of zinc chloride and acrylonitrile buta di-ene rubber (NBR) compounds within the scope of this research.

4.4.1 Curing study

The influence of inorganic metal halide like, $ZnCl_2$ on the curing characteristics of nitrile rubber was investigated based on rheometric studies. NBR based rubber compounds with varying the acrylonitrile (-CN) content was prepared by mixing with 20 phr of zinc chloride in an open two roll mill. Zinc chloride, a well-known Lewis acid, produces effective vulcanization of nitrogen based elastomers e.g., acrylonitrile buta di-ene rubber. The curing of nitrile rubber by zinc chloride is attributed to the co-ordination bond formation between the nitrile groups of the host polymer as well as the unsaturation present in the buta di-ene units as a consequence of reaction with zinc chloride. The curing curve of the corresponding rubber compounds with different amount of acrylonitrile content is shown in Fig. 4.4.1. All the samples were studied with 1h curing time 160 °C. It is clearly observed from Fig. 4.4.1 that N18 (-CN ~ 18%) generates the highest amount of rheometric torque despite the fact that it has the lowest amount of acrylonitrile content amongst the rest. Increased amount of acrylonitrile content and subsequently gradual decrease of buta di-ene group present in the host rubber produce lower torque for the vulcanizates. Apart from the co-ordination crosslinking formed by the –CN group and zinc, zinc chloride also takes part in crosslinking of the unsaturation of the di-ene structure present in NBR chains. Existing literatures [134,

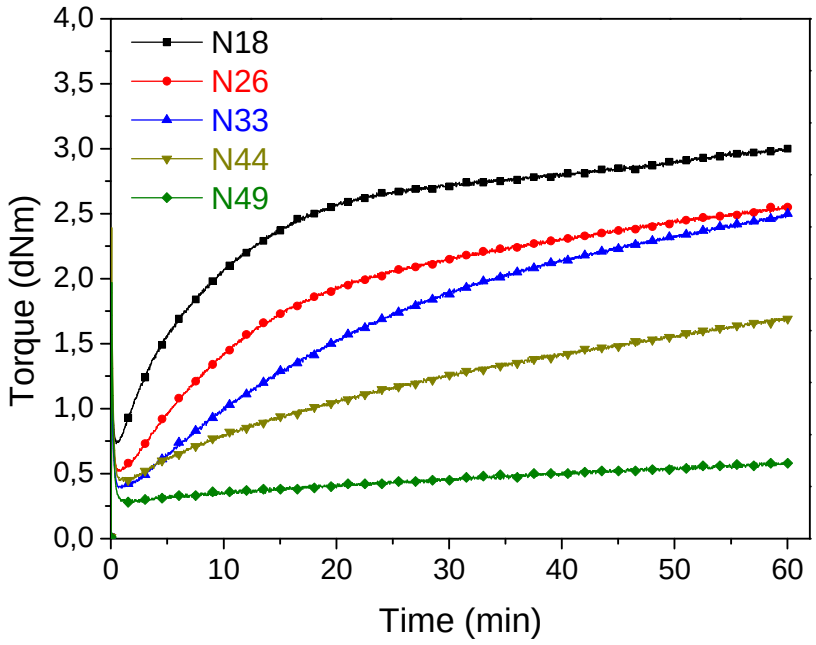

Fig. 4.4.1 Curing isotherms of NBR compound cured with zinc chloride. N18, N26, N33, N44 and N49 represent NBR with acrylonitrile content 18%, 26%, 33%, 44% and 49% respectively. Zinc chloride used in each case is 20 phr

137] provide enough hints that zinc chloride complex formed during the mixing takes part in producing the carbanion atom by attacking the double bond and thus crosslinking takes place (Fig. 4.4.2). Subsequent heating facilitates the crosslinking process and produces strong C-C bonds in the main structures. Such reactions will be more vigorous when the content of unsaturation is higher in the system. This fact therefore obviously explains a definite trend in the increase of the number of bonds and the elasticity as well.

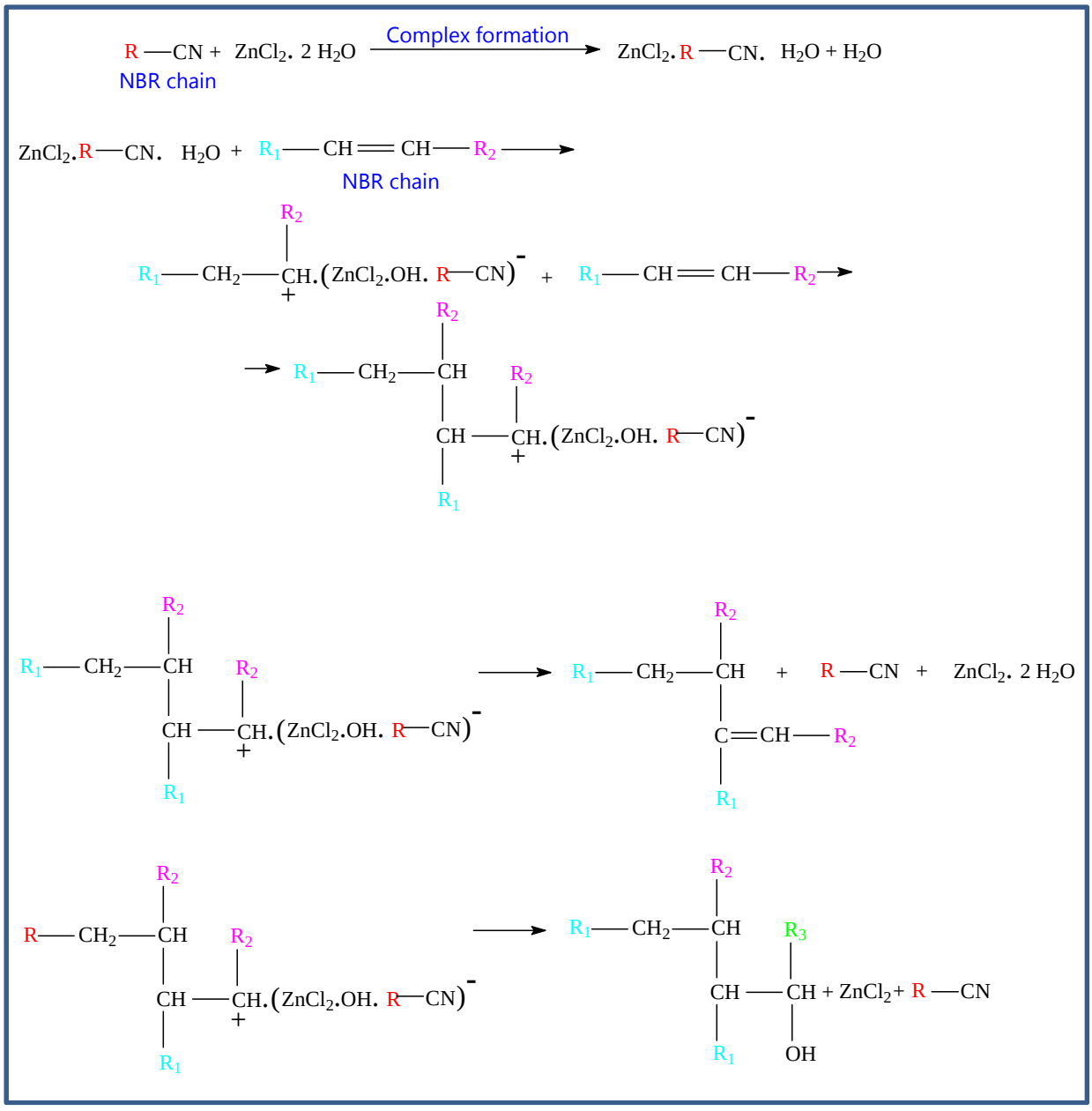

Fig. 4.4.2 Crosslinking reaction mechanism of the unsaturation present in the NBR rubber by zinc chloride complex (R, R_1, R_2 and R_3 are alkyl rubber chains) [136]

It is mostly reported that [135-137], zinc chloride being primarily responsible to form co-ordination bonds with both the unsaturation and nitrogen containing organic substances e.g., -CN, largest tendency is attributed to the reaction with acrylonitrile functionality. Because, both the reactive portions in the rubber molecule can generate the largest electron density on the nitrogen atom of the acrylonitrile group and therefore, the most favored phenomenon is the co-ordination bond formation with the acrylonitrile group [137].

4.4.2 Fourier transform infrared (FTIR) spectroscopy

The infrared spectra of raw NBR 1846 rubber (N18_raw), vulcanized (by zinc chloride) rubber (N18_vulc) and zinc chloride are displayed in Fig. 4.4.3a. Zinc chloride is widely known as a hygroscopic material and therefore, it shows a typical broad absorption peak ranging from 3460 cm^{-1} to 3200 cm^{-1} due to the presence of –OH functional group. The broad peak at ranging from 3700 cm^{-1} to 3100 cm^{-1} for the cured N18 rubber with zinc chloride appears due to the strong intermolecular hydrogen bonding taking place in the vulcanizate [36]. In the raw NBR, due to absence of any water molecule, no peak was seen to appear in the range of 3700 cm^{-1} to 3100 cm^{-1}. Raw NBR showed a typical peak at 2237 cm^{-1} which is

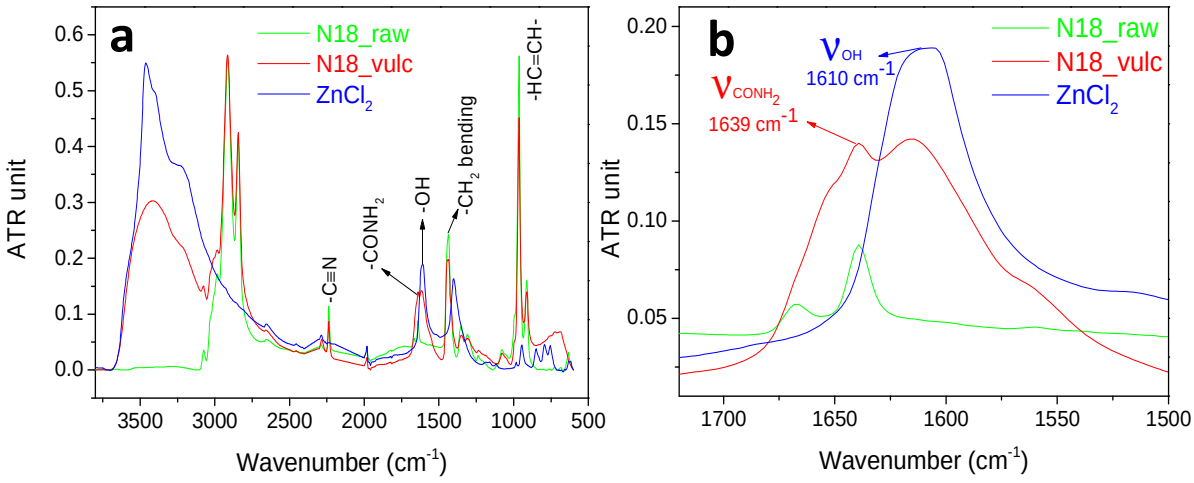

Fig. 4.4.3 (a) FTIR spectra of zinc chloride, raw rubber (N18) and the vulcanized rubber, (b) magnified potion in the range of 1750-1500 cm^{-1}

attributed to the stretching vibration of the –CN group. NBR used for this particular study contains only 18% acrylonitrile content and therefore exhibits a rather weakly intense peak at 2237 cm^{-1}. After vulcanization, the intensity of the peak at 2237 cm^{-1} in N18_vulc significantly decreased but the intensity of the peak at 2281 cm^{-1} was marginally higher than the raw rubber. It is reported that the proposed peak at 2237 cm^{-1} appears due to the 'unreacted' –CN (high in raw rubber) group whereas the peak at 2281 cm^{-1} is attributed to the

'reacted' –CN group (slightly higher in the vulcanizate) formed due to a possible co-ordination complex

4.4.2.1 Co-ordination crosslinking – reaction mechanism

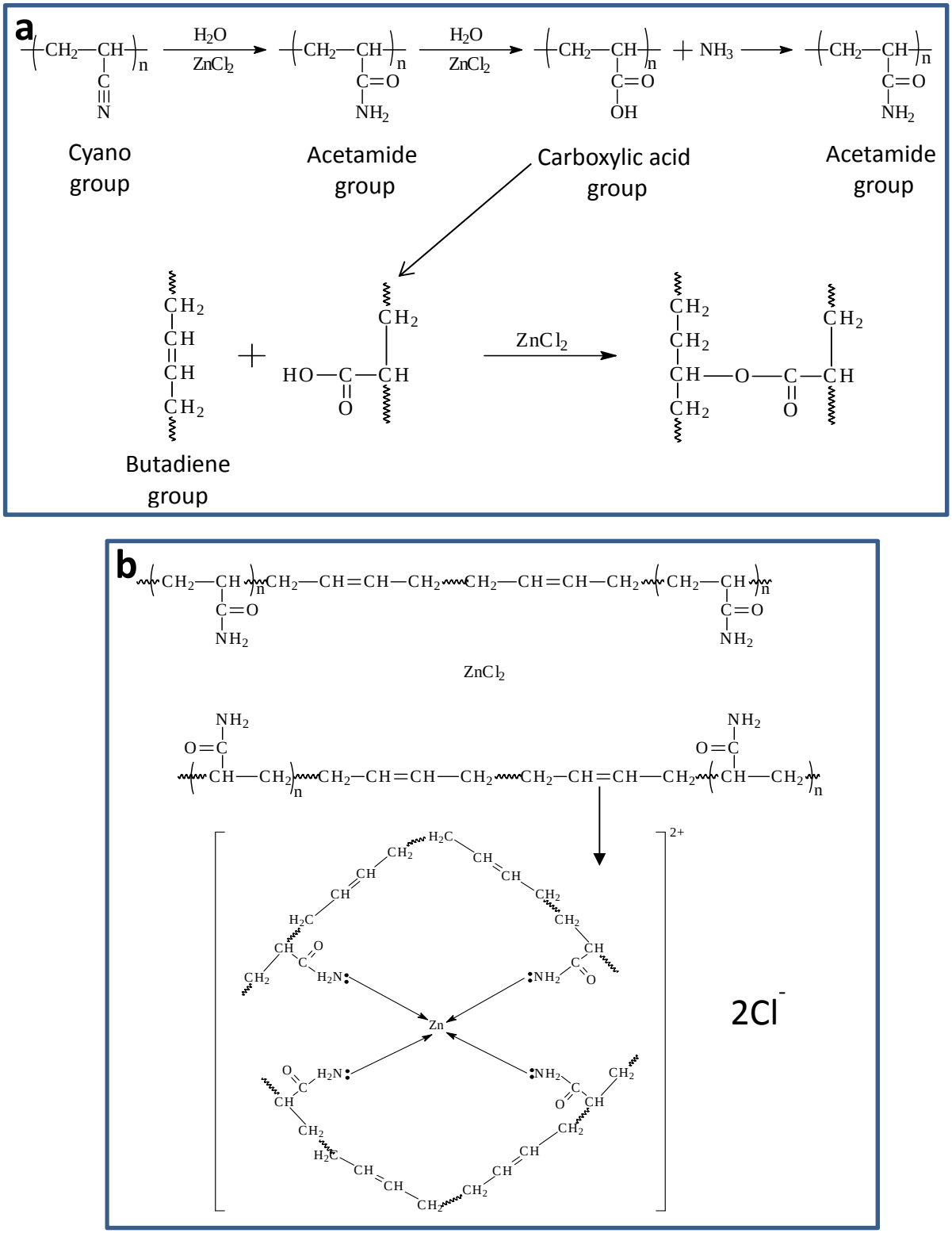

Fig. 4.4.4 (a) Reaction of nitrile group in NBR with $ZnCl_2$, (b) formation of co-ordination complex of zinc with acetamide

between zinc and acrylonitrile group [36,138] . Moreover, the band appearing at 1610 cm^{-1} in case of zinc chloride due to the stretching vibration of –OH of water of crystallization [139] (zinc chloride being hygroscopic contains some water molecules due to exposure to ambient conditions) shifted slightly towards higher wavenumber i.e., 1616 cm^{-1} in case of the rubber vulcanized with zinc chloride. The intensity of the unsaturation of the host rubber (peak at 964 cm^{-1}) also dropped significantly in case of the vulcanizate due to crosslinking by the zinc chloride complex as shown in Fig. 4.4.2. The rubber after mixing with zinc chloride is vulcanized at higher temperature (160°C) and pressure and therefore the water molecule embedded into the zinc chloride evaporates which eventually leads to the shifting of the hydroxyl peak at marginally higher wave number. The nitrile groups in the host polymer being hydrolyzed convert into carboxylic groups which further convert into acetamide groups by the reaction with ammonia generated during the course of the reaction. (See the reaction scheme: 4.4.2.1). A mild peak at 1639 cm^{-1} featuring for the N18_vulc, as shown in Fig. 4.4.3b attributes to the acetamide (-$CONH_2$) group formed during the reaction [140].

With the evidence obtained from the FTIR analysis, we propose the following reaction mechanism taking place when NBR with 18% acrylonitrile content is vulcanized with zinc chloride at 160 °C under pressure. The cyano group, at first, catalyzed by the zinc chloride and the water molecules associated with it converts into acetamide group which further converts into carboxylic acid functionality. The acidic moiety thus produced generates more acetamide functional groups at ammonia atmosphere generated in situ in the reaction medium. Now, evidently the acid groups formed in course of hydrolysis of the cyano groups could not lead to any structure formation, Therefore, it is speculated and proposed that, during vulcanization by the addition of zinc chloride, the acid groups are joined further at the unsaturation present in the host polymer (buta di-ene units) and eventually form ester functional groups (Fig. 4.3.4a). The acetamide complex thus generated by the steps mentioned before eventually form a co-ordination complex with zinc chloride leading to a network structure which induces the crosslinking process of NBR and zinc chloride system (Fig. 4.3.4b).

4.4.3 Crosslink density measurement

In order to gain a deep insight to understand the chemical crosslinking behavior of the vulcanizates cured by zinc chloride, crosslink density was estimated by equilibrium swelling method as well as using Mooney-Rivlin equation. In case of swelling method, ASTM D6814-

02 was followed as discussed in section earlier. The values of crosslink density for the rubber vulcanizates comprising of different grades of NBR (varying acrylonitrile contents) and 20 phr zinc chloride are summarized in Table 4.4.1. The corresponding MR plot is given in Fig. 4.4.5. This equation is widely used to evaluate the degree of the crosslinking of the rubber vulcanizates and mainly based on the phenomenological theory of rubber elasticity [36, 141-143]. For Mooney–Rivlin studies, a plot of reduced stress versus stretching ratio was fabricated and the slope and the intercept obtained by fitting a straight line were taken into consideration to calculate the crosslink density.

$$\text{Reduced stress} = \frac{\sigma}{2(\lambda - 1/\lambda^2)} \qquad (4.11)$$

$$\frac{\sigma}{2(\lambda - 1/\lambda^2)} = c_1 + c_2/\lambda \qquad (4.12)$$

$$\text{Now, Crosslink density } (\upsilon) = 2c_1/RT = \frac{\rho RT}{2M_c} \qquad (4.13)$$

Where, σ = stress of the samples measured by classical stress-strain experiment, λ = stretching ratio, c_1 = intercept of the MR plot, c_2 = slope of the MR plot, M_c = molecular weight of rubber segments between two cross-links [46, 141], ρ = density of rubber, R = universal gas constant (8.314 J K^{-1} mol^{-1}) and T is the ambient temperature (298 K).

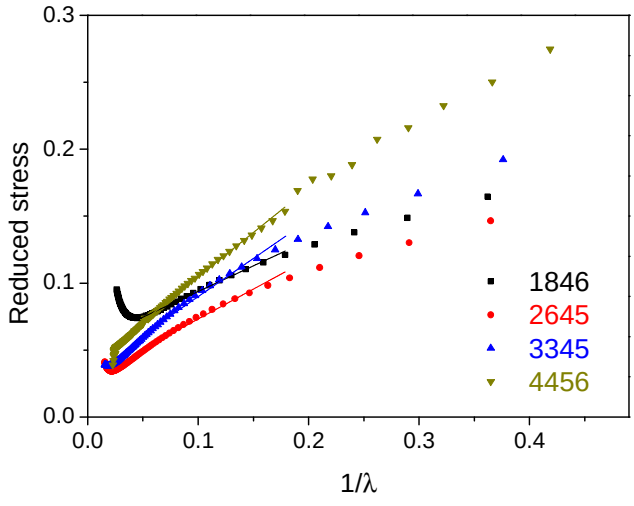

Fig. 4.4.5 Mooney-Rivlin plot for the NBR vulcanizates cured with 20 phr $ZnCl_2$

In both the cases, the crosslink density values are found to be the highest in case of the N18 sample. This estimation correlates the rheological behavior of the vulcanizates as discussed in section 4.4.1.

Table 4.4.1 Crosslink density values calculated for NBR vulcanizates by swelling and Mooney-Rivlin methods

Samples	Swelling method	Mooney – Rivlin technique		
	Crosslink density (mol/cm^3)	Slope (c_2)	Intercept (c_1)	Crosslink density (mol/ cm^3)
N18	6.87 x 10^{-5}	0.1915	0.0277	2.24 x 10^{-5}
N26	9.16 x 10^{-6}	0.2232	0.0143	11.54 x 10^{-6}
N33	11.05 x 10^{-6}	0.2850	0.0165	13.28 x 10^{-6}
N44	13.88 x 10^{-6}	0.3323	0.0190	15.38 x 10^{-6}

4.4.4 Morphology study (SEM)

The SEM micrograph of the N18_Vulc sample is displayed in Fig. 4.4.6. Zinc chloride particles homogeneously dispersed into the nitrile rubber matrix and did not generate any phase separated morphology. The compatibility between zinc chloride and NBR was thus realized [97]. The corresponding EDX spectra of the same sample, as demonstrated in Fig. 4.4.6b, evinced the elemental presence of zinc, chlorine atoms on the surface.

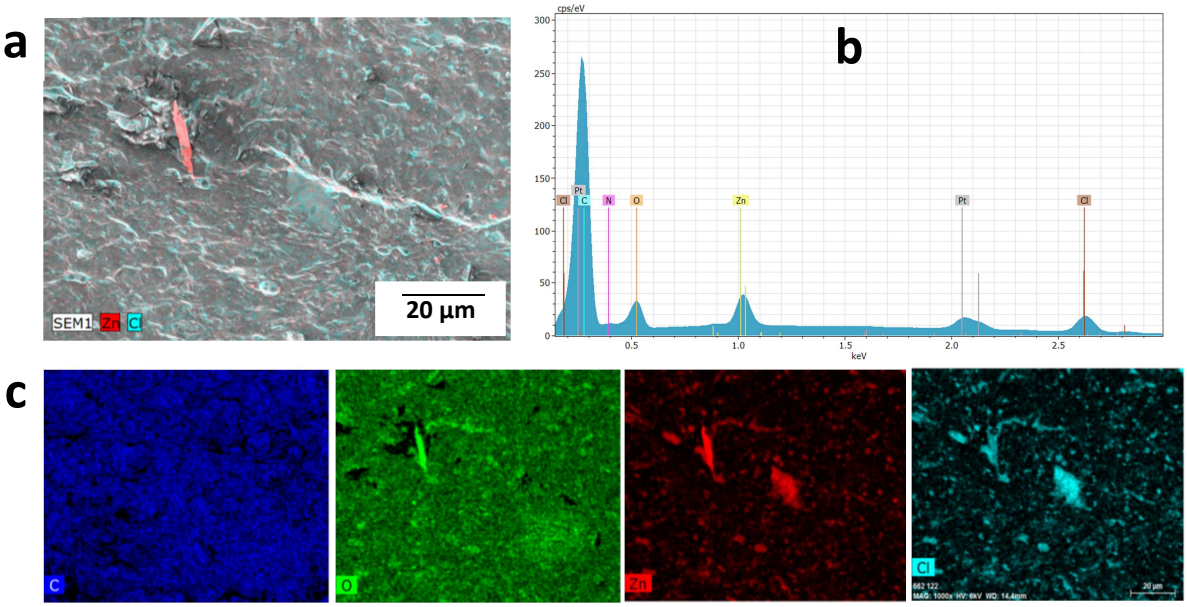

Fig. 4.4.6 (a) SEM micrograph, (b) EDX spectra and (c) carbon, oxygen, zinc and chlorine mapping of N18_Vulc. The peaks in EDX spectra corresponding to Pt originate from the sample holder (sputtering)

After mixing with nitrile rubber, zinc chloride, by the virtue of the co-ordination reaction forms a special type of crosslinking network. Previous report [97], suggested that amount of zinc chloride mixed with nitrile rubber plays a significant role to generate a specific type of microstructure in such compounds. 20 phr zinc chloride produces a 'macro-homogeneous' microstructure with the NBR matrix. However, the 'solubility' of more amount of zinc chloride into the same matrix was not explored in this study. The efficiency of zinc chloride to perfectly mix within the nitrile rubber could facilitate the mechanical properties of the final compounds.

4.4.5 Dynamic mechanical analysis

Fig. 4.4.7 shows the variation of dynamic mechanical properties e.g., storage modulus (E') and loss tangent (tan δ) with temperature for the raw NBR and the vulcanizate. The storage modulus vs. temperature plot, as demonstrated in Fig. 4.4.7a, clearly suggests that the raw rubber due to lack of elasticity typically shows a flowing behavior at higher temperature. On the other hand, NBR vulcanized by zinc chloride shows a higher modulus beyond glass transition temperature with a steady rubbery plateau. Therefore, the higher magnitude of E' was obtained not only due to the filler –like participation of zinc chloride but also the combined effect of the crosslinking process taking place by the co- ordination polar reaction

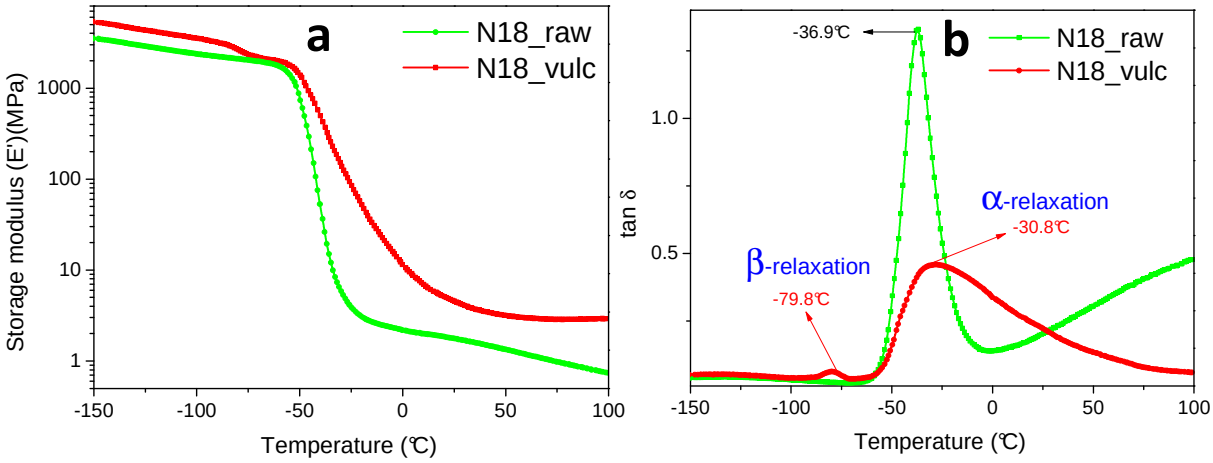

Fig. 4.4.7 (a) Storage modulus and (b) loss tangent plots vs. temperature of the raw rubber and its vulcanizate. High temperature (-30.8 °C) and low temperature (-79.8 °C) processes show α and β transitions respectively for the vulcanizate

between Zn^{2+} and –CN group of acrylonitrile unit and self-curing of buta di-ene chains induces by the thermal process [36]. Now, while looking at the loss tangent plot vs. temperature, a couple of interesting observations were found. The tan δ peak value of the vulcanizate significantly drops down almost 3 times as compared to the raw rubber.

Moreover, the position of the corresponding tan δ peak also shifted a little towards higher temperature (-37 °C to -30 °C) for the vulcanizate. These two observations strongly infer that due to enhanced crosslinked density by incorporating zinc chloride into NBR, the rubber compound is reinforced to some extent. We also recognized that the N18_vulc features with a couple of peaks in the loss tangent vs. temperature spectra (Fig. 4.4.7b). The peak at -36.9 °C corresponds to the glass transition temperature of NBR and termed as the α-relaxation process [144] whereas another peak appearing at relatively lower temperature at -79.8°C is termed as β-transition [144-147]. Zinc chloride by the virtue of the co-ordination complex with the –CN group of NBR, generates a bulky network predominantly produced by the zinc-acetamide chelate compound. Such pendant groups hanging from the main chain of the vulcanizate network usually shows distinct dynamics in the spectra because of their unique relaxation behaviour during the co-operative motion of the macromolecular unit [145-147]. As a result, a distinct association termed as β-relaxation is observed at -79.8 °C. This is the first ever report where the nitrile rubber cured with a novel crosslinking system shows β-transition apart from the usual α-transition associated with the glass transition temperature of the host polymer.

4.4.6 Thermal analysis (TGA and DSC)

Thermogravimetric analysis (TGA)

The thermal stability of the raw rubber (N18_raw) and the vulcanizate (N18_vulc) was investigated by scanning the samples in the temperature range of 0 to 700 °C in N_2 atmosphere in the thermogravimetric analysis with a heating rate of 10K/min. It was clearly observed from Fig. 4.4.8a that, the % char residue for the vulcanizate is substantially higher

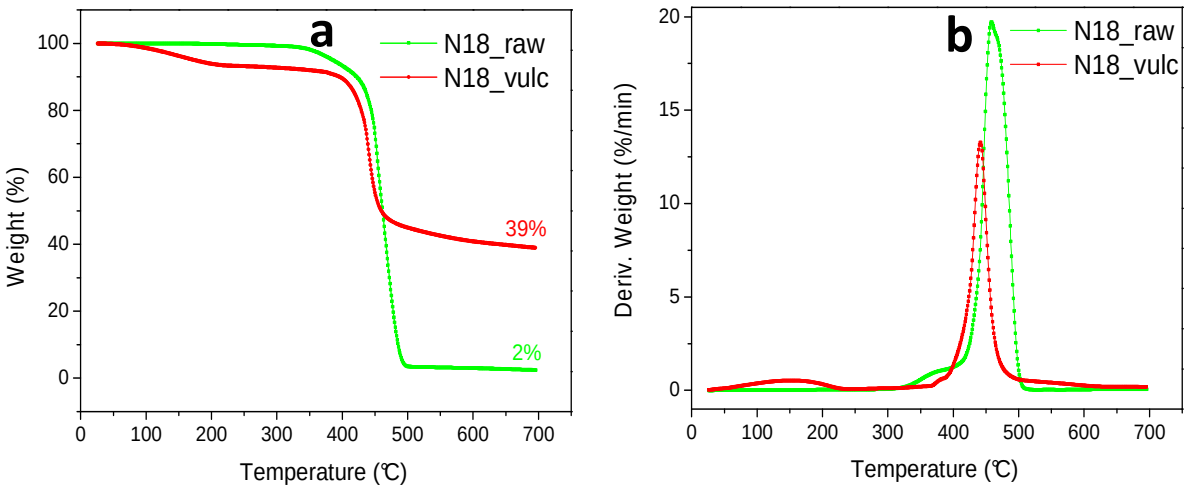

Fig. 4.4.8 (a) TG and (b) DTG plots of the raw rubber and its vulcanizate

(~30%) than the raw rubber (only ~ 2%). It could be obviated that the raw rubber features only one decomposition step while the vulcanizate showed two decomposition steps (Fig. 4.4.8b). Weight loss for the vulcanizate rubber sample at 100-200 °C is attributed to the evaporation of water molecules and hydrogen chloride produced during the vulcanization of NBR with zinc chloride. The onset degradation temperature is also observed to shift slightly towards elevated temperature (~396 °C) for the vulcanizate in comparison to that of the raw rubber sample (~344 °C). All this proves that the vulcanization of nitrile rubber with zinc chloride enhances the thermal stability of nitrile rubber.

Differential scanning calorimetry (DSC)

Differential scanning calorimetry was employed to study the thermal phase behavior of the corresponding samples. The samples were scanned from -160 °C to 100 °C in N_2 atmosphere at the heating rate of 10K/min. The corresponding DSC curves are exhibited in Fig. 4.4.9. The glass transition temperatures obtained for the raw rubber and the vulcanizate are demonstrated to be -48.6 °C and -44.5 °C respectively. The difference in the magnitudes of the T_g in comparison to dynamic mechanical analysis is attributed to the process of measurements in two different characterization techniques. DSC is a static measurement, whereas DMA is known to be a dynamic tool to characterize a specimen. Marginally higher T_g of the vulcanizate relative to the raw rubber coinciding with the DMA results are discussed earlier. Higher value of T_g is ascribed to the higher crosslink density imparted by the zinc chloride particles. Interestingly, in accordance to the DMA plot the vulcanizate showed two glass like

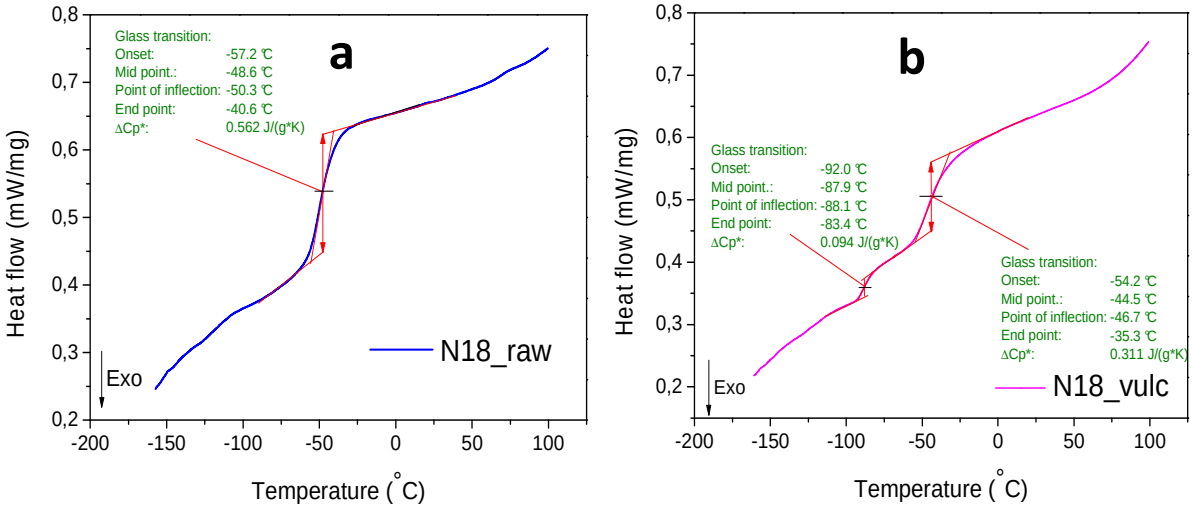

Fig. 4.4.9 Differential scanning calorimetry (DSC) curves of (a) raw rubber and (b) its vulcanizate

transitions in the DSC plot as well. As mentioned earlier, due to the β-relaxation at lower temperature, the NBR-$ZnCl_2$ vulcanizate showed an extra transition at -87.9 °C in the DSC plot. The co-ordination reaction between zinc cations and the nitrile group belonging to NBR is exothermic in nature [148]. Therefore, the exothermic glass like transition at lower temperature is attributed to the formation of the rubber-filler interaction established via the co-ordination bond.

4.4.7 Effect of hydrolysis

To carry out more intensive study about this novel kind of crosslinked network between NBR and zinc chloride established by the co-ordination linkage, the vulcanizate was boiled in water at 100 °C for 48 h. The resulting sample showed some interesting features in the FTIR peak as presented in Fig. 4.4.10. During water treatment, the co-ordination bond formed between zinc atom and the acetamide functional group is completely destroyed due to the extraction of zinc chloride [136] and subsequently new co-ordination linkages are generated between the zinc atom and the oxygen atom (with a lone pair) of the water molecule. The proposed reaction mechanism is exhibited in Fig. 4.4.11. Therefore, quite obviously, free acetamide group is available in the sample. A relatively strong and broad peak at 1639 cm^{-1} for the water treated sample (designated as N18_W) is obtained in the IR spectra. The strong presence of this peak clearly indicates the generation of acetamide functional group due to the reaction mentioned earlier. Hence, it is proposed that with the combined presence of nitrile and amide groups in the rubber, complexes of zinc chloride with amide groups are formed which eventually leads

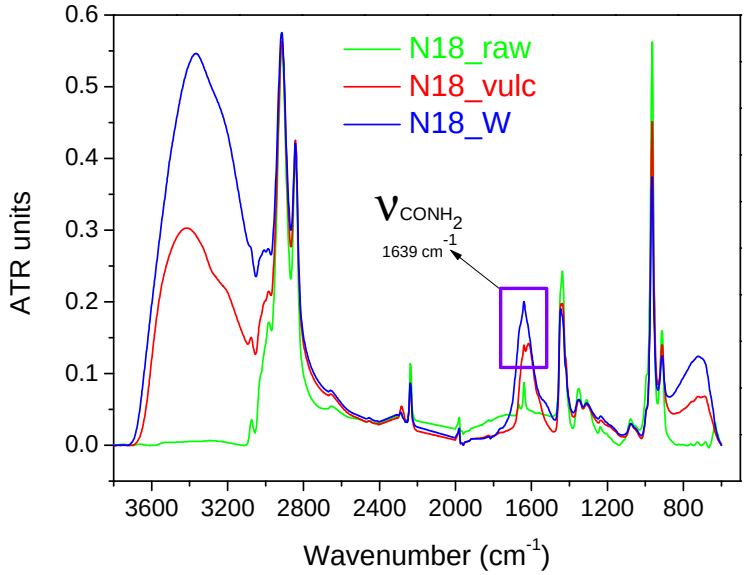

Fig. 4.4.10 FTIR spectra of the raw rubber, vulcanizate and hydrolyzed samples

to the generation of complex units within the vulcanizate [149].While boiling the corresponding vulcanizate in water for 48 h, substantial change in volume was observed afterwards as depicted in Fig. 4.4.12. The change in weight was also obvious. Moreover, to investigate the dynamic and thermal properties of the hydrolyzed sample, DMA and DSC studies were carried out. The peak in the loss tangent vs. temperature spectra (Fig. 4.4.12a) corresponding to the β-relaxation in case of the hydrolyzed sample shifted towards a little bit higher temperature at ~ -64.7 °C because post hydrolysis, higher intensity relaxation seems to occur facilitated by the free acetamide group. The same plot also exhibited a shoulder near -

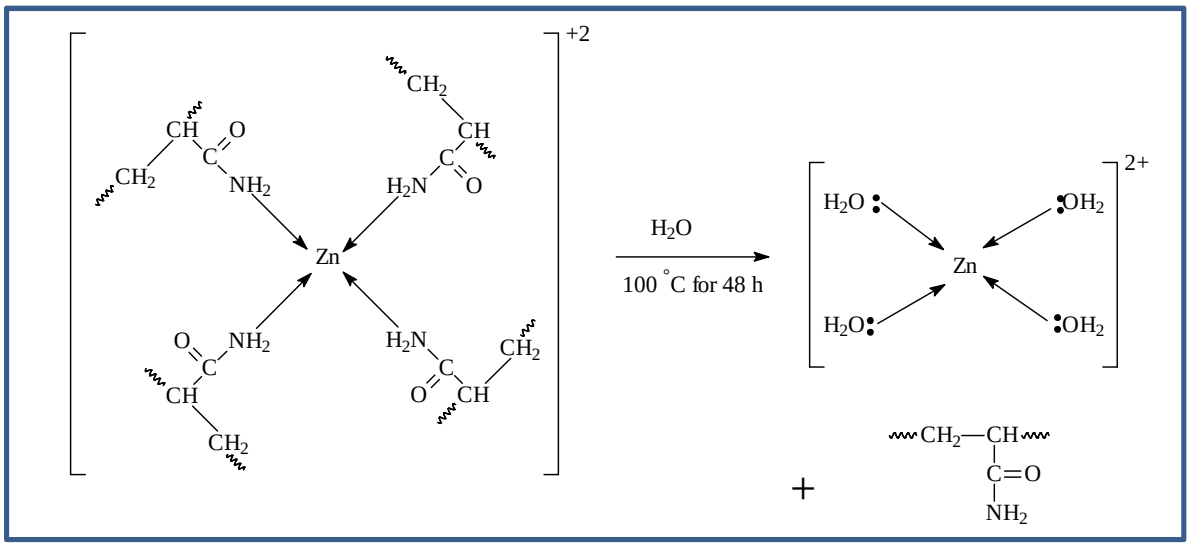

Fig. 4.4.11 Formation of Zn-H_2O based coordinate complex and free acetamide after treating the vulcanizate in boiling water (@100 °C) for 48 h

64.7 °C. This transition is perhaps attributed to the formation of carboxylic zinc compound due to the constant cyclic transformation of the acetamide to acidic functionality induced by water. Surprisingly, the storage modulus vs. temperature plot of the corresponding sample did not show any considerable drop in the magnitude and a plateau modulus was observed as well. Henceforth, it is confirmed that the new co-ordination complex formed (see reaction scheme: 4.4) after the water treatment between the zinc atom and water molecules are quite stable producing comparable dynamic mechanical properties. Detailed study based on DSC was carried out to understand and subsequently interpret the source of appearance of the shoulder at -64.7 °C in the DMA plot. Aqueous swelling behavior of all the vulcanizates with varying acrylonitrile content was studied too. The water uptake capacity of the rubber samples is demonstrated in Fig. 4.4.12d. The degree of swelling plots suggests that upon swelling, all the samples expanded isotropically at a level that is commensurate with the water uptake.

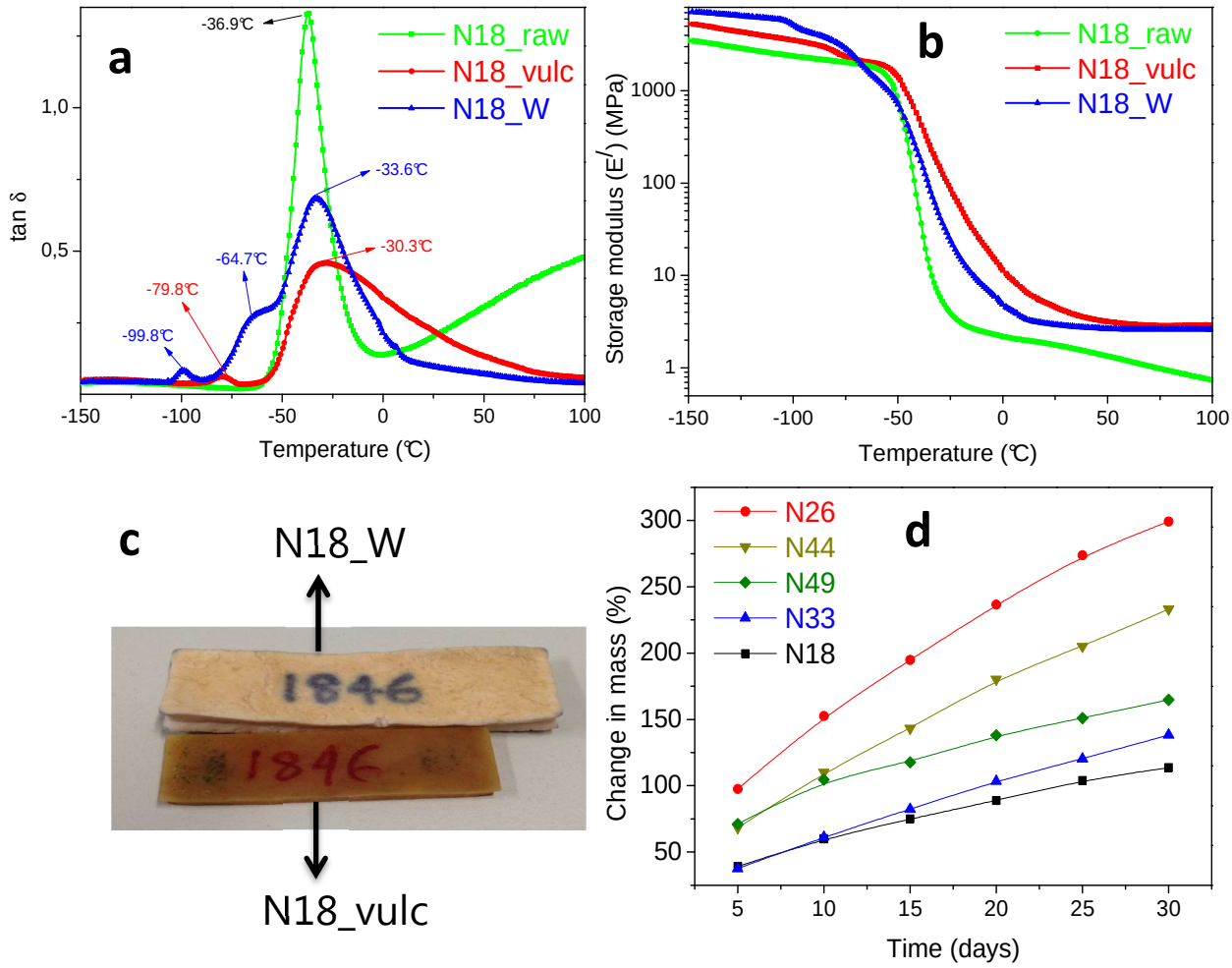

Fig. 4.4.12 (a) loss tangent, (b) storage modulus vs. temperature plots of the raw rubber, vulcanizate and water treated samples, (c) digital picture of the vulcanized and water treated samples, (d) swelling profile of the vulcanized rubber samples with different amount of acrylonitrile contents in water

No real plateau corresponding to equilibrium swelling was obtained for any of the rubber vulcanizates. NBR with least amount of acrylonitrile content (18%) amongst the rest showed the lowest amount of water uptake. The increasing tendency of swelling behavior while treated with water proves that the new type of crosslinking generated in the structure by co-ordination reaction of zinc and the nitrile group of the host polymer facilitates hydrophilicity to some extent. Fig. 4.4.13a shows the DSC plot of the N18_W during heating with a scan rate of 10K/min. Surprisingly the glass like transition belonging to the T_g was not evidently noticed in the DSC plot, however, an endothermic melting peak was also observed at ~ 10 °C

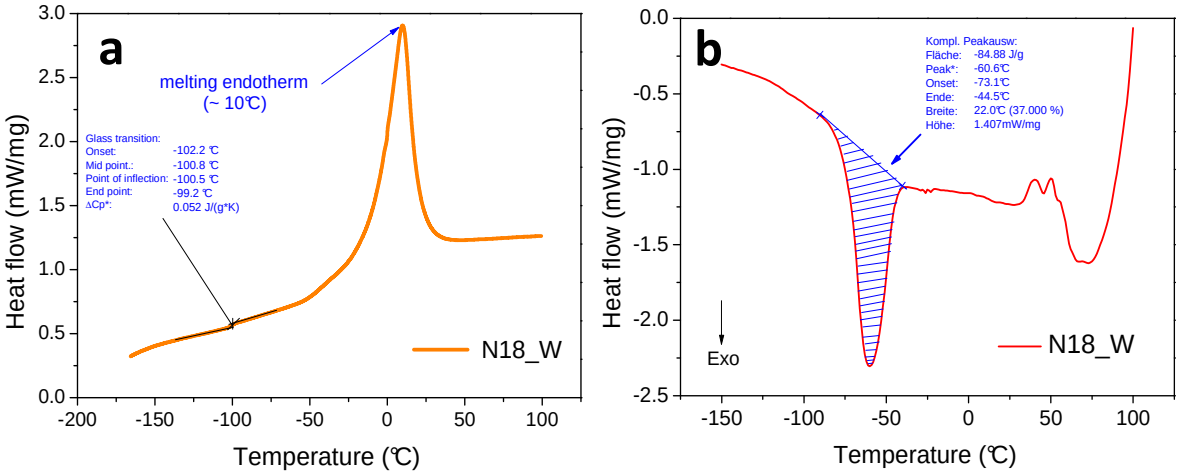

Fig. 4.4.13 DSC thermograms of the hydrolyzed rubber specimen (N18_W) during (a) 2nd heating and (b) cooling

because the water crystallites formed within the structure of the hydrolyzed specimen undergoes melting at higher temperature. The disappearance of the glass transition temperature in the DSC plot of the hydrolyzed specimen could be attributed to the melting of ice formed from the clustered water in the structure and therefore plasticizing effect of water

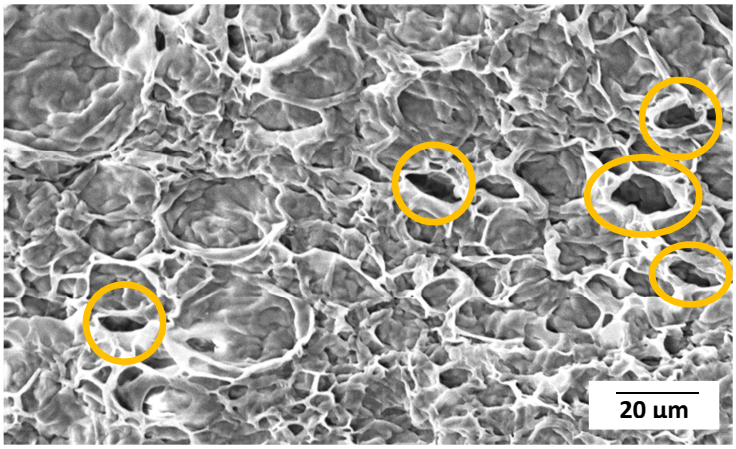

Fig. 4.4.14 SEM micrograph of N18_W. Yellow circles represent the pores generated after water treatment

was primarily responsible for suppressing the glassy to rubbery transition [150-152]. Water-based cross-links tend to form, leading to increased water - water interactions at the expense of water - polymer chain interactions [153]. Henceforth, the absence of the crystallization peaks indicates hydrophilic rubber cannot crystalize or possibly merge with the water crystallization peak below room temperature. A mild glass like transition at 100 °C attributing to the β-relaxation taking place for the bulky co-ordination reaction in the structure was realized though in the plot. This particular transition at low temperature does not alter its position and nature in the DSC plot if compared to the corresponding DMA plot. Fig. 4.4.13b

shows the cooling curve of the hydrolyzed sample at a constant rate of cooling. The ice-melting endotherm at ~ -60°C on the DSC thermogram as depicted in Fig. 4.4.13b resulted from the condensed water crystals in the hydrolyzed specimen [154-158]. The water crystals formed from water molecules had sufficient mobility for intermolecular interactions during rapid cooling (in this case 20K/min) in the DSC. The SEM micrograph of the hydrolyzed sample is displayed in Fig. 4.4.14. N18_Vulc sample after being treated in water generates more rough surfaces in the microstructure. Porous structure seems to be appeared in the whole area of the corresponding rubber specimen. Pores of various sizes were observed as well. The change in the microstructure in case of hydrolyzed sample with respect to the unhydrolyzed (Fig. 4.4.6a) one is pretty obvious. Driven by the phenomenon that a zinc and water based complex was formed after the water treatment, the network structure in the compound significantly alters and therefore the morphological difference is realized. These types of rubber products find applications in the water seals in the storage tanks between the concrete walls, wiper blades used in the cars.

Chapter 5

Conclusion and outlook

Conclusion

Nitrile rubber, a well-known specialty elastomers offers high temperature and oil resistance properties due to presence of polar nitrile groups in the chains. This rubber is the random copolymer with butadiene and acrylonitrile. Sometimes certain part of the acrylonitrile is replaced by a small amount of acrylic acid to synthesize carboxylated nitrile rubber with better performance and properties. The nitrile group as well as the carboxylic groups can also be exploited to generate chemical crosslinks between two polymer chains. On the other hand the use of zinc oxide is inevitable in the sulfur crosslinking process of all diene content polymers. This work is predominantly focused on exploring the role of various zinc containing sources in vulcanizing nitrile rubber and carboxylated nitrile rubber and subsequently investigating the various properties of such compounds. To pursue such a task, fundamental studies have been carried out to understand the basic phenomenon occurring with the zinc based nitrile rubber compounds and at the same time commercial viability of the end products have been taken care of as well.

In this work, we explored the nature of the ionic cross-linking of modified nitrile rubber i.e., carboxylated nitrile rubber produced by the use of different zinc compounds. As the mechanical and dynamic mechanical properties of a finished rubber component are the supreme qualities sought for commercially, we were driven to discover the source of such exceptional properties generated by ionic elastomers generated by XNBR and zinc sources.

Based on the results of different analytical approaches we reached into a conclusion that all the zinc-containing compounds can react with the carboxylic groups of XNBR under the usual vulcanizing conditions i.e., high temperature and pressure, but the final mechanical and dynamic mechanical properties of this rubber depend on the type of zinc compounds used as cross-linking agent. This work successfully elaborates about the fact we revealed associated with the ionomers. We realized that the ionic cross-linking occurs with each of the different zinc curatives used e.g., ZnO, Zn based LDH, and $ZnCl_2$, but they yield distinct curing results,

which is attributed to the formation of different coordination numbers in the ionic cross-links or clusters. By the virtue of formation of a special co-ordination octahedral geometry, a separated polymer phase with high zinc content eventually results within the structure.

After a well-crafted research study, we concluded that only ZnO can produce microphase separation, with a zinc-enriched second phase that we call "*zinc-carboxylate polymer*" that shows high-temperature dynamic mechanical relaxation behavior. This finding could be confirmed on the basis of HR-EFTEM, XRD and FT-IR results reported in this work. Moreover, swelling studies provided direct evidences that all zinc compounds participate in the ionic cross-linking process, but exclusively zinc oxide can offer special polymer microstructure and shows phase separated morphology like a block copolymer.

However, within the scope of this research work, we tried to understand the multiple phases of cross-linked XNBR. As the mechanical properties of the finished elastomeric products depend crucially on their internal phase-structures, i.e. the fraction and local distribution of the phases, their composition and their molecular configuration, special attentions and efforts were made to the chemical aspects of the cross-linking structures. The profound correlation between the mechanical properties and the temperature is mainly governed by the chemistry involved with the XNBR cross-linking with different zinc compounds.

Layered structured clay minerals e.g., montmorillonite, pyrophyllite, vermiculite, hectorite, saponite, perkalite are one of the focused nano-sized fillers which have been explored in different elastomeric matrix to find high performance elastomeric materials. Highly anisotropic feature, ease of synthesis and modification, relatively low cost, non-hazardous nature, processability make this class of inorganic layered material very suitable candidate as alternative fillers for rubbers. However, Layered double hydroxides (LDH) have not been explored to a greater extent with elastomer matrices. This work is focused on investigating the role of LDH clay on nitrile rubber as a multi-functional filler material which would cure the rubber without the assistance of any classical vulcanizing aids and subsequently enhance the required fundamental properties like, mechanical, dynamic mechanical, thermal along with some other sophisticated properties like flame retardancy.

A set of rubber nanocomposites based on zinc containing LDH and XNBR were prepared. It was realized that very high amount of (~100 phr) of LDH loaded in the XNBR matrix allowed us to obtain substantial improvements in the physical properties, such as elastic modulus, thermal decomposition, and flame retardancy. Morphological features based on

TEM micrographs revealed that it is possible to obtain an excellent dispersion of LDH even with a higher concentration (~ 50 wt %). No real tendency of the LDH to form agglomerates was noticed in the microstructures. A direct polymer–filler interaction was suggested by FT-IR spectroscopy. This polymer–filler interaction is supported further by the reported strain-sweep analysis. To get rid of toxic and expensive phosphorous based flame retardants and halogen compounds commercially popular to use as fire retardant materials, LDH was idealized. Excellent enhancement in flame-retardency behavior of the XNBR–LDH composites was obtained. We attribute this to the formation of a thermally insulating layer by the LDH. The improvement in flame-retardant behavior is more pronounced in composites with higher loadings of LDH. Flame retardency effect in this study is even better with respect to a couple of reference systems based on halogenated and Sb_2O_3 based nitrile rubber [159-160]. Finally, the incorporation of even a small amount (4 phr) of LDH in the XNBR allows the compounds to cure at a useful level, without the presence of ZnO. We propose that the interaction at the interface between the XNBR matrix and LDH plays a significant role in the improvement in the mechanical properties of the composites in this study. In the current work, we have proved that a direct rubber–filler chemical interaction improves the mechanical properties, particularly when the size of the filler particles is relatively large compared to the average aggregated particle sizes of the standard reinforcing materials, carbon black and precipitated silica.

Thermo-responsive and mechano-adaptive elastomeric product was prepared by introducing '*zinc soap*' into the ionic elastomer formed by the combination of XNBR and zinc oxide. Increasing the amount of zinc stearate in the compounds with keeping the amount of zinc oxide fixed, strength enhancement of the final products was evidently realized. While curing at elevated temperature, due to melting of zinc stearate particles, the elastic modulus or torque value was dropped for the rubber compounds loaded with higher amount of zinc stearate. This melting behavior of zinc stearate was explored to tune the dynamic properties where the storage modulus could be altered with temperature.

Interesting structural reorientation between of hexa and tetrahedral geometries generated by the ionic elastomers in presence of zinc stearate was observed in the FTIR study. Increasing the amount of crystalline zinc soap only altered the hexa-coordinated structure in the ionomer (1539 cm^{-1}) but the tetra-coordinated structure (1587 cm^{-1}) did not change much. Nano-crystalline zinc stearate particles were seen to form several '*micro-islands*' in the structure acting as the possible reinforcing filler materials whereas phase-separated lamellar

morphology was observed as well generated by the ionic association between the zinc oxide particles and the carboxylic group provided by the host polymer. Microstructures witnessed in the morphological analysis supported the mechanical properties. Both stress strain and fracture mechanical properties of the rubber compounds filled with higher amount of zinc stearate improved substantially. Toughness was also enhanced to some extent. Inspired by the DSC results, the crystallinity aspect of zinc stearate particles was explored. Hence, effect of quenching was investigated. Post fast cooling, the corresponding rubber compound yielded inferior mechanical properties than the slowly cooled sample. Rubber compounds prepared by such compositions could find applications in active damping in the racing car where the mechanical properties need to be tuned as per the requirements with regards to the heat produced during high-speed operations.

Apart from the classical crosslinking mechanisms known to the rubber world in the forms of covalent crosslinking (by sulfur and peroxide vulcanization) and ionic crosslinking, a novel type of crosslinking was studied in nitrile rubber. Vulcanization of acrylonitrile buta di-ene rubber induced by co-ordination reaction was an interesting field for research. An inorganic metal salt i.e., zinc chloride ($ZnCl_2$) was introduced into NBR rubber and the consequent properties of the end products were investigated. The co-ordination reaction between the zinc atom from $ZnCl_2$ and the nitrile group (-CN) from the host polymer fabricated a chelate complex network structure which was the primary driving force to vulcanize the rubber without any classical curing aids like sulfur , accelerator etc. The results obtained from FT-IR, DSC and DMA successfully demonstrated the co-ordination linkage formed between the foreign particles (read, zinc chloride) and the host polymer (read, nitrile rubber). Homogeneity of the system was evinced from the SEM and EDX analyses.

DMA study indicated a couple of relaxation in the spectra. Apart from the usual peak at glass transition temperature characterized by α-relaxation, an extra relaxation was realized to occur at lower temperature for the nitrile rubber compound for the very first time in this work. This particular relaxation was termed as β-relaxation. Due to formation of a bulky co-ordination network induced by zinc acetamide complex, certain degree of restriction in the chain dynamics primarily produced this relaxation. We assumed in this work that the β-relaxation predominantly acts as the precursor of the global motion of the whole unit. Effect of hydrolysis was also investigated on the corresponding vulcanizate. After boiling the sample at 100°C for 2 days, significant change in the physical and chemical natures was observed. The acetamide complex in the vulcanizate before hydrolysis was destroyed and a new co-

ordination complex between zinc atom and water molecule was formed. The truth of this reaction scheme was proved by the FT-IR, DSC and DMA results. Longer exposure in water made the vulcanizate hydrophilic in nature and therefore could be considered to be used commercially as wiper blades, water tank and water seals used in washing machines.

Outlook

Despite the progress made within the scope of this research work, some issues related to these topics still remain as matters of further concerns.

- As the temperature dependent mechanical properties showed remarkable correlations with chemistry, further studies need to be carried out to get more in-depth idea about the role of the zinc compounds e.g., ZnO in developing the new polymer phase of carboxylated nitrile rubber.
- It would be interesting to find the effect of increasing amount of zinc oxide on the development of the lamellar morphology. Selection of another grade of carboxylated nitrile rubber with varying amount of carboxylic acid could also be explored to investigate the stoichiometric configuration of the ionomer formed in situ.
- In this context the influence of sulfur curatives on crystalline character can be further studied. Other mixing additives like MgO or CaO could also be explored to gain better insight about the development of the morphology and associated mechanism involved with.
- Zinc based XNBR system forms ionomers. These ionomers, if properly tuned and modified might potentially generate outstanding self-healing rubbers.
- As LDH being extensively studied with di-ene rubbers to extract better mechanical, dynamic mechanical, thermal and other properties, natural rubber could be an interesting choice as a matrix elastomer. As NR finds a humongous commercial value in tire industries and its components, LDH filled NR system can solve many critical issues related to tire industries. The primary challenge to overcome with this particular system is to disperse LDH effectively into the NR matrix due to the availability of different protein and lipid groups in natural rubber formulation.
- Both zinc and magnesium based LDH are amphoteric in nature. Therefore, while mixing with a polar rubber like XNBR, their structures might undergo some physical and chemical changes. As a consequence, the mechanical properties of the end product

may deteriorate than expected. Ca-Al LDH could be an excellent alternative to explore with XNBR.

- LDH is coming up as an excellent alternative resource to replace the conventional fillers in rubbers. This inorganic clay, if properly explored with different types of rubbers, can yield abundant commercially significant properties in the finished products. Several other smart properties like thermotropicity etc. can also be envisaged in the LDH based rubber nanocomposites [161-162]. Significant interest has been noticed to design such types of thermotropic materials for overheat protection of the solar cells as shown in Fig. 5.1.

Fig. 5.1 Protective materials for overheating solar panel

- Like zinc stearate, a few other compatible crystalline particles could be incorporated into ionic elastomers to extract more fundamental mechanisms involved with the system.
- Relatively rare crosslinking system introduced by co-ordination reaction in the rubber vulcanizates could produce remarkable properties as compared to classically crosslinked samples. The knowledge gained through this research work could be exploited to study more such alternative crosslinking ideas to open a new horizon of rubber elasticity.

In a nutshell, thorough and intensive approaches have been followed in this research work to extract some fundamental understanding about the role of zinc in nitrile rubber compounds. By using some fruitful ideas and of course executing those to results by the help of a series of novel and sophisticated experimental techniques gave new insight into structure-property relationships of nitrile rubber compounded with different zinc sources. Besides understanding the mechanism of the systems, the commercialization opportunity is also taken care of. However, a long term vision and further interest are necessary to draw a comprehensive picture about the relevant topic.

List of figures

List of tables

References

[1] R.B. Simpson, Rubber basics, 2002, Rapra Technology Limited, UK, p.117-123,

[2] B. Slade, Elastomerics, 1985, 117, 11, 34

[3] G. L. M. Vroomen, G. W. Visser and J. Gehring, Rubber World, 1991,205,2,23

[4] B. Thorburn and Y. Hoshi, Rubber World, 1992,206, 4, 17

[5] W. Hofmann, Rubber Technology Handbook, Hanser Publishers, Munich, Germany, 1989, p.404.

[6] A. K. Bhowmick and D. Mangaraj, Rubber Products Manufacturing Technology, Ed., A. K. Bhowmick, M. M. Hall and H. A. Benary, Marcel Dekker Inc., New York, 1994, p.385

[7] A.V. Chapman. Safe rubber chemicals-reduction of zinc levels in rubber compounds. TAARC/MRRA, 1997, 20.

[8] G.J.Fosmire, Zinc toxicity, Am J Clin Nutr, 1990, 51, 225-227.

[9] A.Chapman, T.Johnson, The role of zinc in the vulcanization of styrene-butadiene rubbers. Kautschuk Gummi Kunststoffe, 2005, 58, 7-8, 358-361

[10] A.Das, D.Y.Wang, A.Leuteritz, K.Subramaniam, H.C.Greenwell, U.Wagenknecht, G.Heinrich. Preparation of zinc oxide free, transparent rubber nanocomposites using a layered double hydroxide filler. J Mater Chem, 2011, 21, 7194-7200

[11] D.Basu, A. Das, K.W.Stöckelhuber, U.Wagenknecht, G.Heinrich. Advances in layered double hydroxide (LDH)-based elastomer composites, Progress in Polymer Science, 2014, 39, 3, 594-626

[12] S.B.Eshwaran, D.Basu, B.Kutlu, A.Leuteritz, U.Wagenknecht, K.W.Stöckelhuber, K.Naskar, A.Das, G.Heinrich, Stearate modified zinc-aluminium layered double hydroxides and acrylonitrile butadiene rubber nanocomposites. Polymer-plastics technology and engineering, 2013, 53, 1, 65-73

[13] D.Y.Wang, A.Das, A.Leuteritz, K.Subramaniam, U.Wagenknecht, G.Heinrich, German Patent DE 102010043448 A1, 2011.

[14] D.Basu, A.Das, K.W.Stöckelhuber, D.Jehnichen, P.Formanek, E.Sarlin, J.Vuorinen, G.Heinrich. Evidence for an in-situ developed polymer phase in ionic elastomers, Macromolecules, 2014, 47, 10, 3436-3450

[15] L. Ibarra, A. Rodríguez, I. Mora-Barrantes. Crosslinking of carboxylated nitrile rubber (XNBR) induced by coordination with anhydrous copper sulfate, Polymer International, 2009, 58, 218-226

[16] U.K.Mandal, D.K.Tripathy, S.K.De. Dynamic mechanical spectroscopic studies on plasticization of an ionic elastomer based on carboxylated nitrile rubber by ammonia, Polymer, 1996, 37,25, 5739-5742

[17] P.Antony, S.K.De. Ionic thermoplastic elastomers: A review, Journal of macromolecular science, part C:polymer reviews, 2001, 41, 1-2, 41-77

[18] C.M. Blow, C. Hepburn, Rubber Technology and Manufacture, Butterworth Scientific, London , 1981, 2nd Ed.

[19] J.E. Mark, Science and Technology of Rubber, Academic Press, San Diego, 1994, 2nd Ed.

[20] G. Alliger, Vulcanisation of Elastomers - Principles and Practice of Vulcanisation of Commercial Rubbers, Reinhold Publishing, New York , 1964.

[21] L. Bateman, The Chemistry and Physics of Rubber-like Substances, MacLaren, London, 1963.

[22] M.R. Kresja, J.L. Koenig, Rubber Chemistry and Technology, 1993, 66, 376-410.

[23] M. A. Lo´pez-Manchado, M. Arroyo, B. Herrero, J. Biagiotti, Vulcanization Kinetics of Natural Rubber–Organoclay, Journal of Applied Polymer Science, 2003, 89, 1-15

[24] N.J. Morrison, M. Porter, "Crosslinking of rubbers", in The synthesis, characterization, reactions and applications of polymers, G. Allen, Ed., Pergamon press, 1984, 115

[25] V. Ducháček, Kinetics of thiuram-accelerated sulfur vulcanuization, Journal of applied polymer science, 1974, 18, 125-132

[26] W. Scheele, O. Lorenz, W. Dummer, Rubber Chemistry and Technology, 1956, 29, 1.

[27] L, Bateman, C.G. Moore, M. Porter, and B. Saville in “The Chemistry and Physics of Rubber like Substances,” L Bateman, Ed., Maclaren & Sons Ltd., London, Wiley and Sons, 1963, pp 449.

[28] A.Y. Coran. Vulcanization. Part V. The Formation of Crosslinks in the System: Natural Rubber-Sulfur-MBT-Zinc Ion, Rubber Chemistry and Technology, 1964, 37,3, 679-687

[29] V. Ducháčeˆk, A.Kuta, P.Přibyl. Efficiency of metal activators of accelerated sulfur vulcanization, Journal of Applied Polymer Science, 1993, 47, 4, 743-746

[30] A.Eisenberg. Clustering of ions in organic polymers - a theoretical approach. Macromolecules, 1970, 3, 147-154

[31] A.Eisenberg. B.Hird, R.B.Moore. A new multiplet-cluster model for the morphology of random ionomers. Macromolecules, 1990, 23, 4098-4107

[32] W.J.MacKnight, R.D.Lundberg. Elastomeric ionomers, Rubber Chemistry and Technology, 1984, 57, 3, 652-663

[33] B.Hird, A.Eisenberg. Sizes and stabilities of multiplets and clusters in carboxylated and sulfonated styrene ionomers. Macromolecules, 1992, 25, 6466-6474

[34] W.J. MacKnight. Structure and Properties of Ionomers. NATO ASI Series C Mathematical and Physical Sciences, Vol 198, Ed by Pineri M and Eisenberg A, 1986 p 1.

[35] D.K.Jenkins, E.W.Duck, Ionic Polymers, L.Holliday, Ed., Halstead Press, Wiley, New York, 1975, Ch.3

[36] H.Mou, F.Shen, Q.Shi, Y.Liu, C.Wu, W.Guo. A novel nitrile butadiene rubber/zinc chloride composite: coordination reaction and miscibility. European Polymer Journal, 2012, 48, 4, 857-865

[37] C.Xu, L.Fang, Y.Chen. In situ reactive compatibilized polypropylene/nitrile butadiene rubber blends by zinc dimethacrylate: preparation, structure, and properties. Polymer Engineering and Science, 2013, doi: 10.1002/pen.23789

[38] Y.Lu, L.Liu, C.Yang, M.Tian, L.Zhang. The morphology of zinc dimethacrylate reinforced elastomers investigated by SEM and TEM. European Polymer Journal, 2005, 41, 577-588

[39] B.C.Guo, F.Chen, W.W.Chen, Y.D.Lei, D.M.Jia. Reinforcement of nitrile rubber by in situ formed zinc disorbate. Express Polymer Letters, 2010, 4, 9, 529-538

[40] S.O'Leary, D.O'Hare, G.Seely. Delamination of layered double hydroxides in polar monomers: new LDH-acrylate nanocomposites. Chemical Communications, 2002, 1506-1507

[41] C.Hochstetter. Untersuchung über die Zusammensetzung einigerMineralien. Journal für praktische Chemie 1842 , 27, 375–378.

[42] W.Feitknecht , M.Gerber. Zur Kenntnis der Doppelhydroxyde und basischen Doppelsalze III. über magnesium–aluminium-doppelhydroxyd. Helvetica Chimica Acta, 1942, 25, 131–137.

[43] A.Vaccari. Clays and catalysis: a promising future. Applied Clay Science, 1999, 14, 161-198

[44] F.R.Costa, S.Pradhan, U.Wagenknecht, A.K.Bhowmick, G.Heinrich. XNBR/LDH nanocomposites : effect of vulcanization and organic modifier on nanofiller dispersion and strain-induced crystallization. Journal of Polymer Science Part B : Polymer Physics, 2010, 48, 2302-2311

[45] A.Das, F.R.Costa, U.Wagenknecht, G.Heinrich. Nanocomposites based on choloroprene rubber : effect of chemical nature and organic modification of nanoclay on the vulcanizate properties. European Polymer Journal, 2008, 44, 3456-3465

[46] S.Pradhan, F.R.Costa, U.Wagenknecht, D.Jehnichen, A.K.Bhowmick, G.Heinrich. Elastomer / LDH nanocomposites: synthesis and studies on nanoparticle dispersion,

mechanical properties and interfacial adhesion. European Polymer Journal, 2008, 44, 3122-3132

[47] B.Pradhan, S.K.Srivastava, R.Ananthakrishnan, A.Saxena. Preparation and characterization of exfoliated layered double hydroxide / silicone rubber nanocomposites. Journal of Applied Polymer Science, 2011, 119, 343-351

[48] A. Das , J.J.George, B. Kutlu, A. Leuteritz , D.Y.Wang , S. Rooj , R. Jurk, R. Rajeshbabu , K.W. Stöckelhuber , V. Galiatsatos , G. Heinrich . A novel thermotropic elastomer based on highly-filled LDH–SSB composites. Macromolecular Rapid Communications , 2012, 33,337–42.

[49] A.Laskowska, M.Zaborski, G.Boiteux, O.Gain, A.Marzec, W.Maniukiewicz. Ionic elastomers based on carboxylated nitrile rubber (XNBR) and magnesium aluminium layered double hydroxide (hydrotalcite). Express Polymer Letters, 2014, 8, 374-386.

[50] A. Kołodziejczak-Radzimska, T.Jesionowski. Zinc oxide-from synthesis to application: A review. Materials, 2014, 7, 4, 2833-2881.

[51] A.Moezzi, A.M.McDonagh, M.B.Cortie. Zinc oxide particles: synthesis, properties and applications. Chemical Engineering Journal, 2012, 185-186, 1-22.

[52] D. Basu, A. Das, J.J. George, D.Y.Wang, K.W. Stöckelhuber, U. Wagenknecht, A. Leuteritz, B. Kutlu, U. Reuter, G. Heinrich. Unmodified LDH as reinforcing filler for XNBR and the development of flame-retardant elastomer composites. Rubber Chemistry and Technology, 2014, 87, 4,606-616.

[53] V.Thakur , A.Das , R.N. Mahaling , S.Rooj , U.Gohs , U.Wagenknecht , G.Heinrich . Influence of layered double hydroxides on the curing of carboxylated nitrile rubber with zinc oxide. Macromolecular Materials and Engineering , 2009,294, 561–569.

[54] H.P.Brown. Carboxylic elastomers. Rubber Chemistry and Technology, 1957, 30, 1347-1386.

[55] D.H.Grant, N.Grassie. The thermal decomposition of polymethacrylic acid. Polymer, 1960, 1, 125-134.

[56] D.Y.Wang, A.Das, A.Leuteritz, R.N.Mahaling, D.Jehnichen, U.Wagenknecht, G.Heinrich. Structural characteristics and flammability of fire retarding EPDM / layered double hydroxide (LDH) nanocomposites. RSC Advances, 2012, 2, 3927-3933.

[57] L.Ibarra, M.Alzorriz. Ionic elastomers based on carboxylated nitrile rubber and calcium oxide. Journal of Applied Polymer Science, 2003, 87, 805-813.

[58] L.Ibarra, M.Alzorriz. Ionic elastomers based on carboxylated nitrile rubber and magnesium oxide. Journal of Applied Polymer Science, 2007, 103, 1894-1899.

[59] L.Ibarra, A.Marcos-Fernández, M.Alzorriz. Mechanistic approach to the curing of carboxylated nitrile rubber (XNBR) by zinc peroxide / zinc oxide. Polymer, 2002, 43, 1649-1655.

[60] P.Antony, S.K.De, D.G.Peiffer. Copatibilization of ionomeric polyblends by intermolecular ionic interactions. Rubber Chemistry and Technology, 1999, 72, 449-463.

[61] L.Ibarra, M.Alzorriz. Ionic elastomers based on carboxylated nitrile rubber (XNBR) and zinc peroxide : influence of carboxylic group content on properties. Journal of Applied Polymer Science, 2002, 84, 605-615.

[62] L.Ibarra, M.Alzorriz. Vulcanization of carboxylated nitrile rubber (XNBR) by zinc peroxide. Polymer International, 1999, 48, 580-586

[63] M.Maciejewska, A.Krzywania-Kaliszewska. Thermo-Shrinkable Elastomers. Ch.7, Advanced Elastomers - Technology, Properties and Applications **, e**dited by Anna Boczkowska, ISBN 978-953-51-0739-2, 412 pages, Publisher: InTech, Chapters published September 12, 2012 under CC BY 3.0 license , DOI: 10.5772/2784

[64] M. Przybyszewska, M. Zaborski, The effect of zinc oxide nanoparticle morphology on activity in crosslinking of carboxylated nitrile elastomer, Express Polymer Letters, 2009, 3, 9, 542-552.

[65] N. Hohlbein, T.Pelzer, J. Nothacker, M.von Tapavicza, A. Nellesen, H.Datta, A.M. Schmidt, "Self-healing processes in ionomeric elastomers." *ICSHM 2013: Proceedings of the 4th International Conference on Self-Healing Materials, Ghent, Belgium, June 16-20, 2013*. Ghent University; Delft University of Technology, 2013.

[66] P.J.Flory, J.Rehner. Statistical Mechanics of Cross-Linked Polymer Networks II. Swelling. Journal of Chemical Physics, 1943, 11, 512-521

[67] M.Zaborski, A.Kosmalska. Silica modified by use of organosilanes as a filler for carboxylate butadiene-acrylonitrile rubber. Kautschuk und Gummi Kunststuffe, 2005, 58, 354-357

[68] A.Przepiórkowska, K.Chrońska , M.Zaborski. Chrometanned leather shavings as a filler of butadiene–acrylonitrile rubber. Journal of Hazardous Materials, 2007, 141, 252-257

[69] A.A.Griffith. The phenomena of rupture and flow in solids. Philosophical transactions of the Royal Society of London. Series A, 1920, 221, 163-198

[70] R.S.Rivlin, A.G.Thomas. Rupture of rubber. I. Characteristic energy for tearing. Journal of Polymer Science, 2003, 10, 3, 291-318

[71] T.D. Nguyen, S. Govindjee, P.A. Klein, H. Gao. A material force method for inelastic fracture mechanics. Journal of the Mechanics and Physics of Solids, 2005, 53, 1, 91-121

[72] U.K.Mandal, D.K.Tripathy, S.K.De. Effect of silica filler on dynamic mechanical properties of lonic elastomer based on carboxylated nitrile rubber. Journal of Applied Polymer Science, 1995, 55, 1185-1191

[73] U.K.Mandal, D.K.Tripathy, S.K.De. Moving die rheometry and dynamic mechanical studies on the effect of reinforcing carbon black filler on ionomer formation during crosslinking of carboxylated nitrile rubber by zinc oxide, Polymer, 1993, 34, 3832-3836

[74] U.K.Mandal, D.K.Tripathy, S.K.De, Effect of carbon black fillers on dynamic mechanical properties of ionic elastomer based on carboxylated nitrile rubber . Plastics rubber and composites processing and applications , 1995, 24,19-25.

[75] P. Antony, S. Bandyopadhyay, S.K.De, Synergism in properties of ionomeric polyblends based on zinc salts of carboxylated nitrile rubber and poly(ethylene-co-acrylic acid), Polymer 2000, 41, 787–793

[76] L.Ibarra, M. Alzorriz, Vulcanization of carboxylated nitrile rubber (XNBR) by a mixed zinc peroxide–sulphur system. Polymer International, 2000, 49, 115-121.

[77] L.Ibarra, M. Alzorriz, The effect of crosslinking type on the physical properties of carboxylated acrylonitrile butadiene elastomers. Polymer International, 1999, 73, 927-933.

[78] M. Hara, P. Jar, P, J.A.Sauer, Effect of sample history on ionic aggregate structures of sulphonated polystyrene ionomers, Polymer 1991, 32,1380-1383

[79] W. Clegg, I.R.Little, B.P. Straughan, Zinc carboxylate complexes: structural characterization of the mixed-metal linear trinuclear complexes $MZn_2(crot)_6(base)_2$ (M = Mn, Co, Ni, Zn, Cd, Mg, Ca, Sr; $crot^-$ = crotonate(1-); base = quinoline, 6-methylquinoline) Inorganic Chemistry, 1988, 27, 1916-1923.

[80] D. Min, S.S. Yoon, C. Lee, C., C.Y. Lee, M. Suh, Y.J. Hwang, W.S. Han, S.W. Lee, A zinc(II)-carboxylate coordination polymer constructed from zinc nitrate and 2,6-naphthalenedicarboxylate, Bulletin of the Korean Chemical Society,2001, 22, 531-533

[81] J.A. Andor, O. Berkesi, I. Dreveni, E. Varga, Physical and chemical modification of zinc carboxylate-containing lubricants by molecular structure changes, Lubrication Science, 1999, 11-2, 115-134

[82] J.W. Nicholson, P.J. Brookman, O.M. Lacy, G.S. Sayers, A.D. Wilson, A study of the nature and formation of zinc polyacrylate cement using Fourier transform infrared spectroscopy, Journal of Biomedical Materials Research , 1988, 22, 623-631.

[83] S.S. Chen, J. Fan, T.A. Okamura, M.S. Chen, Z. Su, W.Y. Sun, N. Ueyama, Synthesis, crystal structure, and photoluminescence of a series of Zinc(II) coordination polymers with 1,4-Di(1H-imidazol-4-yl) benzene and varied carboxylate ligands , Crystal growth and design, 2010, 10, 812-822

[84] C. Zhang, Y. Che, Z. Zhang, X. Yang, L. Zang, Fluorescent nanoscale zinc(II)-carboxylate coordination polymers for explosive sensing , Chemical Communications. 2011, 47, 2336-2338.

[85] M.M. Coleman, J.Y. Lee, P.C. Painter, Acid salts and the structure of ionomers, Macromolecules, 1990, 23, 2339-2345.

[86] J. Lin, P.M. Jones, M.D. Lowery, R.R. Gay, S.L. Cohen, Coordination chemistry of ammonia on zinc oxide (0001) and cuprous chloride (111) surfaces: .sigma.-bonding interactions with d10 metal ion sites, Inorganic Chemistry, 1992, 31, 686-695

[87] R.C. Mehrotra, R. Bohra, Metal carboxylates ; Academic: New York, 1983

[88] V.M. Litvinov, P.P. De, Spectroscopy of rubbers and rubbery materials. 2002, Rapra Technology Limited, UK, ISBN: 1-85957-280-4

[89] R.A. Weiss, J.J Fitzgerald, D. Kim, Viscoelastic behavior of plasticized sulfonated polystyrene ionomers, Macromolecules, 1991, 24, 1064-1070.

[90] R.A. Weiss, J.J Fitzgerald, D. Kim, Viscoelastic behavior of lightly sulfonated polystyrene ionomers, Macromolecules, 1991, 24, 1071-1076

[91] H.P. Brown, Crosslinking Reactions of Carboxylic Elastomers, Rubber Chemistry and Technology, 1963, 36, 931-962

[92] K. Sunity, S.K. Chakraborty, S.K. De, Effect of curing systems on polymer-filler interaction, technical properties and fracture mode of carboxylated nitrile rubber, Polymer, 1988, 24, 1055-1062

[93] S. Pierre, A. Eisenberg, Effect of plasticization by amines on the physical properties of an acidic styrene copolymer, Journal of Polymer Science Part B: Polymer Physics, 1988, 26, 569-580

[94] J.J. Lagowski, The chemistry of non-aqueous solvents; Academic Press: New York, vol. III.1970

[95] P.K. Agarwal; R.T. Garner, W.W. Graessley , Counterion and solvent effects on the dilute solution viscosity of polystyrene ionomers, Journal of Polymer Science Part B: Polymer Physics, 1987, 25, 2095-2111.

[96] A. Das, K.W. Stöckelhuber, G. Heinrich, Influence of layered silicate on the self-crosslinking of polychloroprene and carboxylated nitrile rubber, Macromolecular Chemistry and Physics, 2009, 210, 189-199.

[97] H. Mou, F. Shen, Q. Shi, Y. Liu, C. Wu, W. Guo, A novel nitrile butadiene rubber/zinc chloride composite: Coordination reaction and miscibility, European Polymer Journal , 2012, 48, 857-865

[98] H. Dohi, S. Horiuchi, Locating a Silane Coupling Agent in Silica-Filled Rubber Composites by EFTEM, Langmuir, 2007, 23, 12344-12349

[99] I.P. Campbell, C. He, M.P. Stoykovich, Topologically distinct lamellar block copolymer morphologies formed by solvent and thermal annealing, ACS Macro Letters, 2013, 2, 918−923.

[100] W.W. Graessley, Polymeric liquids & networks: dynamics and rheology. 2008, Taylor & Francis (1st edition).

[101] K.W. Stöckelhuber, A. Svistkov, A. Pelevin, G. Heinrich, Impact of filler surface modification on large scale mechanics of styrene butadiene/silica rubber composites, Macromolecules, 2011, 44, 4366-4381

[102] M. Rubinstein, R.H. Colby, Polymer Physics; Oxford University Press: Oxford, U.K., 2003, p330.

[103] T.A. Vilgis, Time scales in the reinforcement of elastomers, Polymer, 2005, 46, 4223–4229

[104] A.V. Chapman. Safe rubber chemicals-reduction of zinc levels in rubber compounds. TAARC/MRRA, 1997, 20.

[105] S.B. Eshwaran, D. Basu, S.R. Vaikuntam, B. Kutlu, S. Wiessner, A. Das, K. Naskar, G. Heinrich. Exploring the role of stearic acid in modified zinc aluminium layered double hydroxides and their acrylonitrile butadiene rubber nanocomposites. Journal of Applied Polymer Science, 2015, doi:10.1002/APP.41539

[106] N.J. Morrison, M. Porter, Comprehensive Polymer Science: The Synthesis, characterization, reactions and applications of polymers: Vol. 6 Polymer Reactions,G. Allen, Ed., Pergamon Press, Oxford 1989, ch. 4.

[107] G. Heideman; R.N. Datta, J.W.M. Noordermeer, Activators in accelerated sulfur vulcanization, Rubber Chemistry and Technology, 2004, 77, 512-541

[108] K. Sahakaro, N. Naskar ,R.N. Datta, J.W.M. Noordermeer , Reactive blending, reinforcement and curing of NR/BR/EPDM compounds for tire sidewall applications, Rubber Chemistry and Technology, 2007, 80, 115-138

[109] G. Kraus, Mechanical losses in carbon black filled rubbers, Journal of Applied Polymer Science, Appl. Polym. Symp., 1984, 39, 75–92.

[110] E.Kanezaki, Effect of atomic ration Mg/Al in layers of Mg and Al layered double hydroxide on thermal stability of hydrotalcite-like layered structure by means of in situ high temperature powdered X-ray diffraction, Materials Research Bulletin, 1998, 33, 773-778

[111] F.R.Costa, A.Leuteritz , U.Wagenknecht, D. Jehnichen, L.Häußler, G.Heinrich, Intercalation of Mg–Al layered double hydroxide by anionic surfactants: Preparation and characterization., Applied Clay Science,2008, 38,3-4,153-164

[112] V. Babrauskas , SFPE technology report 84–10, 1984, Society of Fire Protection Engineers, Boston

[113] C.Huggett, Estimation of rate of heat release by means of oxygen consumption measurements, Fire and Materials, 1980, 4, 61-65

[114] F.R. Costa, U. Wagenknecht, G. Heinrich, LDPE / Mg-Al layered double hydroxide nanocomposite : thermal and flammability properties, Polymer degradation and stability, 2007, 92, 10, 1813-1823

[115] B. Diar-Bakerly, G. Beyer, R. Schobert, J. Breu , Significance of aspect ratio on efficiency of layered double hydroxide flame retardants. ACS symposium series, 2012, 1118, chap. 26, 407-425

[116] Handbook of elastomers, 2nd edition revised and expanded, edited by A.K.Bhowmick and H.L. Stephens, CRC press, ISBN: 0824703839, 2000

[117] T. Ishioka, A.Kiritani, T. Kojiama, Infrared study on annealing effect on conformation of zinc stearate, Spectrochimica Acta Part A, 2007, 66, 1048-1051.

[118] S.K.Ghosh, A.K.Bhattacharya, P.P.De, D.Khastagir, S.K.De, Effect of zinc stearate on properties of melt processable ionomer based on sodium salt of sulphonated maleated EPDM rubber, Plastics, Rubbers and Composites, 2001, 30, 16-23

[119] F. Severcan, P.I. Haris, Vibrational Spectroscopy in Diagnosis and Screening, IOS Press, Jun 15, 2012

[120] M.St.C.Flett, The characteristic infra-red frequencies of the carboxylic acid group, Journal of Chemical Society, 1951, 962-967

[121] Y.Ideka, Y.Yasuda, T.Ohashi, H.Yokohama, S.Minoda, H.Kobayashi, T.Honma, Dinuclear bridging bidentate zinc/stearate complex in sulfur crosslinking of rubber, Macromolecules, 2015, 48, 462–475

[122] K.D. Ziegel, A.Romanov, Modulus reinforcement in elastomer composites. I. Inorganic fillers, Journal of Applied Polymer Science, 1973, 17, 1119-1131

[123] D.Roy, A.K.Bhowmick, S.K.De, Anisotropy in mechanical and dynamic properties of composites based on carbon fiber filled thermoplastic elastomeric blends of natural rubber and high density polyethylene, Polymer Engineering and Science, 1992, 32,971-979

[124] M.Gordon, The Physics of Rubber Elasticity (Third Edition). L. R. G. Treloar, Clarendon Press, Oxford. 1975 pp. xii + 370, British Polymer Journal, 1976, vol 8, issue 1, page

[125] G.Heinrich, E.Straube, G.Helmis, Rubber elasticity of polymer networks: theories, Advanced Polymer Science, 1988, 85, 33-87

[126] L.K. Nash, Entropy and rubbery elasticity, Journal of Chemical Education, 1979, 56, 363

[127] Constitutive models for rubber VI, ed: G.Heinrich, M.Kaliske, A.Lion and S. Reese, CRC press, September 1, 2009, ISBN 9780415563277 - CAT# K11242

[128] R. Stoček, G. Heinrich, M. Gehde, R. Kipscholl, Analysis of Dynamic Crack Propagation in Elastomers by Simultaneous Tensile- and Pure-Shear-Mode Testing, Fracture Mechanics and Statistical Mechanics of Reinforced Elastomeric Blends Lecture Notes in Applied and Computational Mechanics Volume 70, 2013, pp 269-301

[129] S. Rooj, A. Das, I. Morozov, K.W. Stöckelhuber, R. Stocek, G. Heinrich, Influence of "expanded clay" on the microstructure and fatigue crack growth behavior of carbon black filled NR composites, Composites Science and Technology, 2013, 76, 61-68

[130] Y.Nie, B. Wang, G.Huang, L. Qu, P. Zhang, G. Weng, J. Wu, Relationship between the material properties and fatigue crack-growth characteristics of natural rubber filled with different carbon blacks, Journal of Applied Polymer Science, 2010, 117, 3441-3447

[131] A.R.R Menon, C.K.S Pillai1, W.S Jin, C. Nah, Fatigue resistance of silica-filled natural rubber vulcanizates: comparative study of the effect of phosphorylated cardanol prepolymer and a silane coupling agent, Polymer International, 2005, 54, 629-635

[132] M. Klüppel, Evaluation of viscoelastic master curves of filled elastomers and applications to fracture mechanics, Journal of Physics: Condensed Matter; 2009, 21, 035104

[133] A.Erxleben. Structures and properties of Zn (II) coordination polymers, Coordination Chemistry Reviews, 2003, 246,203–228.

[134] Y.B. Lyudvig, A.R. Gantmakher, S.A. Lebedev, Dokl. Akad. Nauk SSSR, 1964, 156, 1163

[135] N.D. Zakharov, G.V. Poroshin, Kauchuk I rezina, 12, 14, 1959

[136] N.D. Zakharov. Vysokomol. Soyed.1963, 5, 1190.

[137] N.D. Zakharov, V.A. Kuznetsova. Vysokomol. Soyed. 5th report in the series ‘’Non-sulphur vulcanization of certain synthetic rubbers’’, A10,2, 331-338, 1968

[138] M. Imoto, T. Otsu, M. Nakabayashi , Vinyl polymerization. LXIX. The polymerization of a complex of acrylonitrile with zinc chloride. Makromol. Chem., 1963, 65, 194–201. doi: 10.1002/macp.1963.020650123

[139] G.Socrates. Infrared characteristic group frequencies. John Wiley & sons, Chichester; New York , c1980, p46

[140] I.K.Bhat, S.K. Chaithanya, P.D.Satyanarayana, B. Kalluraya. The synthesis and antimicrobial study of some azetidinone derivatives with the para-anisidine moiety, Journal of Serbian Chemical Society, 2007, 72, 437-442

[141] J. Furukawa, Y. Onouchi, S. Inagaki, H. Okamoto, Rubber elasticity at very large elongation, Polymer Bulletin, 1982, 6, 7, 381-387

[142] R. Hagen, L. Salmén, B. Stenberg, Effects of the type of crosslink on viscoelastic properties of natural rubber , Journal of Polymer Science, Part B:Polymer Physics, 1996, 34, 1997-2006

[143] A.D. Roberts, Natural rubber science and technology , Oxford University Press: Oxford, UK, 1988

[144] M. Makrocka-Rydzyk, G. Nowaczyk, S. Głowinkowski, S.Jurga. Dynamic mechanical study of molecular dynamics in ethylene–norbornene copolymers, Polymer, 2010,51, 908-912

[145] T. Pakula. A Model of cooperative motions in dense polymer systems by means of closed dynamic loops, Progress in Colloid & Polymer Science, 1987, 75, 171-178

[146] S.Yagihara, K.Hikichi. Cooperative interaction on side-chain motion of Poly (α-amino acid), Polymer Journal, 1982,14, 233-240

[147] K. Saalwächter. Chain dynamics in elastomers as investigated by proton multiple-quantum NMR, Macromolecules , 2006, 39,3291-3303

[148] H.Y. Mou, Y.Y. Cao, F. Shen, X.F. Yuan, C.F. Wu, Study on the non-liquid-phase coordination crosslinking reaction of acrylonitrile–butadiene rubber/copper sulfate composites, Acta Polymerica Sinica, 2008, 9, 910–913

[149] Y.N. Zil'berman, R.Sh. Frenkel', N.B. Vorontsova, N.A. Pitkevich, E.A. Kuz'mina, Mechanism of vulcanization of butadiene-nitrile rubber by zinc chloride. Vysokomol. Soyed. 1973, A15, 5, 1147-1149

[150] M.Y.M. Chiang, M. Fernandez-Garcia, relation of swelling and Tg depression to the apparent free volume of a particle-filled epoxy based adhesive, Journal of Applied Polymer Science, 2003, 87, 1436-1444

[151] R.J.Young, P.A.Lovell, An Introduction to Polymers; Chapman & Hall: London, 1991

[152] H.-G. Elias, An Introduction to Polymer Science, VCH, Weinheim, 1997

[153] G.E. Schaumann, E.J. Leboeuf, Glass transition in peat: their relevance and the impact of water, Environmental Science and Technology, 2005, 39, 800-806

[154] G. Pairoh, T. Tipvarakarnkoon, Thermal analysis of lipid crystallization and water ice on coconut milk emulsions: effect of NaCl concentrations, Journal of Medical and Bioengineering, 2013, 2, 191-195

[155] J.E. House, Jr., C. David Dunbar, A DSC study of the phase transitions in $(CH_3)_3NH[CdCl_3]$, Thermochimica Acta, 1992, 204, 213-219

[156] L.Zhang, A.N.C. van Laak, P.E. de Jongh, K.P. de Jong, Textural characterization of mesoporous zeolites, Zeolites and catalysts – synthesis, reactions and applications, Wiley, vol 1, April 2010, p-252

[157] G.W. Oetjen, P. Haseley, Freeze drying, Wiley, 2008, p60-61

[158] M.Iijima, K.Nakamura, T.Hatakeyama, H.Hatakeyama, DSC studies of the structural change of water restrained by pectins, Recent advances in environmentally compatible polymers, Cellucon'99 proceedings, Woodhead publishing limited, 2001, p-304

[159] P. Rybiński, G. Janowska, Influence synergetic effect of halloysite nanotubes and halogen-free flame-retardants on properties nitrile rubber composites, Thermochimica Acta, 2013, 557, 24-30

[160] P. Rybiński, G. Janowska, Thermal stability and flammability of nanocomposites made of diene rubbers and modified halloysite nanotubes, Journal of Thermal Analysis and Calorimetry, 2013, 113, 31-41

[161] A. Weber, K. Resch, Thermotropic systems with fixed domains exhibiting enhanced overheating protection performance, Journal of Applied Polymer Science, 2014, 12, doi: 10.1002/app.40417.

[162] A. Weber, K. Resch, Thermotropic overheating protection glazings: effect of functional additives and processing conditions on light-shielding efficiency, Journal of Polymer Engineering, 2014, 12, doi: 10.1515/polyeng-2013-0275

Appendix A

The mechanical properties of filled NBR vulcanizates are demonstrated in this article as a percentage change as represented in the following equation:

$$\Delta P\% = \frac{P_f - P_i}{P_i} \times 100$$

Where, $\Delta P\%$ is the percentage change of the mechanical properties, P_f is the value of the corresponding mechanical property of aged NBR specimens and P_i is the value of the

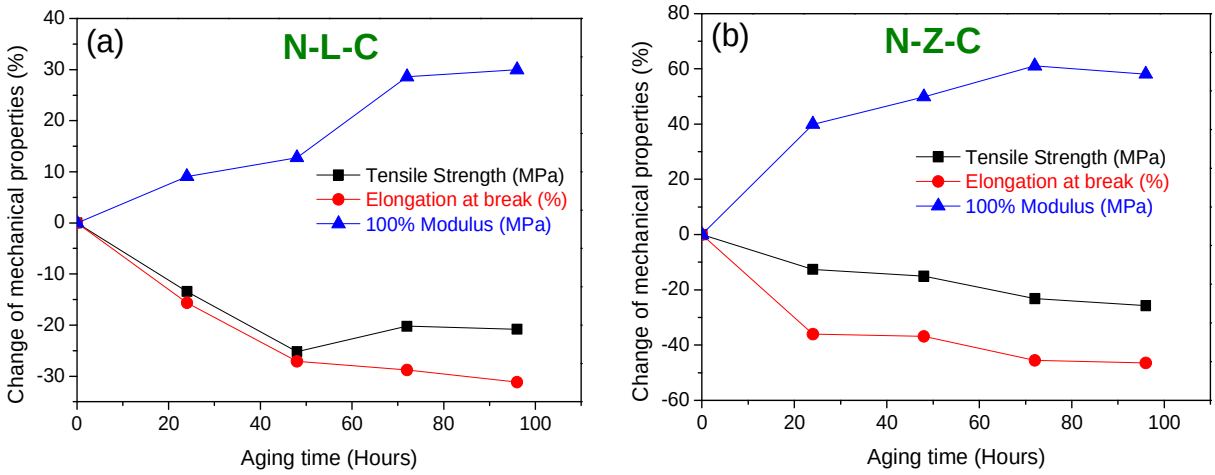

Fig. (a-b) Effect of aging time on the mechanical properties of N-L-C and N-Z-C aged at 100°C (*N-L-C = NBR-Zn Al LDH-CB and N-Z-C = NBR-ZnO-CB*)

corresponding mechanical property of unaged NBR specimens. Fig. (a-b) illustrates the change in the mechanical properties of filled NBR vulcanizates aged at 100°C with different time periods. The heat build-up values for the corresponding compounds are shown in Table.

Table. Heat build-up values for N-L-C and N-Z-C composites. All the specimens are aged for 96 h.

Sample	Aging temperature (°C)	T_g (tan δ)	Hardness	Heat build-up (°C)	
				Center	Surface
N-L-C	unaged	-30.8	68.2	62.8	27.1
	80	-28.8	70.6	---	---
	100	-24.8	72.8	---	---
N-Z-C	unaged	-30.8	70.6	67.2	28.7
	80	-28.8	73.7	---	---
	100	-26.8	74.6	---	---

List of symbols

Tg	Glass transition temperature
S’	Rheometric torque (elastic part)
σ	Stress
Ɛ	Strain
tan δ	Loss tangent
t_{90}	Optimum curing time at 90% crosslinking of the rubber
E’	Storage modulus
E’’	Loss modulus
S	Coefficient of thermal aging
TS_f	Tensile strength after aging
TS_i	Tensile strength before aging
E_f	Elongation at break after aging
E_i	Elongation at break before aging
d	Interlayers distance
θ	Angle between incident beam and planes
λ	Wavelength
V_r	Volume fraction of rubber in swollen gel
D	Deswollen weight of the sample
F	Weight fraction of the insoluble components
H	Initial weight of the sample
χ	Flory-Huggins parameter for polymer-solvent interaction
M_c	Molecular weight between crosslinks
σ_c	Apparent crosslink density
Δυ	Content of ionic crosslinking
U	Strain energy density
k	Temperature dependent rate constant
α	Extent of cure at time t

$d\alpha/dt$	Rate of conversion
E_a	Activation energy of curing
R	Universal gas constant
a_T	Horizontal shift factor
C_1, C_2	WLF constants
T_{VF}	Vogel-Fulcher temperature
α_F	Coefficient of thermal expansion
E'_0	Storage modulus at small amplitude
E'_∞	Storage modulus at high amplitude
γ_c	Critical strain
Φ	Volume fraction of filler
B	Matrix dependent coefficient
λ	Stretching ratio
c_1, c_2	Mooney-Rivlin (MR) constants
da/dn	Crack propagation rate

List of abbreviations

EU	European Uunion
LDH	Layered double hydroxides
NBR	Acrylonitrile buta di-ene rubber
XNBR	Carboxylated nitrile buta di-ene rubber
FTIR	Fourier transform infra-red
SEM	Scanning electron microscopy
TEM	Transmission electron microscopy
HRTEM	High resolution transmission electron microscopy
EFTEM	Energy filtered transmission electron microscopy
DMA	Dynamic mechanical analysis
WAXS	Wide angle X-ray scattering
OLED	Organic light emitting diode
SDBS	Sodium dodecylbenzenesulfonate
TMTD	Tetramethyl thiuram disulfide
ATR	Attenuated total reflection
ISO	International organization for standardization
ASTM	American society for testing and materials
DIN	Deutsches institut für normung
UTM	Universal testing machine
TGA	Thermogravimetric analysis
DTG	Derivative thermogravimetry
DSC	Differential scanning calorimetry
EELS	Electron energy loss spectroscopy
EDX	Energy-dispersive X-ray spectroscopy

List of publications

Articles in Journals:

1. Advances in layered double hydroxide (LDH)-based elastomer composites
   D.Basu, A.Das, K.W.Stöckelhuber, U.Wagenknecht, G.Heinrich
   Progress in Polymer Science, 39, 3, 2014, 594-626

2. Evidence for an in-situ developed polymer phase in ionic elastomers
   D.Basu, A.Das, K.W.Stöckelhuber, D.Jehnichen, P.Formanek, G.Heinrich
   Macromolecules, 47,10, 2014, 3436-3450

3. Unmodified LDH as reinforcing filler for XNBR and the development of flame retardant elastomer composites
   D.Basu, J.J.George, A.Das, D.Y.Wang, U.Wagenknecht, K.W.Stöckelhuber, A.Leuteritz, B.Kutlu, G.Heinrich
   Rubber Chemistry and Technology, 87, 4, 606-616

4. Stearate modified zinc-aluminium layered double hydroxides and acrylonitrile buta diene rubber nanocomposites
   S.B.Eshwaran, **D.Basu**, B.Kutlu, A.Leuteritz, U.Wagenknecht, K.W.Stöckelhuber, K.Naskar, A.Das, G.Heinrich
   Polymer-Plastics Technology and Engineering, 53, 1, 2014, 65-73

5. Rubber composites based on silane-treated stöber silica and nitrile rubber : Interaction of treated silica with rubber matrix
   B.P.Kapgate, C.Das, **D.Basu**, A.Das,G.Heinrich
   Journal of Elastomers and Plastics, 47, 3, 2015, 248-261

6. Naturally occurring amino acids: a suitable substitute of N-N' Di-phenyl guanidine (DPG) in silica tyre formulation
   S.Debnath, A.Das, **D.Basu**, G.Heinrich
   Kautschuk Gummi Kunststoffe, 66, 2013, 25-31

7. Effect of sol-gel derived in situ silica on the morphology and mechanical behavior of natural rubber and acrylonitrile butadiene rubber blends
   B.P.Kapgate, C.Das, A.Das, **D.Basu**, U.Reuter, G.Heinrich
   Journal of Sol-Gel Science and Technology, 62, 2012, 501-509

8. Effect of silane integrated sol-gel derived in situ silica on the properties of acrylonitrile rubber
   B.P.Kapgate, C.Das**,** **D.Basu**, A.Das, G.Heinrich
   Journal of Applied Polymer Science, 131, 40054, doi: 10.1002/app.40531

9. Exploring the role of stearic acid in modified zinc aluminum layered double hydroxides and their acrylonitrile butadiene rubber nanocomposites
   S.B.Eshwaran, **D.Basu**, S.R.Vaikuntam, B.Kutlu, S.Wiessner, A.Das, K.Naskar, G.Heinrich
   Journal of Applied Polymer Science, 132, 41539, doi: 10.1002/app.41539

Articles in Books:

1. Layered double hydroxide (LDH) rubber nanocomposites
   Debdipta Basu, Amit Das, Gert Heinrich
   Invited contribution for a book chapter in **"Encyclopedia of Polymeric Nanomaterials, Kobayashi, Shiro; Müllen, Klaus (Eds.)",** 2015
   Springer
2. Rubber nanocomposites
   Amit Das, **Debdipta Basu**, Gert Heinrich
   Invited contribution for a book chapter in **"Encyclopedia of Polymeric Nanomaterials, Kobayashi, Shiro; Müllen, Klaus (Eds.)",** 2015
   Springer

Conferences:

1. Ionic cross-linking of carboxylated nitrile rubber (XNBR) with different zinc containing additives
   D.Basu, A.Das, K.W.Stöckelhuber, G.Heinrich
   KHK 2012 (10th Fall Rubber Colloquium of DIK-Hannover), November-2012, Hannover, Germany (Proceedings)

2. Exploitation of Layered Double Hydroxide (LDH) – A multifunctional material in rubber
   D.Basu, A.Das, K.W.Stöckelhuber, G.Heinrich
   ICRRM 2013 (International Conference on Rubber and Rubber-like Materials), March-2013, IIT Kharagpur, India (Proceedings)

3. Preparation and properties of flame retardant ethylene propylene di-ene rubber (EPDM) by Layered Double Hydroxides (LDH)
   D.Basu, A.Das, D.Y.Wang, J.J.George, K.W.Stöckelhuber, U.Wagenknecht, G.Heinrich
   EUROMAT 2013 (European Congress and Exhibition on Advanced Materials and Processes), September-2013, Sevilla, Spain (Proceedings)

4. Unmodified LDH as reinforcing filler for XNBR and the development of flame retardant elastomer composites
   D.Basu, B.Kutlu, A.Das, A.Leuteritz, G.Heinrich
   EUROMAT 2013 (European Congress and Exhibition on Advanced Materials and Processes), September-2013, Sevilla, Spain (Proceedings)

5. Phase behavior of carboxylated nitrile rubber
   A.Das, **D.Basu**, K.W.Stöckelhuber, G.Heinrich
   POLYCHAR 22 ,April-2014, Stellenbosch, South Africa (Proceedings)

6. Block co-polymer like phase behavior in ionic elastomer
   D.Basu, A.Das, K.W.Stöckelhuber, D.Jehnichen, P.Formanek, G.Heinrich
   ACS Rubber division, 186th technical meeting October-2014, Nashville, TN, USA
   (Proceedings)

7. Existence of nano-scalic block co-polymer morphology in ionic elastomer
   D.Basu, A.Das, G.Heinrich
   KHK 2014 (11th Fall Rubber Colloquium of DIK-Hannover), November-2014, Hannover, Germany (Proceedings)

8. Designing rubber nanocomposites for ‘green’ and ‘smart’ tire applications
   D.Basu, A.Das, G.Heinrich
   Tire Technology Expo 2015 February-2015, Cologne, Germany (Proceedings)

Curriculum Vitae

Debdipta Basu

Date of birth: 16.01.1985

Nationality: Indian

Education

PhD	**Thesis**: Role of zinc in nitrile rubber
2011-2015	**Supervisor**: Prof. Dr. rer. nat. habil. Gert Heinrich
	At Leibniz-Institute für Polymerforschung (registered student at Technische Universität Dresden, Germany)
M.Sc.	Materials Science
2007-2009	Sardar Patel University, Gujarat, India
B.Sc.	Industrial Chemistry
2003-2006	Calcutta University, West Bengal, India

Honours and awards

- Gold medallist in M.Sc. study (Distinction marks)
- 1st class 1st in B.Sc. in Calcutta University (2003-2006)
- Recipient of prestigious INSPIRE FELLOWSHIP given by Govt. of India

Research interests

- Ionic elastomer
- Self-healing polymer
- Thermoplastic elastomer
- Polymer nanocomposites